A Dissertation

Entitled

Development and Evaluation of Analytical Mobile Source Dispersion Models using Three-Phase Turbulence Parametrization

By

Saisantosh Vamshi Harsha Madiraju

Submitted to the Graduate Faculty as partial fulfillment of the requirements for the

Doctor of Philosophy Degree in Engineering

Dr. Ashok Kumar, Committee Chair

Dr. Liangbo Hu, Committee Member

Dr. Youngwoo (Young) Seo, Committee Member

Dr. Dong-Shik Kim, Committee Member

Dr. Matthew Franchetti, Committee Member

Dr. Scott Molitor, Dean
College of Graduate Studies

The University of Toledo

December 2022

An Abstract of

Development and Evaluation of Analytical Mobile Source Dispersion Models using Three-Phase Turbulence Parametrization

by

Saisantosh Vamshi Harsha Madiraju

Submitted to the Graduate Faculty as partial fulfillment of the requirements for the Doctor of Philosophy Degree in Engineering

The University of Toledo

December 2022

In urban areas, transportation sources are a significant contributor to air pollution emissions including gaseous pollutants and particulate matter (PM). These transportation sources (also called mobile sources) include the vehicles that are normally operated on highways including cars, motorcycles, buses, and trucks. The emissions from mobile sources vary based on the type of combustion, fuel category, the grade of fuel, and the age of moving vehicles. Long-term exposure to mobile source emissions has been associated with adverse health effects such as premature deaths, nonfatal heart attacks, irregular heartbeat, asthma, reduced lung function, and respiratory issues. While for PM the severity of the health effects varies based on the PM size. The level of exposure could be estimated from the ground level concentration of contaminants released from mobile sources. Thus, the role of mobile source air quality modeling is vital in the formulation of air pollution control and management strategies for urban areas.

Many models have appeared in the literature to estimate the nearfield ground level concentrations from mobile sources moving on a highway. However, current models do not account explicitly for the effect of wind shear (magnitude) on the gaseous pollutants near the ground while computing the ground level concentrations near highways from mobile sources. For PM, the available mobile source models do not consider explicitly different ranges of particle size present in the exhaust. It is necessary to predict the downwind concentrations near highways from mobile sources for different particle size ranges to identify the severity of the emissions on public health.

The improvement in the performance of mobile source models over the last 50 years is achieved by improving the theoretical basis of the dispersion equations and developing dispersion coefficients based on either theory or field experiments. This study presents a new Three-Phase Turbulence (TPT) model to calculate the vertical spread of mobile source plume by combining the current concepts of atmospheric turbulence and plume spread observations based on field data. The dispersion coefficients for stable and unstable atmospheric conditions are based on the nearfield parameterization. The initial vertical dispersion coefficient due to the wake effect of mobile sources is incorporated in the dispersion equations.

Three new analytical models based on the solution of the convective–diffusion equation are presented. The first analytical model (SLINE 1.1) is developed by considering highway mobile sources as a line source and incorporates the wind shear near the ground for gaseous pollutants. The second analytical model (SAREA 1.1) is developed by considering highway mobile sources as area sources and incorporates the wind shear near the ground. The third analytical model (SLINE PM 1.1) is based on the analytical solution

and incorporates different particle size ranges for particulate matter released from mobile sources. The SLINE 1.1, SAREA 1.1, and SLINE PM 1.1 follows the proposed TPT model to account for plume/atmosphere interaction. The major inputs of the proposed models include emission rate, wind speed, and turbulence parameters.

The proposed gaseous models (SLINE 1.1 and SAREA 1.1) are evaluated using four different field data sets: CALTRANS, Raleigh, Idaho Falls, and Hyderabad. The SLINE PM 1.1 is evaluated using the Raleigh and Hyderabad datasets for different particle size ranges. The performance of each model is evaluated using several statistical parameters such as Model Bias ($\mu g/m^3$), Fractional Bias, Normalized Mean Square Error, Correlation Coefficient, Geometric Mean Bias, Geometric Mean-Variance, and Fa2 (these indicators are used to evaluate air quality models).

The sensitivity of the SLINE 1.1, SAREA 1.1, and SLINE PM 1.1 models is evaluated using the Sensitivity Index (SI) Method. Intercomparison between the proposed models and the popular models is performed to identify the best-performing model for each category using the statistical indicators mentioned above and using BOOT Software (Version 2.0) to identify the significantly different models.

The results from the BOOT software indicate that SLINE 1.1, SAREA 1.1, ADMS, and SLSM are significantly different with 95% confidence limits. SLINE 1.1 is the best performing gaseous model than SAREA 1.1 and is considered an available model. Results indicate the model predictions of SLINE 1.1, SAREA 1.1, and SLINE PM 1.1 correlate up to 83%, 82%, and 89% respectively with the observed data. Both the gaseous models are highly sensitive to the emission rate, moderately sensitive to wind velocity, and sensitive to the vertical spread of the mobile plume. But the magnitude of sensitivity of SLINE 1.1

model is higher than the SAREA 1.1. The SLINE PM 1.1 is highly sensitive to emission rate, moderately sensitive to wind velocity, and coefficient a, and slightly sensitive to vertical plume spread.

Acknowledgments

I would like to express my gratitude to Dr. Ashok Kumar for his continued academic guidance during the entire program. Without his guidance and persistent help in every step throughout the process, this dissertation would have never been accomplished. I am grateful to my committee members: Dr. Liangbo Hu, Dr. Youngwoo (Young) Seo, Dr. Dong-Shik Kim, and Dr. Matthew Franchetti for their valuable time, suggestions, and comments on my work. My sincere thanks to Dr. Relue (Associate Dean) for the support to complete my research on-time.

I would like to thank my parents (Annam Raju Madiraju and Sailaja Madiraju), sister (Divya), and friends (Venkatesh, Abhiram Pamula, Abhiram Bandreddy, Rutambara, Govind, Yeswanth, Hari Priya, Jaya Chandra, Parul, Goutam, Maruti, Arvind Kumar) for their love and continued support.

I would like to dedicate this dissertation to my parents: Annam Raju Madiraju and Sailaja Madiraju. I am grateful for all the time they spend with me and sacrificed for me. I will always appreciate the things they have done for me throughout my life.

Table of Contents

List of Tables

List of Figures

List of Symbols

u ..... Wind velocity (m/s)
u_1 ..... Wind velocity at a reference height z_1(m/s)
U_e..... Effective wind velocity (m/s)
$U_{\bar{z}}$ ..... Wind velocity at the reference height ($\bar{z}$) (m/s)
u_* ..... Surface friction velocity (m/s)
w_* ..... Convective velocity scale (m/s)
θ ..... Wind angle concerning road (°)
m..... Exponent of power-law profile
s..... Stability parameter
L..... Monin–Obukhov Length (m)
σ_z..... Vertical dispersion coefficient
σ_y..... Horizontal dispersion coefficient
σ_v ..... Standard deviation of lateral wind component (m/s)
σ_{z0} ..... Initial vertical plume spread
$\sigma_\emptyset$ ..... Vertical wind direction
$\sigma_{z_{roads}}$ ..... Vertical plume spread parameter
K ..... Eddy diffusivity at the vertical height
K_1..... Eddy diffusivity at a reference height z_1
n..... Exponent of eddy-diffusivity profile
m_t ..... Additional spread due to the vehicle
a, b_u, b_s, c, d_s, d_u Empirical coefficients
x..... Downwind distance (m)
x_d ..... Downwind distance of monitoring station from the edge of the field
y..... Crosswind distance (m)
Y..... Finite source length (m)
z..... Vertical height of receptor above ground (m)
z_s ..... Height from the ground surface to the tailpipe (m)
Z_{im} ..... Maximum mixed layer height (m)
L_s ..... Finite crosswind line source of length (m)
X..... Highway strip source with width (m)
W..... Width of the road (m)
q..... Emission rate of line source (unit/sec)

Q…… Emission rate of area source (unit/sec)
H…… Average height of car (m)
h……. Mixing box height (m)
Ri……. Richardson Number
dT/σ_z……. Temperature gradient
γ …… Lower incomplete gamma function
Γ ……... Upper incomplete gamma function
r……..……..... Correlation coefficient
C ……... Concentration of pollutants (unit/m^3)
Cp……. Model Predicted Concentration (unit/m^3)
Co…….. Observed Concentration (unit/m^3)
C_{TP}……. Total particulate concentration (unit/m^3)
A_t……... Fractional change in the pollutant concentration rate
V_c……... Fractional change of the input variable
i..... Number of lanes on the highway
V_d ..... Dry deposition velocity of the particle (m/s)
V_g ..... Gravitational settling velocity of the particle (m/s)
R_a ..... Aerodynamic resistance (s/m)
R_p..... Quasilaminar sublayer resistance
P ..... Particle density (g/cm^3)
ρ_{air} ..... Air density (g/cm^3)
d_p ..... Particle diameter (μm)
g..... Acceleration due to gravity (m/s^2)
μ..... Absolute viscosity of air (g/cm/s)
C_2 ..... Air unit's conversion constant ($cm^2/\mu m^2$)
S_{CF}..... Slip correction factor (dimensionless)
V..... Vertical term
D..... Decay term as a function of x

Chapter 1

Introduction

1.1 Background

Highway mobile sources are one of the major contributors to air pollution in the US. The contribution of mobile sources to pollution emissions continue to grow along with the number of vehicles and the total miles traveled. The situation will improve with the use of electric vehicles in the coming years. The mobile source emissions include greenhouse gases (GHGs) that contribute to climate change [1]. They also contain volatile organic compounds (VOCs), nitrogen oxides (NO_x), carbon monoxide (CO), carcinogenic compounds, and fine particulate matter (PM). VOCs and NO_x combine to form ground-level ozone, which causes human health effects like lung infections, asthma, and other respiratory diseases. Ozone also affects plant life that has an impact on agriculture and forestry. CO causes an increased risk of heart disease over a long period of exposure. Carcinogenic compounds (benzene, 1,3butadiene, and aldehydes) cause serious health effects like cancers. PM exposure leads to cardiovascular and raspatory diseases [2].

Air pollution dispersion Modeling allows us to create a simulation of how atmospheric processes disperse pollutants in the ambient atmosphere using mathematical formulations to estimate ground-level concentrations at any downwind distance. The dispersion modeling is based

on the physics and chemistry involved in the process of advection/dispersion of contaminants and could predict and estimate the concentrations of contaminants by considering source origin, composition, emissions, and meteorology. Analytical/numerical techniques are used to simulate ground-level concentration in air quality models. Inputs of air quality modeling include source information, meteorological data, and the surrounding terrain [3], [4]. An important meteorological parameter is an atmospheric stability. The tendency to enhance and resist atmospheric motions is called atmospheric stability. Over the last 50 years, several methods have been proposed to classify atmospheric stability. Some of these methods are based on the variation in temperature with height, wind speed, insolation (daytime), and cloud cover (nighttime). The concentration of pollutants is affected by convective and mechanical turbulence. For unstable atmospheric conditions, more dilution is expected due to convective activities when compared with stable atmospheric conditions [5], [6]. Air pollution dispersion modeling is typically an inexpensive approach when compared to field studies. Most dispersion models use computer programs to simulate the movement of air pollutants in the atmosphere and to estimate the pollutant concentrations in a geographic location. There are different types of models based on the nature of sources (such as point, line, area, and volume sources) [7]. "Line-source models" are generally used to calculate and predict the concentration of pollutants that are continuously emitted from transportation (mobile) sources on the highways. The effect of pollution from line sources is high in an urban environment due to their major contribution to local air quality. Vehicular density, vehicle speed, and emission rate are the major variables to be considered for the prediction analysis of air quality involving mobile sources [8]–[10].

1.2 Literature

The literature review indicated that many line-source air quality models have been developed over the last 50 years. The mathematical formulation of these models can be analytical, statistical, or numerical. The solution of the convective–diffusion equation for a line source was available in the 1950s [10]. During the 1960s and 1970s, many Gaussian-based dispersion models were introduced. These formulations were a function of meteorology, receptor locations, and highway geometry. The differences in formulations were due to the assumptions made during the solution of the convective–diffusion equation or the specification of plume spread rates. However, these models did not perform very well when the predicted results were compared with the observed values. The primary reason was the difficulty in accounting for atmospheric dispersion and turbulence [11]. Subsequently, many experimental field studies have been conducted to improve the models.

HIWAY1 was developed in the early 1970s to predict mobile source emissions near roadways [12]. In 1978, Chock formulated General Motors' (GM) line-source model by incorporating wind speed correction and modified values for vertical dispersion coefficients to address wake turbulence from the vehicles [13]. In 1980, Rao and Keenan evaluated the existing models and suggested new dispersion curves for pollution dispersion near highways [14], [15]. Model development continued from the 1980s onwards to address vehicle-induced turbulence, surface roughness, averaging time, new provisions for plume spread, and other turbulence mixing parameters [16].

The USEPA (the United States Environmental Protection Agency) Office of Research and Development introduced a CALINE (California Line Source) dispersion model in 1972 based on the Gaussian plume model using Pasquill–Gifford (P–G) atmospheric stability classes. CALINE was developed by focusing on the prediction of CO concentration near roadways [17]. In 1975,

formulations for depressed roadways were added to develop CALINE2 [18]. In 1979, the vertical and horizontal dispersion curves were revised along with updating vehicle-induced turbulence, averaging time, and introducing a finite line source to develop CALINE3 to reduce over predictions. In 1984, CALINE4 was introduced with the addition of chemical reactions for CO_2 and PM, intersections, and updating lateral plume spread and vehicle-induced turbulence. CALINE, CALINE2, and CALINE3 are open-source models and are available freely to the public, unlike CALINE4 [19]. In 1989, Luhar and Patil developed a General Finite Line Source Model (GFLSM) based on the Gaussian diffusion equation and evaluated it based on data collected at intersections in Mumbai and New York [20]. Around the early 1990s, the CAL3QHC screening model was developed to auto estimate the queue lengths of vehicles at the intersections. The enhanced version of CAL3QHC is CAL3QHR, a more flexible model than CAL3QHC with a two-tiered approach [21]. In the same decade, the ISCST2 (Industrial Source Complex Short Term 2) model was introduced by incorporating mixing height algorithms. It could estimate the concentration of pollutants with varying emission rates from point sources. According to Eerens, the CAR model was developed in 1993 and evaluated with the data collected in urban areas of the Netherlands [22]. ISCST3 was developed in 1995 by incorporating the new area source option and algorithms of dry deposition [23]. Later, the GFLSM was improved by Sharma based on experiments conducted at intersections in Delhi, India [24]. A road network dispersion model named CARFMI was developed similarly to a CAR model to predict concentrations of pollutants from automobiles near industrial areas [25]. The ROADWAY model was developed while studying vehicle wakes and the dispersion phenomena in pollutants from the vehicles [26]. COPERT and CEM are also major models used to calculate the concentration of pollutants from vehicular emissions [27]. During this period, the ADMS model was developed by CERC, UK [28].

The progress of these model developments has helped regulatory agencies to estimate the impacts of emissions.

A commonly used line-source model, CALINE4, uses a range of traffic and fleet characteristics and a diffusion equation to assess the impacts of a road at a small scale. It is specifically designed for assessing air quality impacts at roadways or intersections and used to predict impacts of changing traffic volumes, signal phasing, or adding additional lanes to a roadway [29]. In New Zealand, a similar model named VEPM was developed, which uses real and lab-based emissions data to predict emissions up to the year 2040 from a roadway [30].

The research has continued to develop, assess, and evaluate the preexisting models and to increase the scope of accuracy for future models. In 2005, the USEPA replaced the ISC model with AERMOD which contains an updated atmospheric stability scheme and the ability to characterize the planetary boundary layer through both surface and mixed layers [31]. In 2007, Gokhale developed a simple semiempirical box model based on the traffic flow rate at the busiest traffic road intersections in Delhi. He estimated hourly average carbon monoxide (CO) concentrations and optimized specific vehicle emission rates based on vehicle category. Through this study, he was able to show that the nature of vehicle flows influences the rate and nature of the dispersion of pollutants which affect pollutant concentrations in the road vicinity [32]. In 2011, Xie conducted a study on both the daily and hourly concentration levels of CO, PM_{10}, CO_2, and O3 during the Beijing Olympic Games, conforming to the Grade II China National Ambient Air Quality Standards. A notable reduction in concentration levels was observed in different regions of Beijing, with the traffic-related air pollution in the downwind northern and western areas. According to Xie, the "Traffic Restriction Scheme (TRS) policy was effective in alleviating traffic-related air pollution and improving short-term air quality during the Beijing Olympic Games" [33].

In 2018, Milando conducted a study near high-traffic roads in Detroit. He evaluated the RLINE/AERMOD by comparing predicted concentrations of NO_x, CO, and $PM_{2.5}$. The model performance for CO and NO_x was found to be best at sites close to major roads, during downwind conditions, during weekdays, and in certain seasons [34]. In 2018, Bowatte investigated the longer-term effects of traffic-related air pollution exposure for individuals with or without existing asthma, and with or without lower lung function. Population groups who fall under the middle age category and live less than 200 m from a major road, could be susceptible to both the development and persistence of asthma. These findings have public health implications for asthma prevention strategies in primary and secondary settings [35]. In 2018, Liang conducted a dorm room inhalation study due to vehicle emissions using a near-road monitor as a surrogate for true exposure and observed acute health effects. This study was conducted near a road, measuring several single traffic indicators at six indoor and outdoor sites [36]. In 2020, Amoatey conducted a comparative study between COPERT and CMEM models. The correlation coefficient for these two models was found to be statistically significant from 0 in the case of combined model comparison across all the traffic locations for both CO and NO_x. He concluded that due to the terrain features of certain roads, weak performance was observed, and the influence of terrain needs to be considered in future studies [37].

Along with the general models for all types of pollutants many models are also available in the literature specifically to predict the concentrations of PM at downwind distances from different sources. Most of these models are aerosol dynamics models considering the particle size method. Each model has its criteria for the particle size that it is used. UHMA (University of Helsinki Multi-component Aerosol Model) is a dispersion model developed at the University of Helsinki with a focus on the growth and development of new particles. The model is evaluated in

the studies conducted by Pirjola et al [38] and Korhonen et al [39]. MONO32 is a model containing 4 size modes and follows a monodisperse approach, especially for the particle size between 7- 450 nm. This model was examined and evaluated by Pohjola et al within 25 seconds after the emission [40]. AERO is a dispersion model developed for particle sizes between 0.01-10μm with 8-size distribution sections and composition was assumed to be uniform [41]. GATOR (Gas Aerosol Transport Radiation Model) is an Eulerian dispersion model used for the moving size or stationary size particles in urban and mesoscale environments [42]. MADRID (Model of Aerosol Dynamics, Reaction, ionization, and Dissolution) is developed for multiple-size particles [43]. AERO-FOR2 is a sectional box model considering 200 evenly distributed sections for the particle size method and externally or internally mixed varying within each size group distributed logarithmically. URM is an Eulerian dispersion model containing four groups under 10μm size. RPM model is considered for the particle sizes between 0.01-0.07 μm. The CIT model developed by the California Institute of Technology is for particle sizes between 0.5-10 μm. All the discussed models consider the effect of condensation/evaporation. The phenomenon of coagulation is considered by all the above-mentioned models except URM and CIT in simulating predictions. The effect of dry deposition is incorporated in all the discussed models. However, the effect of wet deposition is considered only by AEROFOR, URM, and RPM [44].

Researchers in the past performed the model evaluation and comparative studies to evaluate the existing popular models. In 2001, Hanna et al evaluated ADMS, AERMOD, and ISC3 dispersion models concerning non-buoyant tracer releases for point, area, and volume sources with five different field data sets. The results showed that ADMS underpredicts by about 20% and AERMOD underpredicts by about 40%, and both have a scatter factor of about two. The ADMS performance is slightly better than the AERMOD performance and both perform better than ISC3,

an earlier model from the USEPA [3]. In 2005, CALINE4 and CAR-FMI dispersion models were evaluated by Levitin et al. against the near road measurements using the data collected at Elimäki in southern Finland from 15th September to 30th October 1995. The results indicated that the performance of both models was better at 34 m when compared with that at 17 m. However, in most cases, the performance of both the models deteriorated as the wind speed reduced (decreased) and as the wind direction approached a direction parallel to the road [45]. In 2007, the ability of CALINE4 to predict the spatial variation of hydrocarbon concentrations downwind of a motorway was assessed along with the accuracy of COPERT III emission functions. The results indicate that the range of the observed concentrations is higher than that of those modeled. This implies that short-term modeling will tend to underestimate higher percentile concentrations. This affects the model predictions when multiple pollutants are considered [46]. In 2009, Righi et al compared ADMS urban model with an urban air quality monitoring network in Ravenna, Italy by performing a statistical and diagnostic evaluation. The results indicate that the performance of the ADMS urban model is satisfactory. However, the model tends to under-predict the concentration of air pollutants [47]. In 2013, Heist et al. performed a model intercomparison by estimating the near-road pollutant dispersion. AERMOD, CALINE3, CALINE4, ADMS, and RLINE models were used to simulate the predicted concentrations for the Idaho Falls and Caltrans Highway 99 tracer studies. The models performed best for near-neutral conditions in both tracer studies but had mixed results under convective and stable conditions. It was also observed from the results that RLINE, ADMS, and AERMOD had produced similar results and CALINE4 produced significant scatter in the model predictions [17]. In 2017, Agharkar used CALINE4 and GAM (Generalized Additive Models) to perform a model validation and comparative performance evaluation to predict the near-road black carbon. When evaluated based on graphical screening techniques and compared

using descriptive statistics, CALINE4 and GAM exhibited R^2 values of 0.6928 and 0.9415, the slope of linear regression of 0.7341 and 94 respectively. The overall results in this study indicated that both the models showed a good agreement with the measured data [48].

Many dispersion models have been reported in the literature that has applications for highway mobile sources. Some of these are HIWAY4, GM, CALINE series, CAL3QHR, VEMP, GFLSM, CAR-FMI, ROADWAY, AERMOD, CORPET, and CEM. A summary of models used for mobile sources is given in Table 1. Overall HIWAY model was developed for mobile source emissions near roadways. GM model was introduced for line sources incorporating wind speed correction with updated vertical dispersion coefficients. CALINE series was developed by USEPA based on P-G atmospheric stability classes focusing on near roadway pollutants. CAL3QHR is a screening model with a two-tiered approach to auto-estimate the queue lengths of vehicles at the intersections. VEPM is a line dispersion model for the mobile sources to predict future pollutant concentrations from the roadways. GFLSM is based on the Gaussian diffusion equation for the finite line sources, which is evaluated at intersections using data from the conducted field studies. CAR-FMI is a dispersion model developed to predict concentrations of pollutants from automobiles near industrial areas. ROADWAY model was developed while studying the vehicle wakes and the dispersion phenomena in pollutants from the vehicles. COPERT and CEM are also other major mobile source dispersion models used to calculate the concentration of pollutants from vehicular emissions [8].

Currently, USEPA extended the AERMOD for mobile source modeling. AERMOD can be used to perform spot analysis for the $PM_{2.5}$, PM_{10}, and CO. It is also extending its options toward including highway and intersection projects. The current AERMOD uses an elongated area source/set of volume sources for the roadway air quality modeling [19]. The R-LINE is a Research

LINE source model, developed by EPA's Office of Research and Development. R-LINE uses Gaussian dispersion algorithms, like AERMOD [20], which has roadway applications under low wind conditions. AERMOD does not contain algorithms to account for dispersion around solid noise barriers near roadways and roadways within a depression. However, R-LINE has a beta implementation of solid barrier and depressed roadway algorithms for modeling complex configurations of roadways.

Table 1-1: Key features of various air quality models used for mobile source dispersion.

Dispersion Model	**Atmospheric Stability Scheme**	**Significant features related to mobile source dispersion**
HIWAY4	Pasquill-Gifford	New dispersion curves in conjunction with an aerodynamic drag factor are used to account for the change in the wind field due to the moving vehicles [14].
CALINE4	Pasquill-Gifford	This model has an option for modeling roadway intersections. There are new provisions for lateral plume spread and vehicle-induced thermal turbulence [19], [49].
GFLSM	Pasquill-Gifford	This is a simple finite-line source model and could be used for any orientation of wind direction with the roadway and is more suitable for long-term predictions [20], [50].
CAR-FMI	Monin-Obukhov length	A road network dispersion model that estimates the contribution from mobile sources in predicting the emission, dispersion, and chemical transformation [45].
COPERT	Pasquill-Gifford	This model uses emission factors for vehicle fleet composition determined by using a chassis dynamometer test during which a vehicle engine is run over test cycles [51].
ISC3	Pasquill-Gifford	This model has a revised area source algorithm and has the option to specify an initial vertical dimension used to model mechanically generated emission sources from mobile sources [52], [53].
AERMOD	Monin-Obukhov length	ISC3 model revised to develop AERMOD. AERMOD has updated options for the mobile source modeling. It has regulatory applications like transportation conformity hot-spot analyses for particulate matter and carbon monoxide. It has the R-Line feature which offers an additional pathway for the future modeling of mobile sources. Advanced features for mobile sources are still being incorporated into the AERMOD [31], [54].
ADMS 5	Monin-Obukhov length	The mobile source modeling options on roads include traffic-induced turbulence considering the extra turbulence induced by traffic on busy roads and the effect on the model turbulence. It also has the street canyon module which has a separate treatment of traffic-produced turbulence [55], [56].

AERMOD is currently capable of modeling a roadway source as an area/volume source [57], [58]. The R-LINE model has been compared to the concentrations from the Idaho Falls line source tracer experiment [59], the CALTRANS Highway real-world tracer study [19], and 2006

near road study in Raleigh, North Carolina [60]. The R-LINE model showed good performance in a variety of atmospheric conditions, including stable, neutral, and convective conditions; in a variety of wind conditions, including low winds, high winds, and winds parallel to the road; and in a variety of configurations including upwind, downwind, and close to the source [60], [61].

Overall, the literature review of gaseous dispersion models indicates that available line-source dispersion models do not explicitly account for wind shear near the ground under different atmospheric conditions. Therefore, this study focused on developing mobile source dispersion models considering wind shear near the ground for gaseous pollutants. The change in wind velocity with height near the ground is defined as wind shear for this development. The literature review of PM dispersion models shows that the reported models for the estimation of concentrations are not designed for different particle size ranges for infinite and finite-length sources. Mobile source dispersion models could be improved by improving turbulence parametrization of plume or atmospheric interaction based on recent developments.

1.3 Objectives and Significance

The purpose of this study is to develop and evaluate two new mobile (line and area) source models for gaseous pollutants by incorporating wind shear near the ground. For PM emissions from the mobile sources, to develop and evaluate an analytical line-source model to account for different particle size ranges for PM. The objectives of the dissertation are as follows:

1. Development of a Three-Phase Turbulence (TPT) model for mobile plume interaction with atmosphere as plume disperses downwind.

   In the TPT model, the mobile plume interaction with the atmosphere as the plume disperses downwind is categorized into multiple phases based on the findings in different

studies on mobile sources and the conceptual framework suggested by Kumar for dispersion from point sources. The effect of vehicular, thermal, and atmospheric turbulence on the mixing and growth of the mobile source plume is considered during the model development. The magnitude of additional spread due to the vehicles is incorporated in providing the updated turbulence parametrization. The updated turbulence parametrization can be implemented in any analytical mobile source dispersion model.

Hypothesis: An enhanced turbulence model that can be used for mobile source plume dispersion will be developed considering the effect of various critical parameters (e.g. Atmospheric turbulence).

2. Development and Evaluation of a line-source model for gaseous pollutants (SLINE 1.1).
3. Development and Evaluation of an area source model for gaseous pollutants (SAREA 1.1).

For gaseous pollutants, SLINE 1.1 and SAREA 1.1 models were developed by the incorporation of wind shear during the dispersion from mobile (line) and mobile (area) sources using the convective–diffusion equation respectively. The concept of wind shear involving variation of the wind velocity magnitude near the ground for the dispersion of pollutants released from the tailpipe of mobile sources is incorporated through the power-law profile. The updated turbulence parametrization is implemented in both (SLINE 1.1 and SAREA 1.1) models.

Hypothesis: Mobile (line and area) source dispersion models will be developed for gaseous pollutants from the exhaust of the highway mobile sources considering the improved physics of the atmospheric processes. The models will incorporate wind shear and TPT parametrization to

predict downwind ground level concentrations. The model performance will be assessed using the statistical indicators based on simulations for the model predictions.

4. Development and Evaluation of a line-source model for particulate matter of different sizes (SLINE PM 1.1).

   For PM pollutants, SLINE PM 1.1 model is developed based on the analytical solution of the convective–diffusion equation representing the dispersion of particulate pollutants considering the size profile. The particle size concept is incorporated into the equations through the Gravitational settling velocity. The particle diameter is considered while computing the Gravitational settling velocity of the particle. The Gravitational settling velocity is considered in SLINE PM 1.1 while computing the ground level concentrations of the particulate matter. The updated turbulence parametrization is implemented in SLINE PM 1.1 model.

Hypothesis: A mobile source (line) dispersion model will be developed for particulate pollutants from the exhaust of the highway mobile sources considering the improved physics of the atmospheric processes. The model will consider different particle size ranges and TPT parametrization to predict downwind ground level concentrations. The model performance will be assessed using the statistical indicators based on simulations for the model predictions.

5. Identification of the best performing model for mobile source gaseous dispersion model by intercomparing the proposed models with the current models.

   There is a necessity to examine the performance of developed models with respect to the existing popular models. A comparative analysis is performed using developed

models (SLINE 1.1, SAREA 1.1 for gaseous pollutants, SLINE PM 1.1 for PM) with the available models (CALINE4, ADMS, ISC3, SLSM for gaseous pollutants, and SLSM for PM) using statical indicators and graphical visualization to identify the best performing model. The statistical indicators include Model Bias (MB), Fractional Bias (FB), Normalized Root Mean Square Error (NMSE), Correlation Coefficient (r), Geometric Mean Bias (MG), Geometric Variance (VG), and the Factor of two (Fa2) are considered. The graphical visualization is generated by using the Scatter plots, Cp/Co plots, and Q-Q plots. The identification of the significantly different models is performed using Boot software (Version 2.0). This step will highlight the new development in the field.

Hypothesis: The developed models will perform better than the available models to predict the downwind ground level concentrations of air pollutants from the highway mobile sources. The developed models are significantly different from the available models.

1.4 Methodology

The conceptual flow chart of the research methodology is represented in Figure 1-1. The initial step in the research focuses on a new Three-Phase turbulence model for the interaction of mobile plumes with the atmosphere. Then the development of three analytical models based on the solution of the convective–diffusion equation by incorporating the wind shear near the ground for gaseous and particulate pollutants.

The first analytical model is developed by considering highway mobile sources as line sources and named SLINE 1.1. The second analytical model is developed by considering highway mobile sources as area sources and named SAREA 1.1. Then the third model is an analytical model for the PM account for different particle size ranges for particulate matter released from mobile sources and named SLINE PM 1.1. The coordinate system followed by the equations is represented

in Figures 1-2. SLINE 1.1, SAREA 1.1 and SLINE PM 1.1 models incorporate the variation of wind velocity with height.

These models use the proposed Three-Phase turbulence approach through turbulence parametrization. The next step is model evaluation using field data from four different sources. The performance of each model in the model evaluation process is assessed using several statistical indicators including Model Bias (MB), Fractional Bias (FB), Normalized Root Mean Square Error (NMSE), Correlation Coefficient (r), Geometric Mean Bias (MG), Geometric Variance (VG), and the Factor of two (Fa2). The SLINE 1.1 and SAREA 1.1 models are evaluated using the CALTRANS, Raleigh, Idaho Falls, and Hyderabad field data sets. The SLINE PM 1.1 is evaluated using the Hyderabad and Raleigh data.

A comparative analysis is performed between developed models (SLINE 1.1, SAREA 1.1 for gaseous pollutants, SLINE PM 1.1 for PM) and the available models (CALINE4, ADMS, ISC3, SLSM for gaseous pollutants and SLSM for PM). The models used for comparison are widely used today. CALINE4 (the California Line Source Model version 4) is used throughout the world to model near-road pollutant concentrations [62]. ADMS is currently used in UK to identify Low Emission Zones within which only vehicles that have achieved a particular low-emission standard are allowed [63]. ISC3 (The Industrial Source Complex - Short Term regulatory air dispersion model) is one of the popular US EPA models and widely used to assess pollution concentration and/or deposition flux on receptors, from a wide variety of sources [64]. SLSM, a simple line source model from the Textbook by Wark et al [3] was considered in this study along with the available models. More details about the models are provided in Section 7.1.

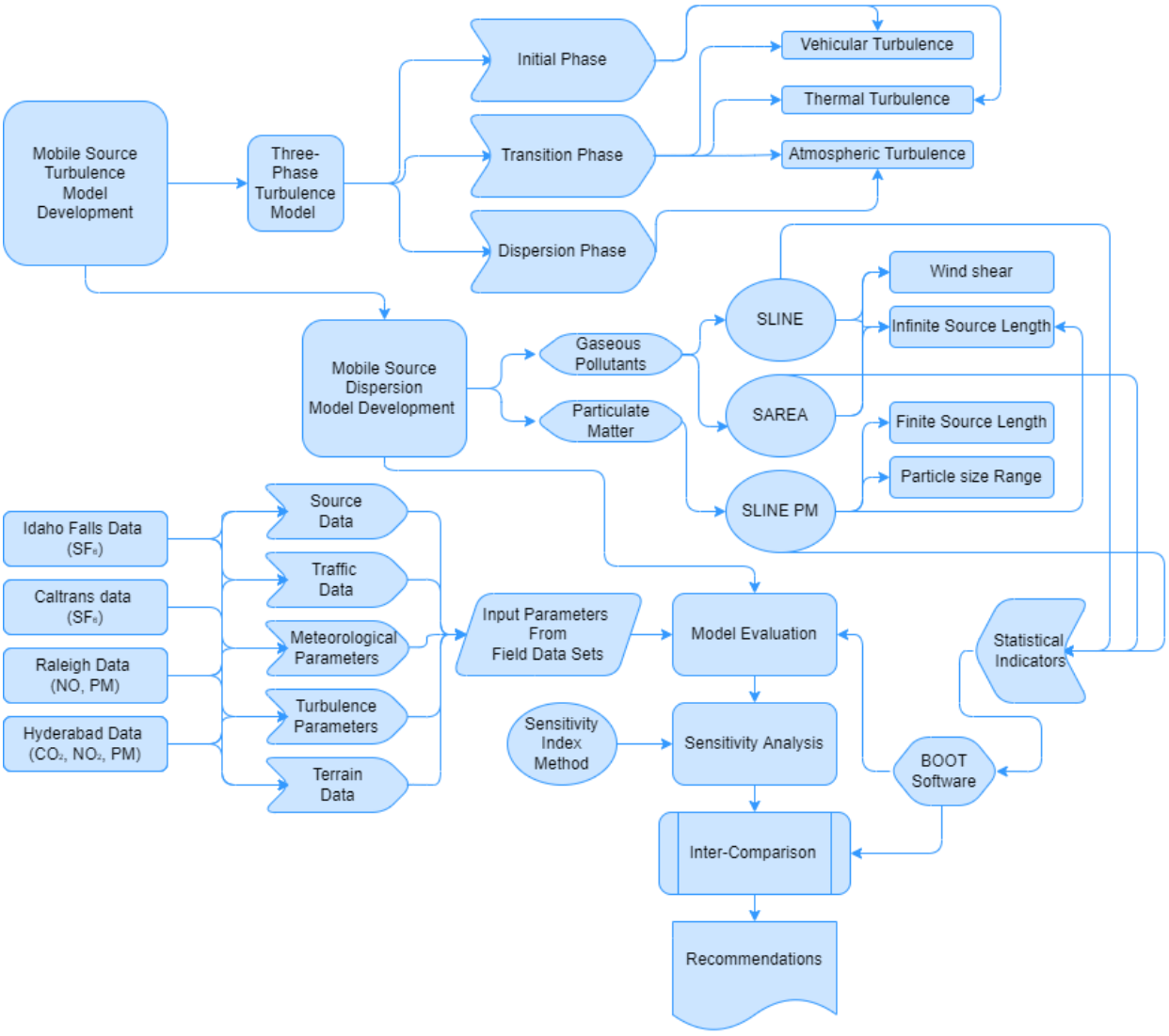

Figure 1-1: Conceptual Flow Chart of Research Methodology

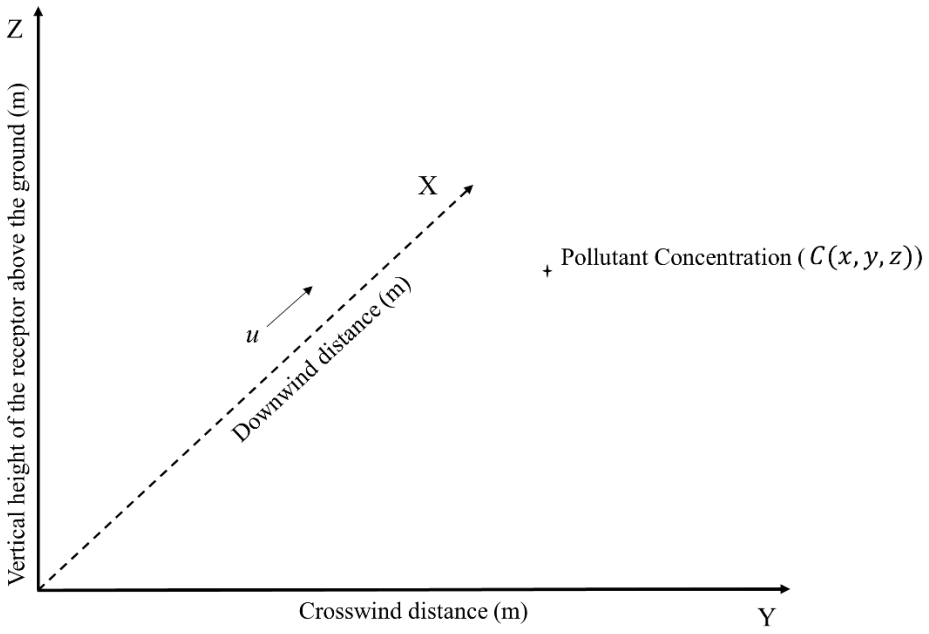

Figure 1-2: Co-ordinate system used for the dispersion calculations.

The sensitivity of the model in predicting ground level concentrations to input variables/parameters is also presented to identify how sensitive each model is towards the independent input variables/parameters. The sensitivity of the SLINE 1.1, SAREA 1.1 , and SLINE PM 1.1 models is tested using the Sensitivity Index (SI) Method (See Section 4.3).

The last step is on the intercomparison of the proposed models and the popular models to identify the significantly different model using Boot software (Version 2.0). SLINE 1.1, SAREA 1.1, CALINE4, ADMS, ISC3, and SLSM models were compared against each other. For SLINE PM 1.1 model, the intercomparison needs to be performed with SLSM.

Chapter 2

Development of a Three-Phase Turbulence model

2.1 Model Development

2.1.1 Flow Regime of the mobile source plume

A highway with mobile source vehicles is considered. wind orientation is at an angle θ (Assumed, θ = 90) to the length of the road. The conceptual turbulence model proposed as mobile plume interaction with the atmosphere as the plume disperses downwind (See Figure 2-1). The proposal is based on the findings in different studies on mobile sources and the conceptual framework suggested by Kumar [65] for dispersion from point sources. The turbulence model includes three flow regimes. They are

1. Initial Phase: The first flow regime (Initial Phase) is near the mobile sources and the highway. The mixing and growth of the plume are due to the turbulence generated from the mobile source [65]. The plume dispersion is dominated by vehicular turbulence (created by the motion of the vehicle) and thermal turbulence (created by the heating of ground due to solar radiation) in this phase. The Initial Phase is observed up to a downwind distance of 6.5 m from the mobile source. As this region is very close to the mobile source, very little plume diffusion can be observed.

2. Transition Phase: The second flow regime (Transition Phase) is in the wake area created by wind flow. The Transition Phase includes the effect of thermal turbulence, vehicular turbulence, and atmospheric turbulence. This phase starts at a distance where the internal turbulence levels of the plume were significantly dropped and the atmospheric eddies in the inertial subrange determine the plume growth [65]. This phase is assumed from the downwind distances of 6.5 m to 50 m. The value of 50 m will depend on the type of vehicles on the highway and could be as high as 150 m for large trucks, as pointed out by Yu et al. [66].
3. Dispersion Phase: The third flow regime (Dispersion Phase) is away from the vehicular wake area. and the plume dispersion is dominated by atmospheric turbulence (created by irregular air motions characterized by winds). In this phase, the plume's turbulence has dropped to a level that the growth of the plume is determined by the energy-containing eddies of atmospheric turbulence [65]. This phase is assumed from the downwind distances greater than 50 m away from the mobile source.

2.1.2 Turbulence Parametrization

σ_z is one of the critical components that affect estimations of the concentration of pollutants from the vehicular exhaust. It is important to incorporate the turbulence parameters related to the wake area created by mobile sources as well as the near field while developing a line source dispersion model near the roadway. Various studies indicate that the initial vertical plume spread (σ_{z0}), depends on the vehicular turbulence, wind velocity, width of the road, residence time, the height and width of the mobile sources within the turbulent mixing zone, and other factors [3], [67], [68] Table 2-1 shows that each of the methods proposed by different studies gives different values of σ_{z0} for different atmospheric conditions. Atmospheric stability influences the value of

σ_{z0}. Benson uses P–G stability classes [69] and the Wake area model by Yu et al. [66], AERMOD [70] uses the surface roughness length and the Monin–Obukhov length (L), and Chock [71] uses the Richardson Number to define stability class. Further details of the atmospheric stability are discussed in Section 3.1.

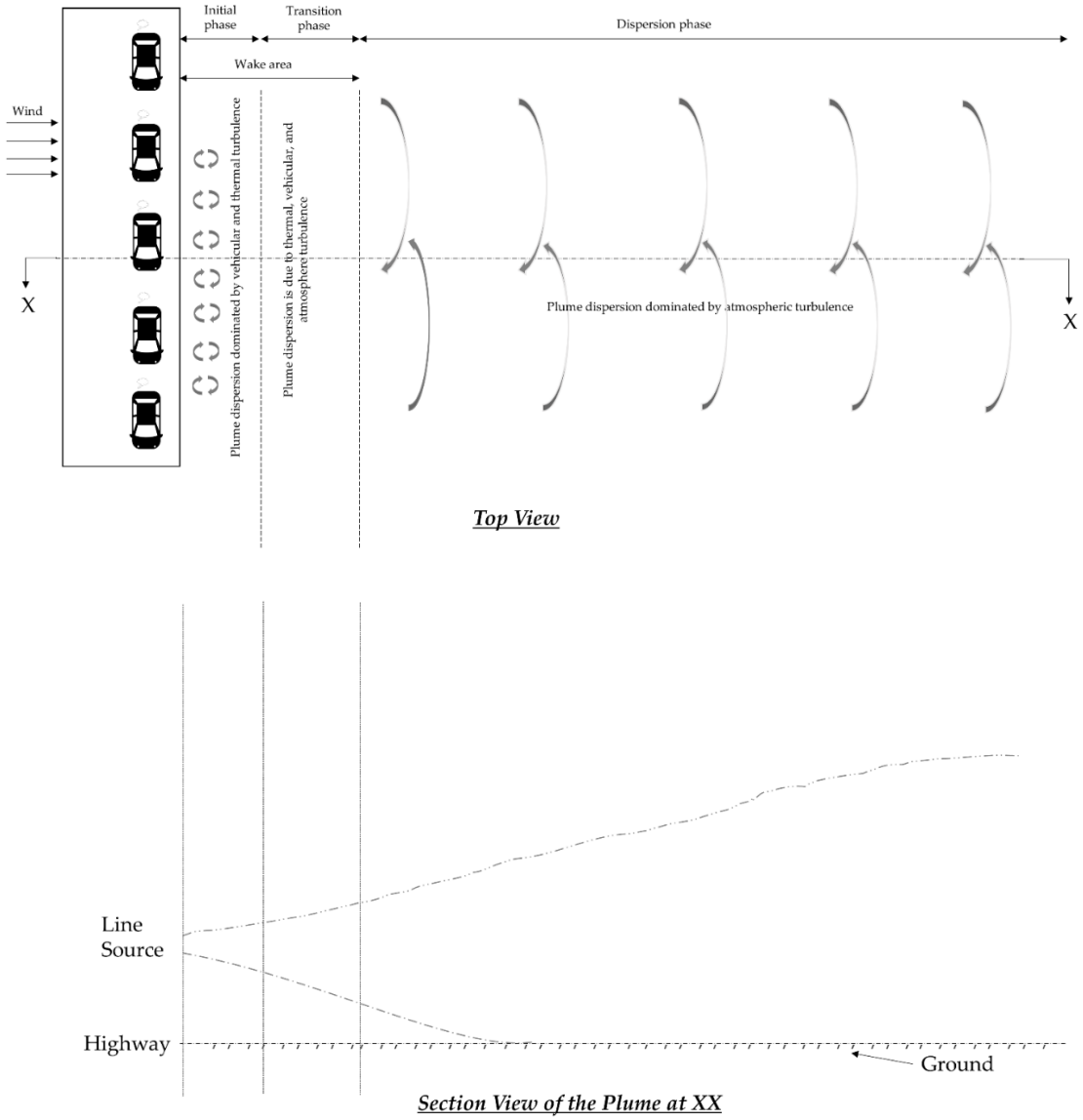

Figure 2-1: Flow regimes of a line source plume.

The width of the mixing zone (i.e., the Initial Phase) in the downwind direction was estimated by Benson as the width of the roadway and an additional 3 m [69]. For this study, it is

assumed that σ_{z0} is constant up to 6.5 m, which is based on the summation of the width of the road 3.5 m and 3 m from the edge of the road. The spread due to the wake turbulence is considered in the calculation of the σ_z in the TPT model by introducing the term σ_{z0} to the σ_z equation.

The procedure for calculating σ_{z0} from four different sources is given by Equations (2.1) to (2.4). Equation (2.1) was given by Chock et al. [71] to calculate the vertical dispersion coefficient using the residence time (2.75 s) [71], Equation (2.2) is given in the paper by Benson [69] by fitting the equation to the experimental data, Equation (2.3) is used in the AERMOD model by USEPA [70], and Equation (2.4) is given by Yu et al. [72].

$$\sigma_{z0} = 1.5 + \frac{\left(1.5 + \frac{0.5W}{U_e \sin\phi}\right)}{10} \tag{2.1}$$

where,

W is the width of the road (m),

U_e is the effective wind velocity (m/s),

θ is the wind angle concerning the road (°).

$$\sigma_z = a_1 x^{b_1} \tag{2.2}$$

where, a_1 and b_1 are the atmospheric diffusion coefficients

$$\sigma_{z0} = \frac{1.7H}{2.15} \tag{2.3}$$

where H is the height of the car.

$$\sigma_{z0} = \text{Effective wake area} \times \text{Vehicle density} \tag{2.4}$$

where the effective wake area is taken as the average vehicle height multiplied by the effective wake length.

The values of σ_{z0} obtained from the above four procedures for a test case are shown in Table 2-1 using the width of the road as 3.5 m. The wind velocity considered was 1.4 m/s, the wind angle concerning the road was taken as 90°, and the average height of the vehicle was H =

1.65 m. The effective wake length was considered as 9.3 m, and the vehicle density on the roadway was 0.125 vehicles/m [69], [71], [72].

Table 2-1: Comparison of σ_{z0} from different studies.

Study	σ_{z0}	Comment
Chock [71]	1.78	Thermal turbulence generated by hot vehicle exhaust that contributed to dispersion in near-roadway environments is considered within the mixing zone. Richardson Number (Ri) > 0.07, which is a stable atmospheric condition.
Benson [69]	1.98	Measured values of σ_z at various distances downwind from the roadway centerline under crosswind conditions were used to fit the curve. The intercept on the y-axis is the approximate value of σ_{z0}. The atmospheric stability conditions are: P-G classes A to E. P–G class E is considered for this value.
	2.78	P–G class F is considered for this value.
AERMOD [70]	1.32	Although RLINE is not a recommended regulatory model, EPA's PM hotspot guidance recommends setting σ_{z0} to the average vehicle height * 1.7/2.15 for all atmospheric conditions (no specific stability conditions are mentioned in the guide for this equation). AERMOD uses the surface roughness length and L to categorize the atmospheric stability.
Wake area model by Yu et al. [66], [72]	1.92	σ_z was parameterized based on vehicle wake, vehicular density, and vehicle types. Assuming that each vehicle provides an independent vehicle wake indicates there is no interaction between vehicles, and the mixing of the pollutant is uniform throughout the vehicle fleet. Atmospheric stability classes were neutral or stable.

The formulation for the vertical plume spread for the different flow regimes in the TPT model is provided in Table 2-2. The vertical dispersion near the mobile source in the Initial Phase is σ_{z0}. The TPT model adopted the formulation for σ_{z0} given by Chock, i.e., Equation (2.1). Based on the study conducted by Yu et al [66] the value of σ_{z0} is considered to be constant until 6.5 m from the mobile source. The formulation for the vertical spread of the plume for stable and unstable conditions from 6.5 m to 50 m downwind distance (Transition Phase) and beyond 50 m downwind distance (Dispersion Phase) for low-level sources is based on theoretical considerations and experimental data and is given by Snyder et al. [61] is presented in Table 2-2. The vehicles in motion on highways create turbulence which can increase the mixing of air pollutants and ambient air in the wake area behind the vehicles. There is a necessity to consider the additional spread due to the vehicles (m_t) on highways to maintain the accuracy of the model-predicted emissions [66]. The vertical spread in the TPT model incorporates the additional spread m_t due to the turbulence

created by moving vehicles in the transition phase. The magnitude of additional spread due to the vehicles is considered to be equivalent to the initial vertical spread in the wake area in the TPT model. The formulation for m_t is presented in Equation (2.10).

Table 2-2: Vertical plume spread formulation for different flow regimes in the TPT model

Flow Regime	**Vertical Plume Spread (σ_z) Formulation**	**Equation No.**	**Downwind Distance (x)**	**Atmospheric Stability**
Initial Phase	σ_{z0}	(2.5)	$\leq$ 6.5 m	Stable and Unstable Atmosphere Condition
Transition Phase	$\frac{a\,u_* x}{U_e\left(1+b_s \frac{u_*}{U_e}\left(\frac{x}{L}\right)^{\frac{2}{3}}\right)} + m_t$	(2.6)	6.5 m $\leq$;& $\leq$ 50 m	Stable Atmosphere Condition
	$a\frac{x\,u_*}{U_e}\left(1 + b_u \frac{u_*}{U_e}\frac{x}{L}\right) + m_t$	(2.7)	6.5 m $\leq$;& $\leq$ 50 m	Unstable Atmosphere Condition
Dispersion Phase	$\frac{a\,u_* x}{U_e\left(1+b_s \frac{u_*}{U_e}\left(\frac{x}{L}\right)^{\frac{2}{3}}\right)}$	(2.8)	50 m $\leq$	Stable Atmosphere Condition
	$a\frac{x\,u_*}{U_e}\left(1 + b_u \frac{u_*}{U_e}\frac{x}{L}\right)$	(2.9)	50 m $\leq$	Unstable Atmosphere Condition

where

$U_{\bar{z}}$ is the wind velocity at the reference height $\bar{z}$,

z_s is the height from the ground surface to the tailpipe of the mobile source, and

w_* is the convective velocity scale.

$$m_t = 1.5 + \frac{\left(1.5+\frac{0.5W}{U_e \sin\phi}\right)}{10} \quad (2.10)$$

The formulation for $U_{\bar{z}}$, U_e and $\bar{z}$ are provided in Equations (4.2), (2.11), and (2.13), respectively. Equations (2.11), (2.12), and (2.13) are considered by Snyder et al. [43]. The standard deviation of the lateral wind component (σ_v) is calculated using Equation (2.12). The best fit values for the empirical constants (a, b_s, and b_u) for TPT model are selected from a trial-and-error process (See Table 2-3).

$$U_e = \sqrt{2\sigma_v{}^2 + U_{(z)}^2} \quad (2.11)$$

$$\sigma_v = \sqrt{(0.6w_*)^2 + (1.9u_*)^2} \quad (2.12)$$

$$\bar{z} = \sigma_z \sqrt{\frac{2}{\pi}} \exp[-\frac{1}{2}(\frac{z_s}{\sigma_z})^2] + z_s \operatorname{erf}\left(\frac{z_s}{\sqrt{2}\sigma_z}\right) \quad (2.13)$$

For the current model for stable atmospheric conditions, $\sigma_v = 1.9u_*$ because the w_* value for stable conditions is approximately 0 (note that the heat flux is either very small or zero). For convective conditions, the value of w_* is given by Equation (2.14) by Akula et al.[73]:

$$w_* = 1.12 \times 10^{-3} z_i \quad (2.14)$$

The existing models use P-G curves to calculate the dispersion coefficients [19]. The dispersion coefficient (σ_z) are typically a function of downwind distance, atmospheric stability, release height, surface roughness, averaging time, and other atmospheric variables [72], [74], [75]. σ_z is revised as follows instead of using a P-G curve for the TPT model. A summary of the values of empirical coefficients for stable and unstable atmospheric conditions for the TPT model are given in Table 2-3. The empirical coefficients (a, b_s and b_u) in the dispersion coefficient expressions were adjusted based on the trial-and-error method to achieve the maximum accuracy at respective atmospheric stability using the curves reported by Benson [69] and Chock [71] for mobile sources. This process involves the computation of σ_{z0} (Initial Phase) using Equation (2.1) in the first step. Then the computation of σ_z is performed considering the respective equations for Transition Phase (Equation 2.6 and 2.7) and Dispersion Phases (Equation 2.8 and 2.9) until 300 m downwind distance from the mobile source. Numerous iterations were performed by varying the values of a, b_s, and b_u to generate σ_z curves with incremental downwind distance (up to 300 m). The base values (i.e., a=0.57 (both stable and unstable atmospheric conditions), b_s=3, b_u=1.5) to initiate the iteration was considered from the Snyder et al. [34], [61]. The numerical values are varied (increased or decreased) to observe the trends (increase or decrease) of σ_z curves. The σ_z curves of TPT model are compared with the reported curves by Benson [69] and Chock [71]

for the mobile sources. During simultaneous iteration and comparison, the values of coefficients are selected from the best-fit curves that achieved the maximum accuracy at respective (stable and unstable) atmospheric stability conditions. These values are the best fit empirical coefficients for the TPT model (See Table 2-3). Since the considered datasets in this study have the observed concentrations of pollutants at downwind distances of less than 300 m, the numerical values considered for the empirical coefficients (presented in Table 2-3) are consistent. Note: The empirical coefficients for the larger downwind distances (> 300 m) can be generated by following the same approach while considering the TPT model to predict ground-level concentrations of pollutants from the mobile sources.

Table 2-3: Empirical coefficients used TPT model for different atmospheric stability conditions**.**

Atmospheric Stability	**Empirical Coefficient**	**Value**
Stable conditions	a	0.55
	b_s	2.50
Unstable conditions	a	0.50
	b_u	1.90

Chapter 3

Field Data

3.1 Atmospheric stability

Atmospheric stability influences the value of the plume spread in the horizontal as well as vertical direction. P-G stability is the most common method used to categorize atmospheric turbulence in the earlier literature. It is based on wind speed, incoming solar radiation (daytime), and cloud cover (nighttime) [3].

Other methods have been used to define stability class (See Table 3-1) including Monin-Obukhov Length (L), Richardson Number (Ri), temperature gradient (dT/σ_z), and standard deviation of vertical wind direction ($\sigma_\emptyset$) [3], [76].

The ranges of atmospheric stability indicators are given in Table 3-1. The atmospheric stability of the field data is categorized based on Table 3-1 depending upon the available information from the field study. The model predictions are simulated using the generic expressions discussed in Section 7.1 for stable and unstable atmospheric conditions and compared with the observed concentration values of the gaseous and particulate pollutants in the field.

Table 3-1: Typical values of five stability indicators under different atmospheric conditions.

Atmospheric Stability	**Pasquill Class** [3]	**Monin Obukhov Length (m)** [76]	**Richardson Number (Ri)** [76]	**Temperature Gradient (Degree Centigrade/100m)** [3]	**Standard Deviation of Vertical Wind Direction ($\sigma_\emptyset$) (Degree)** [3]
Extremely unstable conditions	A	−2 to −3	−0.86	≤−1.9	≤12
Moderately unstable conditions	B	−4 to −5	≥−0.86 to <−0.37	−1.9 to ≤−1.7	≥10 to <12
Slightly unstable conditions	C	−12 to −15	≥−0.37 to <−0.10	−1.7 to ≤−1.5	≥7.8 to <10
Neutral conditions	D	Infinite	≥−0.10 to <0.053	−1.5 to ≤−0.5	≥5 to <7.8
Slightly stable conditions	E	35 to 75	0.053 ≤ to <0.134	−0.5 to ≤−1.5	≥2.4 to <5
Moderately stable conditions	F	8 to 35	0.134≤	1.5 to ≤4.0	<2.4
Extremely Stable	G	-	-	>4.0	-

3.2 Field Data

The data considered in this study are from the experiments reported in the literature. A total of four of the data sets collected were used in the evaluation of considered dispersion models. CALTRANS99 (Data 1), Idaho Falls Tracer Experiment (Data 2), Raleigh NO experiment (Data 3), Hyderabad field study (Data 4). Data 1, 2, and 3 were the field studies conducted to evaluate the RLINE model being incorporated in the AERMOD regulatory model by USEPA [17], [61]. The Q-Q plots which represent the distribution of data are represented in Figures 3-1 to Figure 3-22. These are cumulative frequency distributions that provide a graphical characterization of the distribution of observed data. They provide a visual characterization of how the observations are spread for the central value. In these plots, the sample quantiles indicate the concentration values ($\mu g/m^3$) and theoretical quantiles represent the data distribution with a central value of 0.

3.2.1 CALTRANS Data

The CALTRANS highway 99 Tracer experiment was conducted in the 1980s in California near Highway 99 in two directions for the northbound (NB) and southbound (SB) lanes to measure SF_6. The emission factors for SF_6 are slightly different for the NB and SB. The line sources in NB and SB lanes were specified with a unit emission rate. Nearly 35,000 vehicles were observed in traffic daily. Since the line sources were long and the emissions were uniform along the lines, only one median receptor was modeled. The terrain is fairly flat. The samplers were placed 1 m above the ground level. The concentrations of SF_6 were measured at 0 m, 32.14 m, 64.28 m, and 128.56 m downwind distances in both North and South directions. The wind speed ranges are observed to be 0.2 m/s–6 m/s. The atmospheric stability provided was based on P-G stability categories [17].

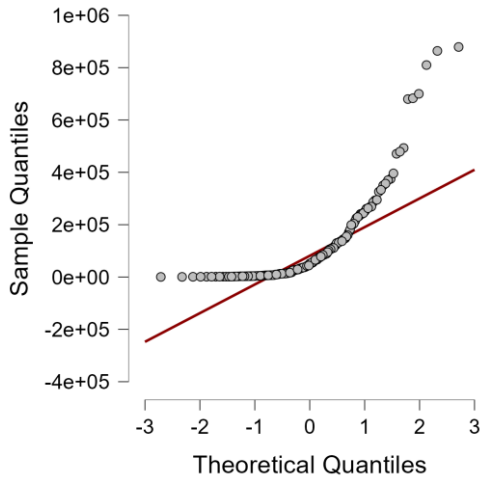

Figure 3-1: Q-Q plot of the CALTRANS data (SF_6) for stable atmospheric conditions

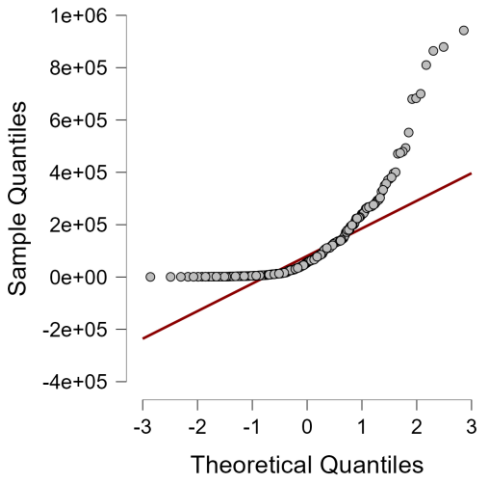

Figure 3-2: Q-Q plot of the CALTRANS data (SF_6) for unstable atmospheric conditions

3.2.2 Idaho Falls Data

The Idaho Falls Tracer experiment was conducted to measure SF_6 in 2008 at Idaho Falls, a city in Idaho. As part of this study, two simultaneous experiments were conducted, one had a barrier downwind of the line source to represent a roadside sound wall, and the other had no barrier. In this analysis, we only use the data from the no-barrier experiment to test the model

concentrations for a flat roadway case. The line source in the experiment was 54 m long, the field results have been processed to represent what would have been measured had the source been infinitely long. Therefore, the input source is very long (1 km) and only one receptor is only modeled at each perpendicular downwind distance. The source is modeled with a unit emission rate because the measured emission rates are slightly different for each day. The emission rates for day 1, 2, 3, and 5 are 0.05 g/s, 0.04 g/s, 0.03 g/s, and 0.03 g/s respectively. The surface meteorology file contains only the 15 min periods where the wind direction was within 25 degrees of perpendicular to the line source. Additionally, day 4 is omitted completely because the winds were rather erratic, and the receptor grid was not always downwind of the line source. The SF_6 is measured in this field experiment for 18 m, 36 m, 48 m, 66 m, 90 m, 120 m, and 180 m downwind distances [17].

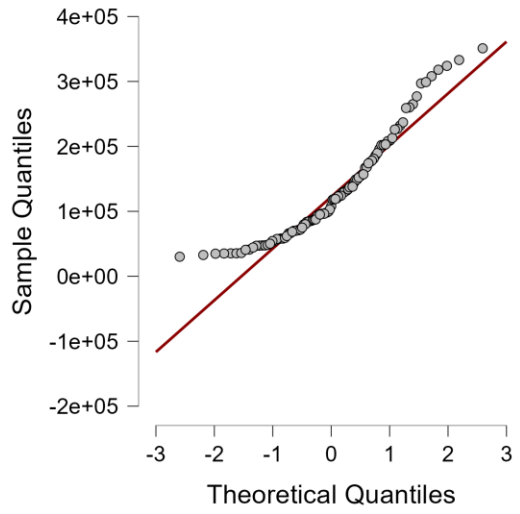

Figure 3-3: Q-Q plot of the Idaho Falls data (SF_6) for stable atmospheric conditions

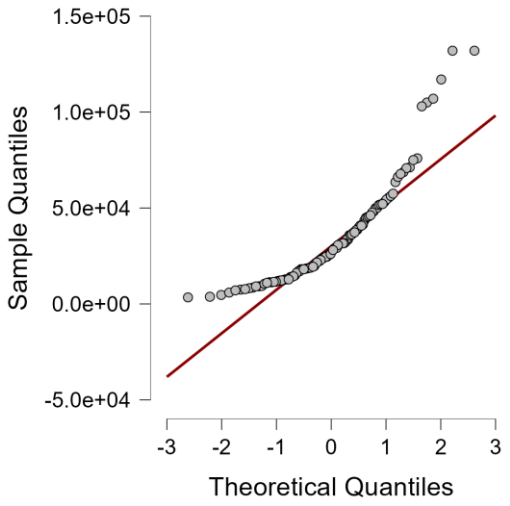

Figure 3-4: Q-Q plot of the Idaho Falls data (SF_6) for unstable atmospheric conditions

3.2.3 Raleigh Data

The Raleigh 2006 experiment was conducted to measure NO in Raleigh, North Carolina. The line sources were run with unit emission rates so they can be multiplied by the traffic and

emission factor to determine the modeled concentration. The line source was 1 km long, and 8 lanes were used (4 lanes on each side of the median).

The emission factor used was 0.5 g/vehicle/km from Venkatram 2007. The data are available for every 10 min of air [59]. In the same experiments the concentrations of $PM_{0.1}$, $PM_{2.5}$, and PM_{10} were measured at 5m, 20m, 50m, 100m, and 300m downwind distances from the road. The average time of sampling frequency was 24 hours [77].

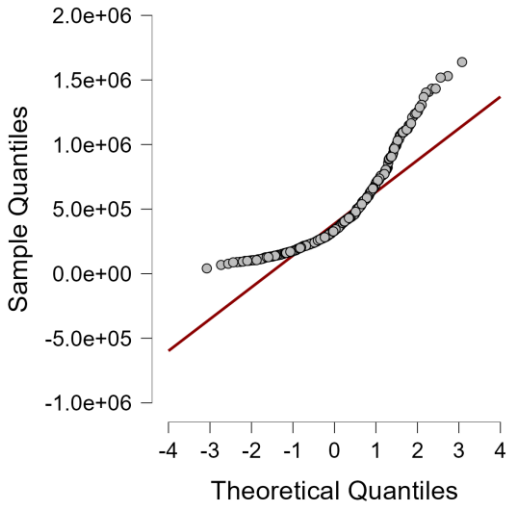

Figure 3-5: Q-Q plot of the Raleigh data (NO) for stable atmospheric conditions

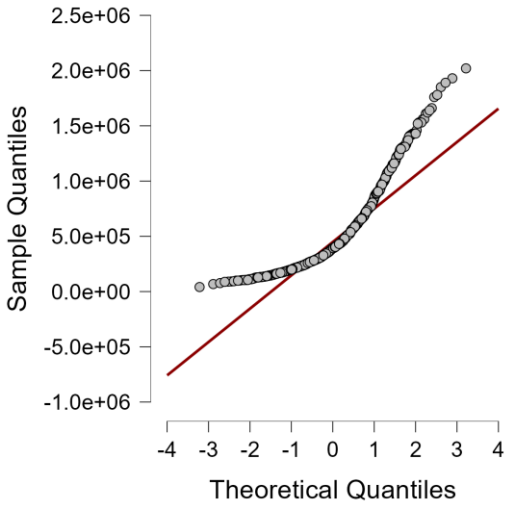

Figure 3-6: Q-Q plot of the Raleigh data (NO) for unstable atmospheric conditions

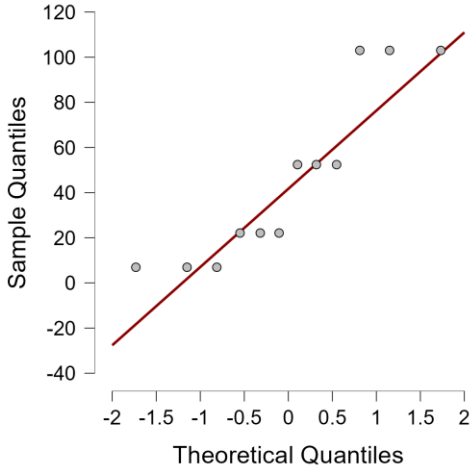

Figure 3-7: Q-Q plot of the Raleigh data (PM between 10 and 2.5 µm) for stable atmospheric conditions

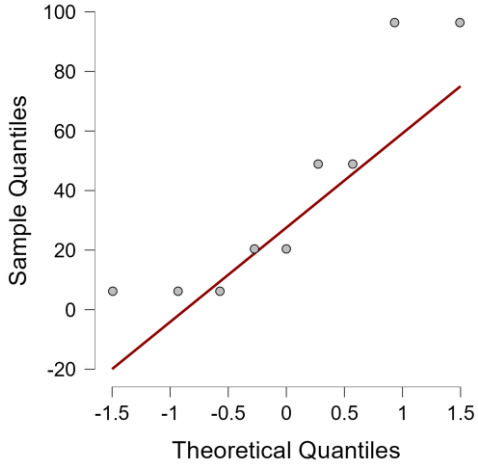

Figure 3-8: Q-Q plot of the Raleigh data (PM between 2.5 and 0.1 µm) for stable atmospheric conditions

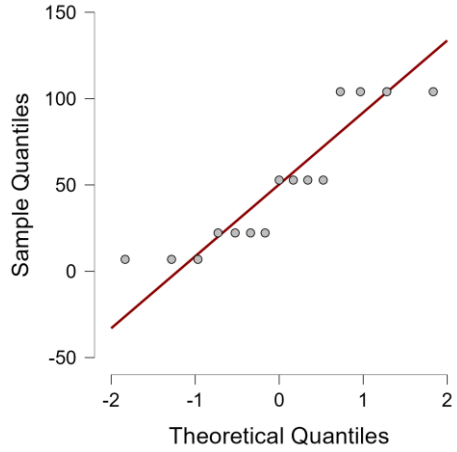

Figure 3-9: Q-Q plot of the Raleigh data (PM < 0.1 µm) for stable atmospheric conditions

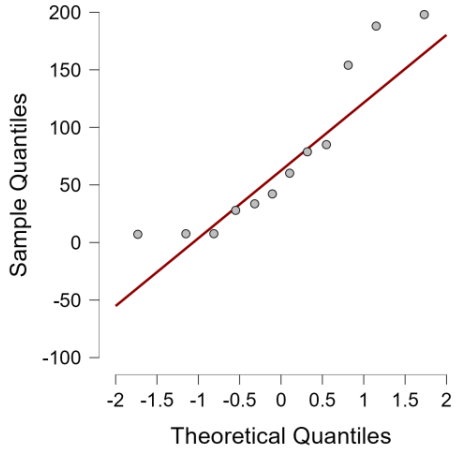

Figure 3-10: Q-Q plot of the Raleigh data (PM between 10 and 2.5 µm) for unstable atmospheric conditions

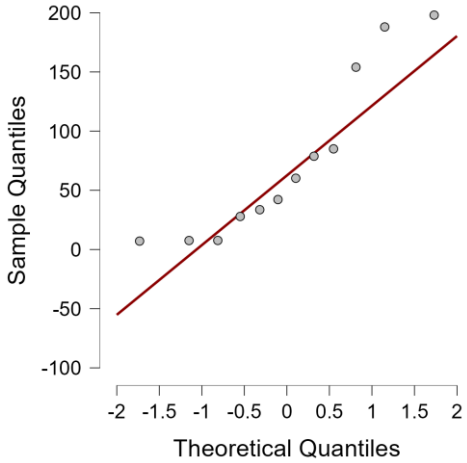

Figure 3-11: Q-Q plot of the Raleigh data (PM between 2.5 and 0.1 µm) for unstable atmospheric conditions

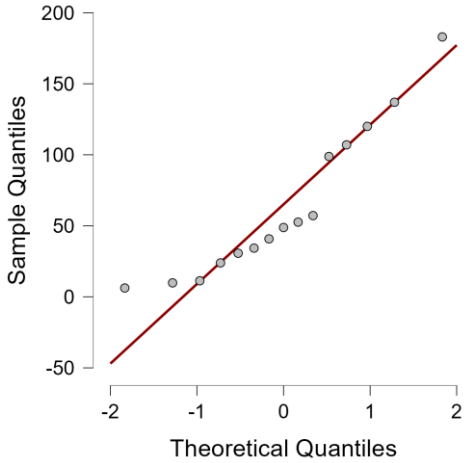

Figure 3-12: Q-Q plot of the Raleigh data (PM < 0.1 µm) for unstable atmospheric conditions

3.2.4 Hyderabad Data

The data used in this study were collected by Madiraju (under the direction of PVS Gopi Raghunadh and K Ravi Kumar) in Hyderabad, India in 2016 [78]. The concentrations of $PM_{2.5}$ and PM_{10} were collected from January to April. The concentrations of $PM_{2.5}$ and PM_{10} were measured at 3.5 m, 7 m, 10.5 m, and 14 m downwind distances from the traffic intersections using a dust sampler. The data were collected at five major traffic intersections in the city at Balanagar, Jeedimetla, Zoo Park, MGBS, and JNTU. The sampling readings were analyzed in the VNR VJIET

environmental laboratory. The atmospheric conditions varied from extremely unstable to moderately unstable during the daytime of measurement. The readings were collected at around noon every day for 90 days (January 2nd to April 1st, 2016) continuously. Gaseous pollutants were also measured during these experiments and are published by Madiraju et al [78] in 2020.

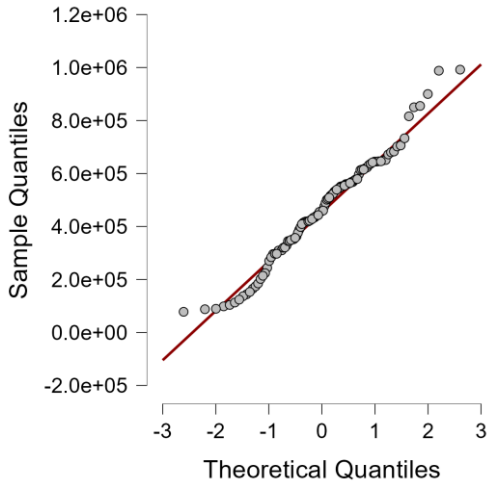

Figure 3-13: Q-Q plot of the Hyderabad data (CO_2) for stable atmospheric conditions

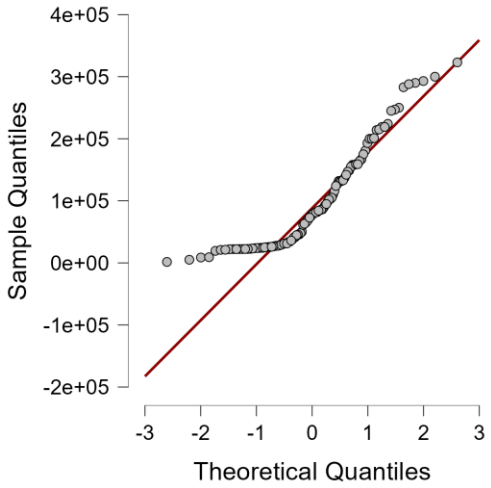

Figure 3-14: Q-Q plot of the Hyderabad data (CO_2) for unstable atmospheric conditions

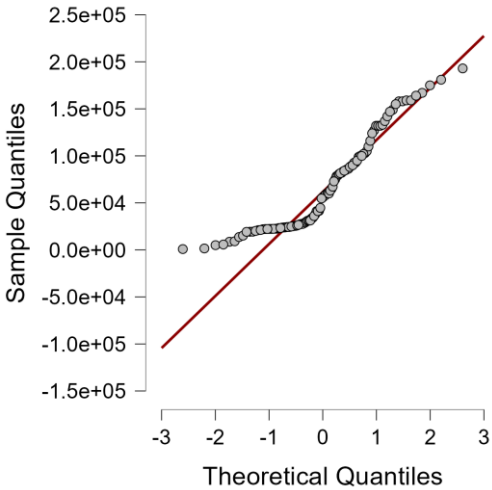

Figure 3-15: Q-Q plot of the Hyderabad data (NO_2) for stable atmospheric conditions

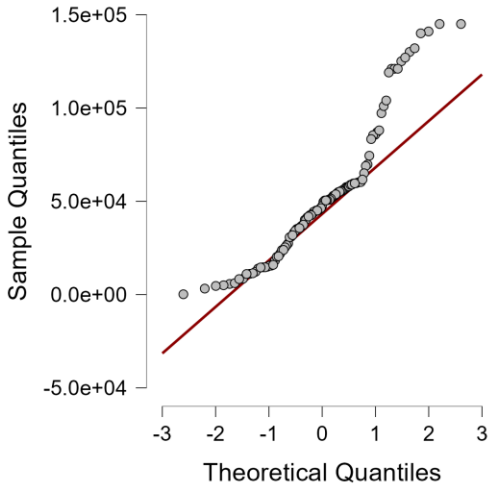

Figure 3-16: Q-Q plot of the Hyderabad data (NO_2) for unstable atmospheric conditions

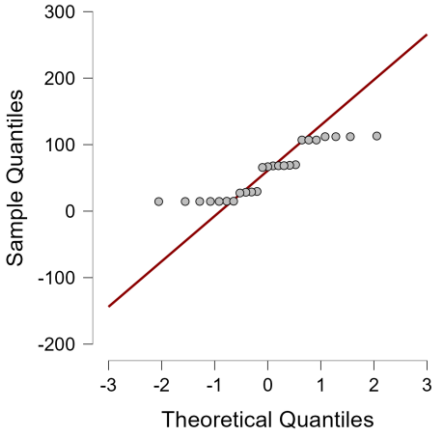

Figure 3-17: Q-Q plot of the Hyderabad data (PM >10 µm) for stable atmospheric conditions

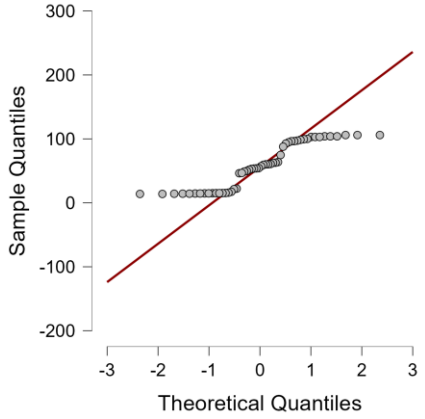

Figure 3-18: Q-Q plot of the Hyderabad data (PM between 10 and 2.5 µm) for stable atmospheric conditions

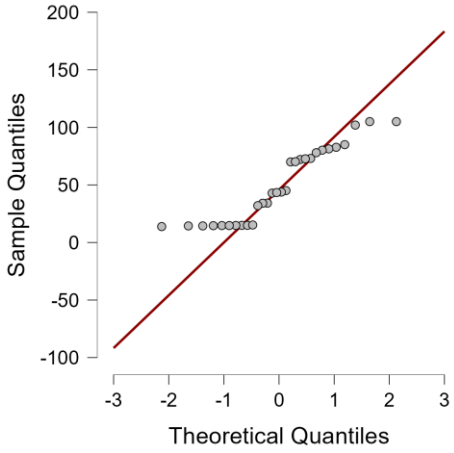

Figure 3-19: Q-Q plot of the Hyderabad data (PM <2.5 µm) for stable atmospheric conditions

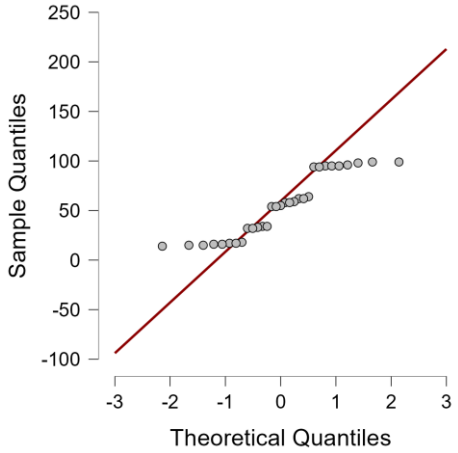

Figure 3-20: Q-Q plot of the Hyderabad data (PM >10 µm) for unstable atmospheric conditions

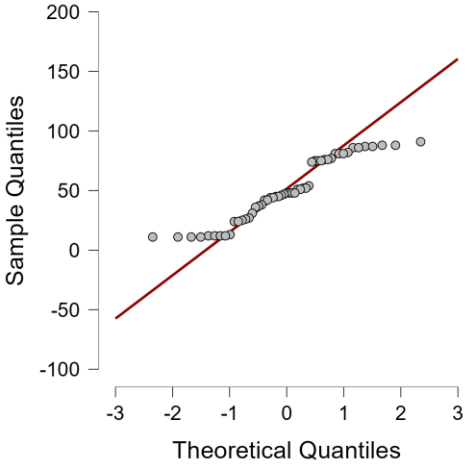

Figure 3-21: Q-Q plot of the Hyderabad data (PM between 10 and 2.5 µm) for unstable atmospheric conditions

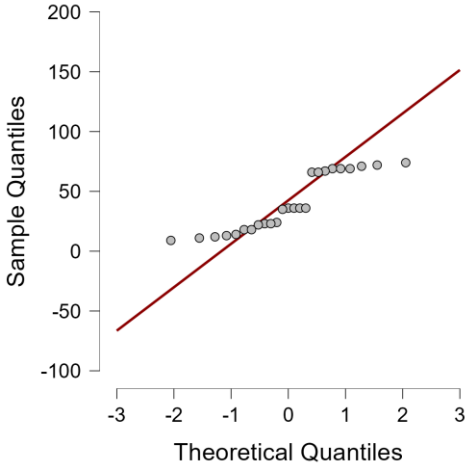

Figure 3-22: Q-Q plot of the Hyderabad data (PM <2.5 µm) for unstable atmospheric conditions

Chapter 4

Development and Evaluation of a Line Source Analytical Dispersion Model (SLINE 1.1)

4.1 Methodology

4.1.1 Development of SLINE 1.1 model

The basic approach to developing the SLINE 1.1 model was the incorporation of wind shear during the dispersion from a line source using the convective–diffusion equation. It is important to consider the variation of the wind velocity magnitude near the ground for the dispersion of pollutants released from the tailpipe of mobile sources. This physical phenomenon was incorporated in the derivation of the dispersion and transport equation for the SLINE 1.1 model. The model was based on the analytical solution of the convective diffusion equation of a line source given in the book by Sutton, O.G. [10].

The assumptions used in deriving the equation were:

(i) The wind direction is always perpendicular to the highway.

(ii) The dispersion is of a non-fumigation type.

(iii) The velocity profile with height above ground level is assumed to be the same for all downwind distances.

(iv) A power law profile is assumed for the velocity, i.e., the magnitude of the wind velocity near the ground level changes rapidly and follows a power law.

(v) The eddy diffusivity profile is a conjugate of velocity profile as given in equation (4.3) below; and

(vi) The emission rate is constant.

The convective–diffusion equation representing the dispersion from mobile sources [10] is given as:

$$u(z)\frac{\partial C}{\partial x} = \frac{\partial}{\partial x}\left(K(z)\frac{\partial C}{\partial x}\right) \tag{4.1}$$

where,

C is the concentration of pollutants at a point (x, z),

x is the downwind distance,

z is the vertical height of the receptor above the ground, and

u and K are the wind velocity and eddy diffusivity at the vertical height z, respectively. The profiles of wind velocity and eddy diffusivity are given by Equations (4.2) and (4.3):

$$u = u_1\left(\frac{z}{z_1}\right)^m \tag{4.2}$$

$$K = K_1\left(\frac{z}{z_1}\right)^n \tag{4.3}$$

where u_1 and K_1 are the wind velocity and eddy diffusivity at a reference height z_1, respectively. m is the exponent of the power law velocity profile, and n is the exponent for the eddy diffusivity profile. Note that $n = 1 - m$ to satisfy assumption (v) given above, and the value of m lies between 0 and 1.

The stability parameter (s) is calculated based on m and n using Equation (4.4):

$$s = \frac{(m+1)}{(m-n+2)} \tag{4.4}$$

The analytical solution of Equation (4.1) to calculate the concentration of pollutants at any downwind distance when the wind and eddy diffusivity profiles are given by Equations (4.2) and (4.3) [10] is given by Equation (4.5):

$$C_{(x,z)} = \frac{q}{u_1 \gamma(s)} \left[\frac{u_1}{(m-n+2)^2 K_1 x}\right]^s \exp\left[-u_1 \frac{z^{m-n+2}}{((m-n+2)^2 K_1 x)}\right] \quad (4.5)$$

where q is the emission rate of the mobile source per unit length, and $\gamma(s)$ is the lower incomplete gamma function of s.

The value of u_1 is based on the field measurement, and K_1 is computed using Equation (4.6) used by Rao et al. [15], [26] and Nimmatoori and Kumar [79]:

$$K = \left(\frac{\sigma_z^2 u}{2x}\right) \quad (4.6)$$

where, σ_z is the standard deviation of concentration in the z-direction.

Equations (4.5) and (4.6) are as follows if the wind is not perpendicular to the highway:

$$C_{(x,z)} = \frac{q}{u_1 \sin\theta \, \gamma(s)} \left[\frac{u_1}{(m-n+2)^2 K_1 x}\right]^s \exp\left[-u_1 \frac{z^{m-n+2}}{((m-n+2)^2 K_1 x)}\right] \quad (4.7)$$

$$K = \left(\frac{\sigma_z^2 u \sin\theta}{2x}\right) \quad (4.8)$$

Where θ is the angle between the wind direction and the line source.

Equations (4.8) and (4.3) indicate that K as well as K_1 are a function of downwind distance x. However, the derivation of Equation (4.1) assumes that the K profile is constant as the plume moves downwind. It is assumed during the application of Equation (4.7) that the concentration is predicted in the SLINE 1.1 model at a downwind distance by updating the value of K_1 in the model for that downwind distance. It is expected that this approach will improve the model performance.

The vertical spread of the plume for stable and unstable conditions beyond 50 m downwind distance (Dispersion Phase) for low-level sources is based on theoretical considerations and experimental data and is given by Snyder et al. [61] as Equations (2.8) and (2.9).

Expression of K_1 (See Equations 4.9 and 4.10) can be obtained as follows by substituting Equation (2.8) for the stable condition and Equation (2.9) for the unstable condition in Equation (4.6) with the help of Equation (4.2):

$$K_1 = \frac{\sigma_z^2\, u_1 \mathrm{Sin}\theta}{2x} = \left[\frac{a\, u_* x}{\left(U_e + b_s u_* \left(\frac{x}{L}\right)^{\frac{2}{3}}\right)} + m_t\right]^2 \frac{u_1 \mathrm{Sin}\theta}{2x} \tag{4.9}$$

$$K_1 = \frac{\sigma_z^2\, u_1 \mathrm{Sin}\theta}{2x} = \left[\frac{a\, u_* x}{U_e}\left(1 + b_u \frac{u_*}{U_e}\frac{x}{L}\right) + m_t\right]^2 \frac{u_1 \mathrm{Sin}\theta}{2x} \tag{4.10}$$

The expression for concentration for stable conditions is:

$$C_{(x,z)} = \frac{q}{u_1 \mathrm{Sin}\theta\, \gamma(s)} \left[\frac{2}{\left[\frac{a\, u_* x}{U_e + b_s u_* \left(\frac{x}{L}\right)^{\frac{2}{3}}} + m_t\right]^{2\,(m-n+2)^2}}\right]^s \exp\left[-\frac{2\, z^{m-n+2}}{\left[\frac{a\, u_* x}{U_e + b_s u_* \left(\frac{x}{L}\right)^{\frac{2}{3}}} + m_t\right]^{2\,(m-n+2)^2}}\right] \tag{4.11}$$

The expression for unstable conditions is:

$$C_{(x,z)} = \frac{q}{u_1 \mathrm{Sin}\theta\, \gamma(s)} \left[\frac{2}{\left[\frac{a\, u_* x\left(1 + b_u \frac{u_* x}{U_e L}\right)}{U_e} + m_t\right]^{2\,(m-n+2)^2}}\right]^s \exp\left[-\frac{2\, z^{m-n+2}}{\left[\frac{a\, u_* x\left(1 + b_u \frac{u_* x}{U_e L}\right)}{U_e} + m_t\right]^{2\,(m-n+2)^2}}\right] \tag{4.12}$$

Equations (4.19) and (4.20) represent the final developed concentration equations for the SLINE 1.1-line source dispersion model for the calculation of downwind concentrations under stable and unstable atmospheric conditions, respectively. Note that the $m_t = 0$ in the dispersion phase because the additional effect due vehicle after the wake area is negligible.

4.2 Statistical Model Evaluation

The quantitative performance of the model could be studied by computing the statistical indicators suggested in the literature over the last five decades. The performance measures of the SLINE 1.0 model used include MB (µg/m^3), FB, NMSE, r, MG, VG, and Fa2. These statistical

performance measures are based on the suggestions given in the literature [44], [47], [48], [80]–[85]. If Cp - Model Predicted Concentration, Co - Observed Concentration then the model formulation is as follows:

(a) Fractional Bias: The FB is a ratio between the difference of the average values and the summation of the average values of the observed and predicted concentration of pollutants, multiplied by two. It is a dimensionless number. In the ideal case, the value of FB is equal to zero. However, if its value is between −2.0 and +2.0, then the model can be referred to as better performing. If the FB value is less than −0.67, then the model is underpredicting, and if the value is less than −2.0, then the model is extremely underpredicting. If the value is higher than +0.6, then the model is overpredicting, and if the value is higher than +2.0, then the model is extremely overpredicting. The value of FB is influenced by infrequently occurring high concentration values [86], [87].

$$\mathrm{FB} = 2\left(\frac{\overline{C_o} - \overline{C_p}}{\overline{C_o} + \overline{C_p}}\right) \tag{4.13}$$

(b) Normalized Root Mean Square Error: The scatter in the data collected is then normalized by the product of the average values of observed and predicted concentrations of pollutants. In the ideal case, the value of NMSE is zero. A smaller NMSE value denotes that the model is better performing. NMSE values cannot be used for accessing the model predicted concentrations that are over- or underpredicted [86], [88].

$$\mathrm{NMSE} = \frac{\overline{(C_p - C_o)^2}}{\overline{C_o}.\overline{C_p}} \tag{4.14}$$

(c) Correlation Coefficient: The correlation coefficient, r, gives an indication of the linear relationship between the predicted and observed values. r is insensitive to either an additive or a multiplicative factor. A perfect r = 1 is necessary, but not a sufficient condition for a perfect model [86], [89].

$$\mathbf{r} = \frac{\mathbf{n}(\Sigma \mathbf{C_o C_p}) - (\Sigma \mathbf{C_o})(\Sigma \mathbf{C_p})}{\sqrt{[\mathbf{n}\Sigma \mathbf{C_o^2} - (\Sigma \mathbf{C_o})^2]\left[\mathbf{n}\Sigma \mathbf{C_p^2} - (\Sigma \mathbf{C_p})^2\right]}} \quad (4.15)$$

where n is the number of data points, Σ is the summation notation, and 'i' represents the i^{th} value of concentration.

(d) Geometric Mean Bias: The MG value is reliable when the magnitude of the observed and predicted concentrations of the pollutants varies significantly. Extremely low values of concentrations also have strong influences on the MG value. In the ideal case, the MG value is equal to 1. If the MG value is equal to +0.5, then the model is underpredicting, and if the value is equal to +2.0, then the model is overpredicting [86], [90].

$$\mathrm{MG} = \exp(\overline{\ln \mathrm{C_o}} - \overline{\ln \mathrm{C_p}}) \quad (4.16)$$

(e) Geometric Variance: In ideal cases, VG values are equal to 1. Similar to MG, the VG value also shows similar properties of performance measures except in the identification of over- and underprediction [86], [91].

$$\mathrm{VG} = \exp \overline{(\ln \mathrm{C_o} - \ln \mathrm{C_o})^2} \quad (4.17)$$

(f) The factor of two: Fa2 is defined as the percentage of predictions within a factor of two of the observed values. The ideal value for the factor of two is 1 (100%). Fa2 is the most robust statistical indicator. The value of Fa2 should be greater than 0.8 for an acceptable air quality model [86].

It is always recommended to consider multiple performance measures to accurately assess models. The distribution of each variable considered determines the significance of the model performance measure. Characteristics of the statistical indicators for better performing model are presented in Table 4-1.

For model evaluation, model-predicted concentrations are evaluated against observed concentrations for different field studies. Observed concentrations are directly measured by

instruments. It is important to recognize that different degrees of uncertainty are associated with different types of observed concentrations. Furthermore, it is important to define how the predicted concentrations are to be compared with the observed concentrations.

Table 4-1: Characteristics of the statistical indicators for a better performing model

Statistical Indicator	**MB ($\mu g/m^3$)**	**FB**	**NMSE**	**r**	**MG**	**VG**	**Fa2**
Ideal Values	0	0	0	1	1	1	1
Suggested range from the literature	Minimal Mean error	$-0.5 \leq FB \leq +0.5$	Smaller values	Close to unity	$0.75 \leq MG \leq 1.25$	$0.75 \leq VG \leq 1.25$	$0.80 \leq Fa2$

Table 4-2: Model evaluation results for the SLINE 1.1 model

Statistical Indicator	**MB ($\mu g/m^3$)**	**FB**	**NMSE**	**r**	**MG**	**VG**	**Fa2**
CALTRANS stable conditions	12.34	0.11✓	0.05✓	0.88✓	0.89✓	1.20✓	0.84✓
CALTRANS unstable conditions	-14.97	−0.16✓	0.14✓	0.87✓	1.28	1.13✓	0.85✓
Idaho Falls stable conditions	6.75✓	0.15✓	0.05✓	0.75✓	0.88✓	1.22✓	0.81✓
Idaho Falls unstable conditions	-3.64✓	−0.11✓	0.02✓	0.87✓	1.11✓	1.11✓	0.92✓
Raleigh stable conditions	15.02	0.14✓	0.04✓	0.80✓	0.86✓	1.22✓	0.83✓
Raleigh unstable conditions	-15.72	−0.12✓	0.03✓	0.85✓	1.13✓	1.24✓	0.87✓
Hyderabad stable conditions	13.02	0.13✓	0.32✓	0.81✓	1.26	1.32	0.84✓
Hyderabad unstable conditions	-13.56	-0.19✓	0.17✓	0.82✓	1.21✓	1.24✓	0.88✓

The evaluation results for SLINE 1.1 using the CALTRANS, Idaho Falls, Raleigh, and Hyderabad data as model inputs for the statistical indicators mentioned earlier are given in Table 4-2. The numerical result gives a quantitative relationship between observed and predicted values. The values with '✓' denote the interpretation of statistical criteria which were satisfied by the suggested range from the literature for a better performing model.

The MB values of the model indicate that there is a minimal error of 3% to 16% is observed for SLINE 1.1 for overall predictions. Since the ideal value of 0 is very difficult to achieve, a minimal error of less than 10% is acceptable for better performing model. If the values of FB are between -0.5 and 0.5 then the model is better performing [86]. Since the values of FB ranging from -0.19 to 0.15 are between -0.5 and 0.5 indicates that SLINE 1.1 is a better performing model. Based

on FB results it can be said that the model is over-predicting in sable conditions and slightly under-predicting in unstable conditions. It should be noted that there may be an influence of infrequently occurring high concentration values on the FB. The values of NMSE values are close enough to 0 which indicates that the model is performing better [88]. All the NMSE results are less than unity indicating SLINE 1.1 is better performing. According to the 'r' values the predicted concentrations are 75% to 88% correlated to the observed concentrations, which indicates the accuracy of the model. If the MG and VG values are between 0.75 and 1.25 then the model is a better performing model [86]. Considering MG, the model is performing better for 6 out of 8 data sets, and Considering VG the model is performing better for 7 out of 8 data sets. Overall, the Fa2 values indicate that the model is predicting more than the 81st fraction of data between 0.5 and 2 of the observed concentrations for all the data sets.

4.3 Sensitivity Analysis

4.3.1 Sensitivity Index (SI) Method

The sensitivity analysis is the quantification of uncertainty in the model results (concentration in this study), based on its inputs and associated parameters. There are many techniques to perform sensitivity analysis. In this study, the sensitivity analysis was performed on SLINE 1.1 using the SI method. The SI is defined as the fractional change in the pollutant concentration rate over the fractional change of the concerned input variable [92]. This method is used to assess air quality model performance and reliability and identify the sensitivity of the model based on small inaccuracies in input parameters and model formulation [93]. Air quality model performance and reliability are sensitive to small inaccuracies in input parameters and model formulation. The sensitivity analysis is the quantification of uncertainty in the model conclusions based on its input variables. SI method is used in this study to understand the

sensitivity of the SLINE 1.1, SAREA 1.1 (See Chapter 5), and SLINE PM 1.1 (See Chapter 6), model in predicting downwind concentrations. The SI (See Equation 4.18) is defined as the fractional change in the pollutant concentration rate (C_t) over the fractional change of the concerned input variable (V_c)

$$SI = \frac{d(C_t)}{d(V_c)} \tag{4.18}$$

The SI method represents the degree of sensitivity of each input variable used in the model. Categorization of the degree of sensitivity based on SI results is indicated in Table 4-3.

Table 4-3: Categorization of the degree of sensitivity [92].

SI	**Degree of sensitivity**
Large Value	Highly Sensitive
Zero	Insensitive
Small Value	Slightly Sensitive
Negative Value	Inversely Proportional
Positive Value	Directly proportional

4.3.2 Test Case

The important input variables/parameters required for running SLINE 1.1 include the emission rate of a line source (q), wind velocity at reference height (u_1), the coefficient a, coefficient b_s (only for stable conditions), coefficient b_u (only for unstable conditions), and surface friction velocity (u_*). These variables represent the emission rate, meteorology, and turbulence used in SLINE 1.1. The values in the considered range chosen for each variable/parameter were based on a trial-and-error process, which varied up to ±25%. The test case input values and standard values considered are presented in Table 4-4 and Table 4-5 respectively. One could choose another set of ranges. In general, the values were selected based on the possible errors in the specification of each variable. Sensitivity runs were performed on these variables/parameters for two different atmospheric stability conditions (stable and unstable) at near-field downwind distances of 5 m, 50 m, and 300 m. These three downwind distances were

specifically chosen in the sensitivity analysis because, at 5 m, it represents the concentration near the Initial Phase (mixing zone near the source); at 50 m, it represents the concentration at the boundary of the Transition Phase (after which additional vertical spread due to the turbulence created by the vehicles is neglected); and at 300 m, it represents the concentration during the Dispersion Phase (where plume dispersion is dominated by atmospheric turbulence) (See Figure 2-1). The executed simulations for each input to calculate predicted concentrations and calibration residuals by adjusting the variables in the considered range were presented in Madiraju et al [94].

Table 4-4: Input data and associated parameters for the test case of the SLINE 1.1 model.

Parameter	**Stable**	**Unstable**
q (g/m-s)	0.0028	0.0028
z (m)	0.1	0.1
u_1 (m/s)	1.4	0.7
n	0.7	0.15
m	0.3	0.85
s	0.813	0.685
γ(s)	1.28	1.32
Z_{10} (m)	10	10
h (m)	50	50
h^n	15.462	1.798
n+1	1.7	1.15
a	0.57	0.57
u_* (m/s)	0.05	0.15
b_s	3	-
b_u	-	1.5
L (m)	134	−30
z_s (m)	0.5	0.5
σ_v (m/s)	0.095	0.730
W_* (m/s)	0	1.120
z_i (m)	1000	1000

Table 4-5: Standard input values considered for the sensitivity analysis.

Atmospheric conditions	**q (g/m-s)**	**u_1 (m/s)**	**m**	**u_* (m/s)**	**a**	**b_s**	**b_u**
Stable	0.0028	1.4	0.3	0.05	0.57	3	-
Unstable	0.0028	0.7	0.85	0.15	0.57	-	1.5

The results of SI method for stable atmospheric conditions are discussed in this section. The sensitivity results of SLINE 1.1 model using the test case data (discussed in section 4.1) for the sensitivity analysis are computed and tabulated for 5 m, 50 m, and 300 m in Table 4-6.

i. The emission a line source (q): The SI method results show that the model is highly sensitive to the emission rate and is directly proportional to model predicted concentrations. The magnitude of SI values increases with an increase in downwind distances. Results indicate that as the q value increases the model predicted concentrations significant impact along with the downwind distances.

ii. The exponent of the power-law profile (m): The SI method results show that the model is inversely proportional and moderately sensitive to m and the magnitude of SI values decreases with an increase in downwind distances. Results indicate that the exponent of the power-law profile (m) has a significant impact on the model predicted concentrations at higher downwind distances than that of the lower downwind distances.

iii. Wind velocity (u_1): According to the SI method results, the model is inversely proportional and highly sensitive to the u_1. The magnitude of SI values is slightly increasing with the increase in downwind distances. Results indicate that the u_1 have a significant impact on the model predicted concentrations at all the downwind distances.

iv. The coefficient a: According to the SI method results, the model is inversely proportional and highly sensitive to the a. The magnitude of SI values is slightly increasing with the increase in downwind distances. Results indicate that the coefficient a has a significant impact on the model predicted concentrations at lower downwind distances.

v. Coefficient b_s: The SI method results indicate that the model is directly proportional and very slightly sensitive to the b_s. The magnitude of SI values is slightly increasing with the increase in downwind distances. Results show that the impact of b_s is minimal on the model predicted concentrations.

vi. Surface friction velocity (u_*): The SI method results indicate that the model is inversely proportional and moderately sensitive to the u_*. Results indicate that the Surface friction velocity (u_*) has less impact on the model predicted concentrations at lower downwind distances than larger downwind distances.

Table 4-6: The sensitivity index results of SLINE 1.1 for the stable atmospheric conditions.

Model Input Variables/ Parameters	**Downwind distances**		
	5 m	**50 m**	**300 m**
q	19.41	20.13	20.52
m	-6.43	-3.69	-2.77
u_1	-3.93	-4.57	-11.66
a	-11.76	-14.05	-15.84
b_s	0.07	0.24	0.48
u_*	-3.10	-4.52	-4.71

The results of SI method for unstable atmospheric conditions are discussed in this section. The sensitivity results of SLINE 1.1 model using the test case data (discussed in Table 5-2) for the sensitivity analysis are computed and tabulated for 5 m, 50 m, and 300 m in Table 4-7.

i. The emission rate of a line source (q): According to SI method results the SLINE 1.1 is highly sensitive and is directly proportional to q at the 5 m, 50 m, and 300 m downwind distances. The magnitude of SI values is increasing with the increase in downwind distances. Results indicate that the model predicted concentrations are impacted by changes in q for all downwind distances.

ii. The exponent of the power-law profile (m): The SI index method results indicate that SLINE 1.1 is moderately sensitive and inversely proportional to the coefficient m at

the 5 m, 50 m, and 300 m downwind distances. The magnitude of SI values is increasing with the increase in downwind distances. Overall, two methods indicate that the exponent of the power-law profile (m) has a significant impact on the model predicted concentrations at higher downwind distances than that of the lower downwind distances.

iii. Wind velocity (u_1): The SI model results show that at all the downwind distances the SLINE 1.1 is inversely proportional to u_1. The magnitude of SI values is increasing with the increase in downwind distances and has higher values. This shows that the wind velocity has a higher impact on predicted concentrations at higher downwind distances than the near source downwind distances. However significant impact can be observed at all downwind distances.

iv. The coefficient a: As per the SI method results, the model is highly sensitive to coefficient a and the effect is inversely proportional. The SI values are increasing with the increase in downwind distances. The results indicate that the coefficient a has a significant impact on the model predicted concentrations irrespective of the downwind distances. A slightly higher impact can be observed at higher downwind distances.

v. Coefficient b_u: The SI method results indicate that the model is slightly sensitive to the coefficient b_u and the changes in predicted concentrations are directly proportional to b_u. Overall, the two methods show that the impact of b_u is very minimal on the model predicted concentrations due to minimal increment in lower magnitudes.

vi. Surface friction velocity (u_*): SI method results show that the model is moderately sensitive and is inversely proportional to the u_*. The magnitude of SI values is increasing with the increase in downwind distances up to 300 m. The results indicate

that moderate impact on the model predictions with incremental downwind distances up to 300 m.

Table 4-7: The sensitivity index results of SLINE 1.1 for the unstable atmospheric conditions.

Model Input Variables/ Parameters	**Downwind distances**		
	5 m	**50 m**	**300 m**
q	22.36	23.23	23.70
m	-8.57	-9.68	-9.95
u_1	-22.24	-23.41	-24.10
a	-22.88	-24.05	-24.81
b_u	1.65	1.86	1.95
u_*	-8.60	-9.42	-9.85

4.4 Conclusions

A new model, SLINE 1.1, has been presented to compute downwind concentrations from line sources on a highway. The model was evaluated with four different data sets. The results indicate that SLINE 1.1 is an acceptable model based on qualitative analysis and quantitative analysis of model performance. Qualitative analysis showed that there was a strong correlation between the observed and predicted values. The statistical indicators representing the model performance of SLINE 1.1 were within the acceptable range of a better-performing model and also indicate that the model is overpredicting.

The most sensitive input variables were identified for SLINE 1.1. up to 300 m downwind from the source using SI method.

For stable atmospheric conditions, the model is

- Highly sensitive to q and an at all the three phases,
- Moderately sensitive to m at the initial phase,
- Moderately sensitive to u_1 at dispersion phase,
- Almost insensitive to b_u at all the phases, and

- Moderately sensitive u_* at all the phases.

For unstable atmospheric conditions, the model is

- Highly sensitive to q and an at all the three phases,
- Moderately sensitive to m at all the phases,
- Highly sensitive to u_1 at all three phases,
- Slightly sensitive to b_u at all the phases, and
- All most highly sensitive u_* at all the phases.

Chapter 5

Development and Evaluation of a Line Source Analytical Dispersion Model (SAREA 1.1)

5.1 Methodology

5.1.1 Development of SAREA 1.1 model

Similar to SLINE 1.1, SAREA 1.1 model incorporates the wind shear near the ground for gaseous pollutants but by considering highway mobile sources as area sources. The basic approach to developing the SAREA 1.1 model origin from the convective–diffusion equation as well. The SAREA 1.1 model focuses on deriving the analytical solution from the convective-diffusive equation with the use of a vertical velocity profile.

The fundamental assumptions made while deriving the analytical solution are:

(i) Continuous emission at a constant rate from the source.

(ii) Constant meteorological conditions and steady-state flow.

(iii) The direction of the wind is perpendicular to the mobile sources.

(iv) The dispersion is of the non-fumigation type.

(v) Conservation of mass in the plume.

(vi) The velocity profile with height above the ground level is assumed to be the same for all downwind distances.

(vii) A power-law profile is assumed for the velocity i.e. The magnitude of the wind velocity near the ground level changes rapidly and follows a power law, and

(viii) The eddy diffusivity profile is a conjugate of the velocity profile.

The SAREA 1.1 is based on the integration of the concentration equation for a point source given by Sutton [10] (See Equation (5.1)) :

$$C(x,z) = \frac{Q}{u_1 \Gamma(s)} \left[\frac{u_1}{(m-n+2)^2 K_1 x}\right]^s \exp\left[-u_1 \frac{z^{m-n+2}}{((m-n+2)^2 K_1 x)}\right] \quad (5.1)$$

where Q is the emission rate of the mobile (area) source per unit length, and $\Gamma(s)$ is the upper incomplete gamma function of s.

The velocity profile with height above the ground level is assumed to be the same for all downwind distances. The magnitude of the wind velocity near the ground level changes rapidly. Therefore, for the ground level discharge of the pollutant, it is very important that the variation of the wind velocity magnitude is incorporated in the dispersion and transport equation. This incorporation is performed using the power law profile formulation presented through Equation (4.2). Input parameters related to meteorological (weather conditions in the ambient environment), traffic (road network) , terrain (features that reflects the nature of the terrain), and source (mobile source) are collected during the field measurement. However, the turbulence input parameters are computed using the formulation provided by the TPT model (See Chapter 2) for the SAREA 1.1 (Similar to SLINE 1.1).

In the proposed model, the eddy diffusivity K is a function of downwind distance x. However, the derivation of the convective–diffusion equation representing the dispersion from mobile sources assumes that the K profile is constant as the plume moves downwind. It is assumed during the application of Equations (5.2) and (5.3) that the concentration is predicted in the SAREA 1.1 model at a downwind distance by updating the value of K in the model for that

downwind distance. The K value is updated by incorporating the vertical spread formulation of TPT model. The updated formulation of K is presented in the Equation (4.9) (for stable atmospheric conditions) and Equation (4.10) (for unstable atmospheric conditions). It is expected that this approach will improve the model performance.

Equation (5.1) for a highway strip source with width X, and infinite length having the origin of x ordinate at the center of the strip is integrated from x-(X/2) to x+(X/2) to estimate the concentration from the strip. The integrated equation is given by Bhat and Kumar (2011) [95] as Equation (5.2) and Equation (5.3):

$$C(x,z) = \sum_1^i Q \frac{z^{a^{s-1}}}{A}\left[\frac{A+x^{1-s}B\exp\left(\frac{B}{x_i}\right)+D}{S-1}\right]_{x_i-(\frac{X}{2})}^{x_i+(\frac{X}{2})} \quad \text{for } z > 0 \tag{5.2}$$

$$C(x) = \sum_1^i \left[\frac{Q}{\Gamma(s)(m+n-2)^2K_1}\ln(x_i)\right]_{x_i-(\frac{X}{2})}^{x_i+(\frac{X}{2})} \quad \text{for } z = 0 \tag{5.3}$$

$$a = (m - n + 2) \tag{5.4}$$

$A = \Gamma(s)$, where Γ is the upper incomplete gamma function. (5.5)

$$B = -u_1\frac{z^a}{a^2K_1}, \tag{5.6}$$

$$D = \gamma(s,(\frac{-B}{x})), \tag{5.7}$$

where the total concentration of the pollutant is given by Equations (5.2) and (5.3) after considering the 'i' number of strips in the area source and the strips are assumed to be adjacent. The integration is performed considering the centerline of the strips. The formulation for computation of x_i values are provided in Equations (5.9) and (5.10).

The vertical spread in the SAREA 1.1 model incorporates the additional spread m_t due to the turbulence created by moving vehicles. m_t is considered for the downwind distance ≤ 50m for computing the vertical spread of the plume [66]. The Three-Phase approach suggested by Madiraju and Kumar [96] to develop the formulation of atmospheric/plume turbulence is followed in this

study. The development of SAREA 1.1 model is expanded for unstable and stable atmospheric conditions in the following sections.

The concentration of the pollutant under stable atmospheric conditions can be computed for a highway strip of width X, and infinite length having the origin of x ordinate at the center of the strip to obtain the concentration from the strip using the Equation (5.7) for z > 0 and Equation (5.8) for z = 0.

$$C(x,z) = q\frac{z^{a^{s-1}}}{A}\left[\frac{A+x^{1-s}\dfrac{-2xz^{a}}{\left[\dfrac{a\,u_{*}x}{u_1+b_s u_{*}\left(\frac{x}{L}\right)^{\frac{2}{3}}}+m_t\right]^{2}a^{2}}\exp\left(\dfrac{-2z^{a}}{\left[\dfrac{a\,u_{*}x}{u_1+b_s u_{*}\left(\frac{x}{L}\right)^{\frac{2}{3}}}+m_t\right]^{2}a^{2}}\right)+D}{S-1}\right]_{x_i-(\frac{X}{2})}^{x_i+(\frac{X}{2})} \qquad z > 0 \qquad (5.7)$$

$$C(x) = \sum_1^i\left[\frac{2x_i q}{A(m+n-2)^2\left[\dfrac{a\,u_{*}x}{u_1+b_s u_{*}\left(\frac{x}{L}\right)^{\frac{2}{3}}}+m_t\right]^{2}u_1}\ln(x_i)\right]_{x_i-(\frac{X}{2})}^{x_i+(\frac{X}{2})} \qquad z= 0 \qquad (5.8)$$

where,

$$x_i = x_d + {}^{X}/_{2} \qquad (\text{if, } i=1) \qquad (5.9)$$

$$x_i = x_{i-1} + X \qquad (\text{if, } i>1) \qquad (5.10)$$

and x_d is the downwind distance of the monitoring station from the edge of the field.

The concentration of the pollutant under unstable atmospheric conditions could be computed for a highway strip of width X of infinite length having the origin of x ordinate at the center of the strip using Equations (5.7) and (5.8). The concentration from the strip using Equation

(5.11) for z > 0 and Equation (5.12) for z = 0. The total concentration of the pollutant is given by the following equation after considering the 'i' number of strips (lanes on the highway) in the area source.

$$C(x,z) = \sum_1^i q \frac{z^{a^{s-1}}}{A} \left[\frac{A + x^{1-s} \frac{-2xz^a}{a^2\left[a\frac{xu_*}{U_e}\left[1+b_u\left(\frac{xu_*}{U_eL}\right)\right]+m_t\right]^2} \exp\left(\frac{-2z^a}{a^2\left[a\frac{xu_*}{U_e}\left[1+b_u\left(\frac{xu_*}{U_eL}\right)\right]+m_t\right]^2}\right)+D}{S-1} \right]_{x_i-\left(\frac{X}{2}\right)}^{x_i+\left(\frac{X}{2}\right)} \quad z > 0 \qquad (5.11)$$

$$C(x) = \sum_1^i \left[\frac{2x_i q}{A(m+n-2)^2\left[a\frac{Ux}{U_e}\left[1+b_u\left(\frac{Ux}{U_eL}\right)\right]+m_t\right]^2 u_1} \ln(x_i) \right]_{x_i-\left(\frac{X}{2}\right)}^{x_i+\left(\frac{X}{2}\right)} \quad z = 0 \qquad (5.12)$$

The strip on the highway refers to the number of lanes in practical conditions [79], [95]. The expression to calculate the ground-level concentrations of the pollutants released from highway mobile sources when considered as an area source are represented by Equations (5.7), (5.8), (5.11), and (5.12). Also, note that the vertical spread due to wake turbulence induced by mobile sources is considered until 50 m downwind distance. It is assumed the wake turbulence is negligible after the 50 m downwind distance from the source release [66], [72].

5.2 Statistical Model Evaluation

It is unrealistic to achieve the ideal case values in the results of statistical indicators. The values with '✓' denote the interpretation of statistical criteria which were satisfied by the suggested range from the literature for a better-performing model. The Model bias values of the model indicate that there is a minimal error of 8% to 24% is observed for SAREA 1.1. Even though more than 10% mean error is observed, which is a positive error. This positive error indicates the model is overpredicting. Also, the FB values are observed to be less than 0.5 which indicates the model is performing better since the values are close to 0 (ideal value). Only one negative value is observed in Hyderabad data for stable conditions, this can be due to infrequent high concentration

values. The values of NMSE are slightly higher than that of SLINE 1.1 but they are close enough to 0 (ideal value) which indicates that the model is performing better. According to the 'r' values the predicted concentrations are 79% to 85% correlated to the observed concentrations. Even though the lower range of correlation is higher than that of SLINE 1.1 the upper range of correlation is equal to that of SLINE 1.1. Considering MG, the model is performing better for 6 out of 8 data sets and considering VG the model is performing better for 7 out of 8 data sets. MG and VG value rages of SAREA 1.1 are the same as SLINE 1.1. Similar to SLINE 1.1, the Fa2 values SAREA 1.1 indicate that the model is predicting more than the 81st fraction of data between 0.5 and 2 of the observed concentrations for all the data sets.

Table 5-1: Model evaluation results for the SAREA 1.1 model.

Statistical Indicator	**MB (µg/m3)**	**FB**	**NMSE**	**r**	**MG**	**VG**	**Fa2**
CALTRANS stable conditions	15.86	0.34✓	1.61✓	0.81✓	1.32	1.20✓	0.82✓
CALTRANS unstable conditions	23.12	0.35✓	1.73✓	0.78✓	1.37	1.26	0.86✓
Idaho Falls stable conditions	11.32	0.31✓	1.25✓	0.84✓	1.19✓	1.11✓	0.83✓
Idaho Falls unstable conditions	23.09	0.46✓	1.18✓	0.79✓	1.20✓	1.18✓	0.81✓
Raleigh stable conditions	8.01✓	0.18✓	0.89✓	0.83✓	1.05✓	1.07✓	0.86✓
Raleigh unstable conditions	16.07	0.20✓	1.1✓	0.85✓	1.10✓	1.03✓	0.89✓
Hyderabad stable conditions	14.94	-0.07✓	0.28✓	0.79✓	1.12✓	1.17✓	0.81✓
Hyderabad unstable conditions	13.03	0.10✓	0.14✓	0.81✓	1.23✓	1.25✓	0.84✓

The results for the statistical evaluation of models are mentioned in Table 5-1, But the key identifications in the results are discussed as follows.

5.3 Sensitivity Analysis

5.3.1 Test Case

The important input variables/parameters required for running SAREA 1.1 include the emission rate of an area source (Q), wind velocity at reference height (u_1), the coefficient a, coefficient b_s (only for stable conditions), coefficient b_u (only for unstable conditions), and surface friction velocity u_*.These variables represent the emission rate, meteorology, and

turbulence used in SAREA 1.1. The sensitivity of the SAREA 1.1 model is determined using data collected from the literature for stable and unstable atmospheric conditions. The results simulated from the model are analyzed to conclude the sensitivity to the independent variable parameters. Mobile sources emitting exhaust gases from the tailpipe on a highway are considered. The wind is assumed to be perpendicular to the motion of the vehicle with a speed of 1.4 m/s at 10 m. The approximate count of vehicles is 8000 per hour. Each vehicle travels at an average speed of 40 miles per hour. The number of vehicles was computed to be 0.125 per meter. The emission rate of an air pollutant is estimated to be 0.0028 g/s-m using the appropriate emission factor.

Table 5-2: Input data and associated parameters for the test case of the SAREA 1.1 model.

Parameter	**Stable**	**Unstable**
q (g/m-s)	0.0028	0.0028
z (m)	0.1	0.1
u_1 (m/s)	1.4	0.7
n	0.7	0.15
m	0.3	0.85
s	0.813	0.685
γ(s)	1.28	1.32
Z_{10} (m)	10	10
h (m)	50	50
h^n	15.462	1.798
n+1	1.7	1.15
a	0.57	0.57
u_* (m/s)	0.05	0.15
b_s	3	-
b_u	-	1.5
L (m)	134	−30
z_s (m)	0.5	0.5
σ_v (m/s)	0.095	0.730
W_* (m/s)	0	1.120
z_i (m)	1000	1000

Table 5-3: Standard input values considered for the sensitivity analysis.

Atmospheric conditions	**Q (g/m-s)**	**u_1 (m/s)**	**m**	**u_* (m/s)**	**a**	**b_u**	**b_s**
Stable	0.0226	1.4	0.3	0.05	0.57	3	-
Unstable	0.0226	0.7	0.85	0.15	0.57	-	1.5

The surface friction velocity used for the analysis is 0.05m/s and the average height from the ground surface to the tailpipe of the mobile sources (z_s) is 0.5 m. The concentration of the pollutant is estimated along the downwind distance (y = 0). The results of the SAREA 1.1 model using the sample data for the sensitivity analysis are computed and tabulated for 5 m, 50 m, and 300 m (See Tables 2-5).

The results of the SI method for stable atmospheric conditions are as follows:

The results of SI method for SAREA 1.1 model using the test case (discussed in Table 5-2) for the sensitivity analysis are computed and tabulated for 5 m, 50 m, and 300 m in Table 5-4.

i. The emission rate of an area source (Q): The SI method results show that the model is highly sensitive to the emission rate and is directly proportional to model predicted concentrations. The magnitude of SI values increases with an increase in downwind distances. As the Q value increases there is a significant impact along with the downwind distances on the model predicted concentrations.

ii. The exponent of the power-law profile (m): The exponent of the power-law profile (m) has a significant impact on the model predicted concentrations at lower downwind distances than that at higher downwind distances. Because the SI method results show that the model is inversely proportional and moderately sensitive to m and the magnitude of SI values decreases with an increase in downwind distances.

iii. Wind velocity (u_1): According to the SI method results, the model is inversely proportional and highly sensitive to the u_1.The magnitude of SI values is drastically increasing with the increase in downwind distances. It can be said that impact of the exponent of the Wind velocity (u_1) on the model predicted concentrations at is increasing with incremental downwind distances.

iv. The coefficient a: According to the SI method results, the model is inversely proportional and moderately sensitive to the a. The magnitude of SI values is slightly increasing with the increase in downwind distances. The coefficient a has a significant impact on the model predicted concentrations at higher downwind distances than that of the lower downwind distances.

v. Coefficient b_s: The SI method results indicate that the model is very slightly sensitive to the coefficient b_s and the changes in predicted concentrations are directly proportional to b_s. The results show that the impact of b_s is very minimal on the model predicted concentrations and also no impact at near source.

vi. Surface friction velocity (u_*): The SI method results indicate that the model is inversely proportional and moderately sensitive to the u_*. Results indicate that the surface friction velocity (u_*) has less impact on the model predicted concentrations at lower downwind distances than that of larger downwind distances.

Table 5-4: The sensitivity index results of SAREA 1.1 for stable atmospheric conditions.

Model Input Variables/ Parameters	**Downwind distances**		
	5 m	**50 m**	**300 m**
Q	12.34	14.86	14.45
m	-5.98	-3.24	-2.32
u_1	-2.91	-3.55	-10.64
a	-10.87	-13.16	-14.95
b_s	0.09	0.26	0.51
u_*	-2.25	-3.67	-3.86

The results of SI method for unstable atmospheric conditions are discussed as follows:

The results of both these methods for SAREA 1.1 model using the test case data (discussed in Table 5-2) for the sensitivity analysis are computed and tabulated for 5 m, 50 m, and 300 m in Table 5-5.

i. The emission rate of an area source (Q): According to SI method results the SAREA 1.1 is highly sensitive and is directly proportional to Q at the 5 m, 50 m, and 300 m downwind distances. The magnitude of SI values is increasing with the increase in downwind distances. The model predicted concentrations are impacted by changes in Q for all downwind distances. The impact of Q on model predicted concentrations at stable and unstable atmospheric conditions are the same. However, the magnitude of the impact varies.

vii. The exponent of the power-law profile (m): The SI index method results indicate that SAREA 1.1 is moderately sensitive and inversely proportional to the coefficient m at the 5 m, 50 m, and 300 m downwind distances. The magnitude of SI values is increasing with the increase in downwind distances. The exponent of the power-law profile (m) has a significant impact on the model predicted concentrations at higher downwind distances than that of the lower downwind distances.

viii. Wind velocity (u_1): The SI model results show that SAREA 1.1 is highly sensitive to u_1. The magnitude of SI values is increasing with the increase in downwind distances. The results indicate the u_1 has a higher impact on predicted concentrations at higher downwind distances than the near source downwind distances. But overall u_1 has a significant impact on model predicted concentrations.

ix. The coefficient a: As per the SI method results, the model is highly sensitive to coefficient a and the effect is inversely proportional. The SI values are increasing with the increase in downwind distances. The coefficient a has a significant impact on the model predicted concentrations irrespective of the downwind distances.

x. Coefficient b_u: The SI method results indicate that the model is directly proportional and slightly sensitive to the b_u. The magnitude of SI values is slightly increasing with the increase in downwind distances. The impact of b_u is minimal on the model predicted concentrations and the model sensitivity to b_u is slightly increasing with downwind distance.

xi. Surface friction velocity (u_*): SI method results show that the model is moderately sensitive and is inversely proportional to the u_*. The magnitude of SI values is increasing with the increase in downwind distances up to 300 m.

Table 5-5. The sensitivity index results of SAREA 1.1 for the unstable atmospheric conditions.

Model Input Variables/ Parameters	**Downwind distances**		
	5 m	**50 m**	**300 m**
Q	23.04	23.91	24.38
m	-12.56	-17.67	-18.94
u_1	-21.31	-22.48	-23.17
a	-22.45	-23.62	-24.38
b_u	1.67	1.85	1.96
u_*	-11.32	-13.44	-14.09

5.4 Conclusions

A new area source model, SAREA 1.1 model developed and evaluated it using multiple field data sets and assess its quantitative performance. SAREA 1.1 is a dispersion model for gaseous pollutants associated with highway mobile sources. This model is based on an analytical solution of the convective-diffusion equation after incorporating wind shear near the ground. The revised turbulence model is used in this study for the SAREA 1.1. The ranges of statistical indicators for the SAREA 1.1 are observed to understand its performance. The model evaluation results show that the model is overpredicting, and the predicted values are significantly correlated with the observed values.

The sensitivity analysis is performed on SAREA 1.1 using SI method to identify the sensitive input variables for which model is sensitive.

For stable atmospheric conditions, the model is

- Highly sensitive to q at all the three phases,
- Moderately sensitive to m at the initial phase and slightly sensitive in transition and dispersion phase,
- Slightly sensitive to u_1 at initial and transition phase and moderately sensitive to u_1 at dispersion phase,
- Almost insensitive to b_s at all the phases,
- Moderately sensitive to the initial phase and significantly sensitive to the dispersion phase and
- Moderately sensitive u_* at all the phases.

For unstable atmospheric conditions, the model is

- Highly sensitive to q, a and u_1 at all three phases,
- Moderately sensitive to m at the initial phase and highly sensitive at transition and dispersion phase,
- Very slightly sensitive to b_u at initial and transition phase, and slightly sensitive at dispersion phase
- Slightly moderate sensitive to u_* at the initial phase and moderately sensitive at transition and dispersion phases.

A sensitivity analysis of comparing of four generic mobile source dispersion models was performed by Madiraju et al [97] on SLINE 1.0 and SAREA 1.0. The current results shows that the sensitivity improved in the updated model versions.

Chapter 6

Development and Evaluation of a Ground Level Line Source Analytical Dispersion Model (SLINE PM 1.1) for Particulate Matter

6.1 Methodology

6.1.1 Model development

The basic approach to developing the SLINE PM 1.1 model is based on the analytical solution of the convective–diffusion equation representing the dispersion of particulate pollutants from a point source. (See Equation (6.2)). The analytical solution is derived by Ermak [98] from study state form of atmospheric convective–diffusion equation (See Equation (6.1)).

The assumptions used in deriving the equation were:

(i) The source emits a non-reacting pollutant.

(ii) The terrain is assumed to be flat.

(iii) The average wind velocity is constant. The wind speed is assumed to be sufficiently large for diffusive transport of pollutant.

(iv) The atmosphere is unlimited in the vertical direction.

(v) A Cartesian coordinate system is used with the x-axis oriented in the direction of the constant wind, the y-axis in the horizontal crosswind direction, and z-axis oriented in the vertical crosswind.

(vi) The diffusion coefficients in the y- and z-directions are taken to be functions of only the down-wind distance from the source. Since the pollutant particles travel downwind at a constant speed.

The study state form of atmospheric convective–diffusion equation is given as:

$$u\frac{\partial C}{\partial x} = \left(K(y)\frac{\partial^2 C}{\partial y^2}\right) + \left(K(z)\frac{\partial^2 C}{\partial z^2}\right) + \left(V_g\frac{\partial C}{\partial z}\right) \quad (6.1)$$

The analytical solution of the convective–diffusion equation representing the dispersion of particulate pollutants from a point source at emitting at a constant emission rate is given as:

$$C_{(x,y,z)} = \frac{q}{2\pi\sigma_y\sigma_z u}\exp\left\{\frac{-y^2}{2\sigma_y^2}\right\}\exp\left\{\frac{-V_g(z-h)}{2K} - \frac{V_g^2\sigma_z^2}{8K^2}\right\}\left[\exp\left\{\frac{-(z-h)^2}{2\sigma_z^2}\right\} + \exp\left\{\frac{-(z+h)^2}{2\sigma_z^2}\right\} - \sqrt{2\pi}\frac{V_1\sigma_z}{K}\exp\left\{\frac{V_1(z+h)}{K} + \frac{V_1^2\sigma_z^2}{2K^2}\right\}\operatorname{erfc}\left\{\frac{V_1\sigma_z}{\sqrt{2}K} + \frac{z+h}{\sqrt{2}\sigma_z}\right\}\right] \quad (6.2)$$

where,

$C_{(x, y, z)}$ = concentration (units/m^3)

q = emission rate (units/s)

u = wind speed (m/s)

σ_y = horizontal dispersion coefficient (m)

σ_z = vertical dispersion coefficient (m)

z = the height measured from the surface of the ground (m)

h = height of the source.

$V_1 = (V_d - V_g)/2$

V_d = dry deposition velocity of the particle (m/s)

V_g = gravitational settling velocity of the particle (m/s)

K = eddy diffusivity (m^2/s)

The Equation (6.2) can be reduced to the Gaussian plume model, when gravitational settling is neglected and the vertical diffusion coefficient K_z, is constant. The Equation (6.2) allows us to incorporate the variation of the wind velocity magnitude near the ground during the dispersion of PM released from mobile sources. The velocity field is represented by a power law (See Equation (4.2)). The profiles of wind velocity and eddy diffusivity at a given downwind distance are given in Equations (4.2) and (4.3).

The concentration Equation (6.1) given by Ermak [98]; and used by Nimmatoori and Kumar [79] for a point at (x, y, z) from an elevated source is used for developing SLINE PM 1.1.

The downwind concentrations from a line source are obtained by integrating Equation (6.2) for a point source. There are two choices (finite and infinite) while carrying out the integration depending on the chosen length of the line source.

The finite length (Y) equation given by Nimmatoori and Kumar [79] is adopted for calculating downwind concentrations. They obtained Equation (6.3) by integrating Equation (6.2) from Y/2 to Y/2.

$$C_{(x,y,z)} = \frac{q}{2\sqrt{2\pi}\sigma_z u}\exp\left\{\frac{-V_g(z-h)}{2K} - \frac{V_g^2\sigma_z^2}{8K^2}\right\}\left[\exp\left\{\frac{-(z-h)^2}{2\sigma_z^2}\right\} + \exp\left\{\frac{-(z+h)^2}{2\sigma_z^2}\right\} - \sqrt{2\pi}\frac{V_1\sigma_z}{K}\exp\left\{\frac{V_1(z+h)}{K} + \frac{V_1^2\sigma_z^2}{2K^2}\right\}\operatorname{erfc}\left\{\frac{V_1\sigma_z}{\sqrt{2}K} + \frac{z+h}{\sqrt{2}\sigma_z}\right\}\right]\left[\operatorname{erf}\left(\frac{\frac{Y}{2}}{\sqrt{2}\sigma_y}\right) - \operatorname{erf}\left(\frac{-\frac{Y}{2}}{\sqrt{2}\sigma_y}\right)\right] \quad (6.3)$$

An infinite length source equation was derived from Equation (6.2) and is given as Equation (6.3) for computing ground-level concentrations.

$$C_{(x,y,z)} = \frac{q}{\sqrt{2\pi}\sigma_z u}\exp\left\{\frac{-V_g(z-h)}{2K} - \frac{V_g^2\sigma_z^2}{8K^2}\right\}\left[\exp\left\{\frac{-(z-h)^2}{2\sigma_z^2}\right\} + \exp\left\{\frac{-(z+h)^2}{2\sigma_z^2}\right\} - \sqrt{2\pi}\frac{V_1\sigma_z}{K}\exp\left\{\frac{V_1(z+h)}{K} + \frac{V_1^2\sigma_z^2}{2K^2}\right\}\operatorname{erfc}\left\{\frac{V_1\sigma_z}{\sqrt{2}K} + \frac{z+h}{\sqrt{2}\sigma_z}\right\}\right] \quad (6.4)$$

The expressions for the vertical and horizontal dispersion coefficients for stable conditions are given as Equation (2.6) and Equation (6.5), and for unstable conditions are given as Equation (2.7) and Equation (6.6) respectively. The vertical spread coefficient equations of SLINE PM 1.1 are based on TPT model (See Chapter 2). The horizontal spread coefficient equations of SLINE PM 1.1 are based on the work of Snyder et al. [61] and include an additional term m_t to account for the additional vertical spread due to the vehicular turbulence as suggested by Madiraju and Kumar [94], [96].

$$\sigma_y = c\frac{\sigma_v}{u_*}\sigma_z\left(1 + d_s\frac{\sigma_z}{|L|}\right) \tag{6.5}$$

$$\sigma_y = c\frac{\sigma_v}{u_*}\sigma_z\left(1 + d_u\frac{\sigma_z}{|L|}\right)^{-\frac{1}{2}} \tag{6.6}$$

The particle size concept is incorporated into the equations through the gravitational settling velocity. The particle diameter is considered while computing the gravitational settling velocity of the particle. The gravitational settling velocity is considered in SLINE PM 1.1 while computing the ground level concentrations of the particulate matter. Gravitational settling velocity is the terminal velocity that the particle settles on the ground under the action of gravity [99]. Dry deposition velocity is also considered in the SLINE PM 1.1 model which describes the speed of atmospheric particulate matter deposit to the ground surface [100]. The dry deposition velocity (V_d) and gravitational settling velocity (V_g) of the particles are computed using the algorithms used in the AERMOD by USEPA [101]. The expressions are given as Equations (6.7) and (6.8).

$$V_d = \frac{1}{R_a + R_p + R_a R_p V_g} + V_g \tag{6.7}$$

where,

R_a = Aerodynamic resistance (s/m)

R_p = Quasilaminar sublayer resistance

$$V_g = \frac{(\rho - \rho_{air}) g d_p^2 C_2}{18\mu} S_{CF} \quad (6.8)$$

where,

P = particle density (g/cm^3),

ρ_{air} = air density (g/cm^3),

d_p = particle diameter (μm),

g = acceleration due to gravity (m/s^2),

μ = absolute viscosity of air (g/cm/s),

C_2 = air unit's conversion constant (cm^2/μm^2), and

S_{CF} = slip correction factor (dimensionless).

6.1.2 Application of the model

The developed model is applied as follows depending on the availability of particle size profile for emitted PM.

1. Emission data with given particle size profile: If the input data available to simulate to predict the ground level concentration of the PM includes the details on the distribution of the particle sizes, then the formulation provided in the Equations (2) or (3) is first applied to each range of particle size distribution. The total particulate concentration (C_{TP}) will be the sum of concentrations for each size range.
2. Emission data with no particle size distribution: If the input data available to simulate to predict the ground level concentration of the PM does not include the detailed distribution of the particle sizes, then the formulation provided in the Equations (2) or (3) is used.

6.2 Statistical Model Evaluation

The statistical evaluation of the model is performed for each location. The statistical indicators considered in this study are MB (μg/m^3), FB, NMSE, r, MG, VG, and Fa2. The model

evaluation results are provided in Table 3. The ideal case values of each indicator are given in the 2nd column of the table to assess the performance of the model.

The values with '✓' denote the interpretation of statistical criteria which were satisfied by the suggested range from the literature for a better-performing model. The Model bias values of the model indicate that there is a minimal error of 2% to 24% is observed for SLINE PM 1.1. It can be observed from the results that a very minimal error is observed for the particle size ranges <0.1 µm.

Table 6-1: The statistical model evaluation results for the five monitoring locations.

Data	**Statistical Indicators**							
	MB ($\mu g/m^3$)	**FB**	**NMSE**	**r**	**MG**	**VG**	**Fa2**	**Particle size ranges (µm)**
Hyderabad data stable conditions	21.65	1.16✓	1.01✓	0.79	1.47	1.33	0.77	>10
Hyderabad data unstable conditions	23.14	1.02✓	0.97✓	0.74	1.09✓	0.96✓	0.71	>10
Hyderabad data stable conditions	-6.22✓	0.91✓	0.76✓	0.85✓	1.06✓	1.02✓	0.82✓	10-2.5
Raleigh data stable conditions	5.36✓	0.99✓	1.11✓	0.84✓	1.01✓	0.98✓	0.81✓	10–2.5
Hyderabad data unstable conditions	25.98	1.26	3.19	0.74	1.25✓	1.21✓	0.69	10–2.5
Raleigh data unstable conditions	8.33✓	1.02✓	1.26✓	0.79	1.24✓	1.16✓	0.70	10–2.5
Hyderabad data stable conditions	20.37	1.14✓	1.03✓	0.77	1.16✓	1.12✓	0.73	<2.5
Raleigh data stable conditions	12.88	1.22✓	1.29✓	0.84✓	1.36	1.29	0.81✓	0.1-2.5
Hyderabad data unstable conditions	14.85	1.01✓	1.27✓	0.81✓	1.45	1.31	0.80✓	<2.5
Raleigh data unstable conditions	12.39	0.88✓	4.97	0.72	1.22✓	1.18✓	0.68	0.1-2.5
Raleigh data stable conditions	3.35✓	0.97✓	1.12✓	0.89✓	1.25✓	1.19✓	0.82✓	<0.1
Raleigh data unstable conditions	2.39✓	0.98✓	1.26✓	0.85✓	1.16✓	1.07✓	0.80✓	<0.1

FB values for 11 out of 12 data sets were in the satisfactory range of a better-performing model. The values of NMSE are close enough to 0 (ideal value) which indicates that the model is performing better [73] except in two data sets where the NMSE values are over the range of better performing model. According to the 'r' values the predicted concentrations are 72% to 89% correlated to the observed concentrations. Considering MG and VG, the model is performing better for 9 out of 12 data sets. The Fa2 values SLINE PM 1.1 indicate that the model is prediction ranging from 69^{th} to 81^{st} fraction of data between 0.5 and 2 of the observed concentrations for all the data sets.

6.3 Sensitivity Analysis

6.3.1 Test case

Table 6-2: Input parameters and data

Parameters	Data or Value
Emission rate	Daily emission data
Source release height	0.5 m
Receptor height	1 m
Study area type	Urban
Atmospheric Stability	Extremely unstable conditions/Moderately unstable conditions
Wind speed (u_1)	Varied depending on the sampling day and time
Ambient Temperature	Varied depending on the sampling day and time
Downwind distances (x)	5 m, 50 m, and 300 m
Surface friction velocity (u_*)	0.18 m/s
Monin-Obukhov Length (L)	-2 to -5 m
The average height of car (H)	1.6 m
a	0.4, 0.75
b_u	2, 3.5
c	1.6
V_g	0.004 m/s
V_d	0.07 m/s
V_1	0.033 m/s

The data used for the sensitivity analysis was collected by Madiraju (under the direction of PVS Gopi Raghunadh and K Ravi Kumar) in Hyderabad, India in 2016 [78]. The concentrations of PM were collected from January to April. The atmospheric conditions varied from extremely unstable to moderately unstable during the daytime of measurement. The readings were collected at around noon every day for 90 days (January 2nd to April 1st, 2016) continuously. The details of the test case input data from the field studies were provided in Table 6-2.

The data is divided into different particle size ranges. PM≤0.1 μm: particles with a size less than or equal to 0.1 μm also known as 'ultra-fine' particles. PM < 2.5 μm: particles with a size less than or equal to 2.5 μm also known as 'fine' particles. PM between 10-2.5 μm: particles with a size less than 10 μm and greater than 2.5 also known as 'coarse' particles [93]. The emission rates were

calculated using the measured traffic data in the field. The diameter of the particle is considered in the SLINE PM 1.1 model through the calculation of Vg.

Table 6-3: Sensitivity analysis results using the SI method for stable atmospheric conditions

Model Input Variables/Parameters	**Downwind distances**		
	5 m	**50 m**	**300 m**
q	14.02	17.77	26.25
m	-2.55	-4.92	-15.68
u_1	-10.03	-16.16	-29.63
a	-9.30	-14.23	-26.63
b_s	1.13	1.57	0.04
u_*	-6.57	-9.71	-20.64

Table 6-4: Sensitivity analysis results using the SI method for unstable atmospheric conditions

Model Input Variables/Parameters	**Downwind distances**		
	5 m	**50 m**	**300 m**
q	22.53	23.55	24.64
m	-5.57	-13.16	-14.95
u_1	-2.91	-14.86	-14.45
a	-7.78	-17.67	-18.86
b_u	0.94	0.26	0.51
u_*	-0.14	-3.24	-2.32

The sensitivity of the SLINE PM 1.1 is analyzed using SI method.

For stable atmospheric conditions, the model is

- Highly sensitive to q at all three phases and the sensitivity is increasing with incremental downwind distances,
- Slightly sensitive to m in the initial phase and moderately sensitive in the transition phase and highly sensitive in the dispersion phase,
- Moderately sensitive to u_1 at initial and transition phase and highly sensitive to u_1 at dispersion phase,
- Slightly sensitive to b_s at the initial phase and transition phase almost insensitive to b_s at dispersion phase,

- Moderately sensitive to the initial phase and significantly sensitive to the transition and dispersion phase,
- Moderately sensitive u_* at initial and transition phase and highly sensitive in the dispersion phase.

For unstable atmospheric conditions, the model is

- Highly sensitive to q at all the three phases,
- Moderately sensitive to m at the initial phase and highly sensitive at transition and dispersion phase,
- Moderately sensitive to u_1 at initial and transition phase and highly sensitive to u_1 at dispersion phase,
- Moderately sensitive to the initial phase and highly sensitive to the transition and dispersion phase,
- Almost insensitive to b_u In all the three-phase,
- Very slightly sensitive to u_* at the initial phase and moderately sensitive in a transition phase and the magnitude of significance is reduced at dispersion phases.

6.4 Conclusions

The development and evaluation of SLINE PM 1.1, an analytical line source dispersion model to predict ground-level concentrations for PM for different particle size ranges are presented. Separate dispersion equations are presented for the infinite as well as finite-length mobile sources. The application of the SLINE PM 1.1 model for emission data with a given particle size profile and emission data with no particle size distribution is presented.

The sensitivity results indicate that u_1, u_*, m and a are inversely proportional to the model predictions. q, b_s, and b_u are directly proportional to the model predictions. The results also show

that the model is highly sensitive to q because if the emission from the source increases, then the model predictions increase. The model is moderately sensitive (relatively to q) to the u_1 because the dispersion is relatively affected by the wind speed. The model is also moderately sensitive (relatively to q) to coefficient a because it is an empirical coefficient contributing to the vertical dispersion coefficient. The model is moderately sensitive to the u_* due to the dependence of vertical and horizontal dispersion. The model is moderately sensitive to Coefficient m and almost insensitive to Coefficient b_s and b_u.

A sensitivity analysis was performed by Madiraju et al [102] on SLINE PM 1.0. The current results shows that the sensitivity improved in the updated model version.

Chapter 7

Inter-comparison of Developed and Available models

7.1 Discussion of Available Dispersion Models

The four generic model formulations of the available models (CALINE4, ADMS, ISC3, and SLSM) discussed in this section are used in this study to simulate the predictions based on the four available data sets. The data sets used in this study are discussed in Section 3.2. Note that the ability of a dispersion model to predict the concentrations of the air pollutants under varying conditions could only be evaluated after field measurements are taken under similarly varying conditions. All the available dispersion models used in this study are currently being used widely across the globe for compliance, educational and industrial purposes.

7.1.1 CALINE4

CALINE4 is a line-source Gaussian plume dispersion model used for regulatory purposes for predicting the concentrations of pollutants near roadways. The roadway geometry, worst-case meteorological parameters, anticipated traffic volumes, and receptor positions are the initial input parameters for the model for regulatory work. The approach followed by CALINE4 assumes (i) a homogeneous wind flow field (both vertically and horizontally), (ii) steady-state conditions, and (iii) negligible along-wind diffusion. The horizontal and vertical dispersion is adequately described

as unimodal. The CALINE4 model contains improved algorithms for vertical and horizontal dispersion. However, the focus of this study is on the generic equation (see Equation (7.1)) of CALINE4 [103].

$$C_{(x,y)} = \frac{q}{\pi u \sigma_z} \int_{y_1-y}^{y_2-y} \exp\left(\frac{-y^2}{2\sigma_y^2}\right) dy \tag{7.1}$$

where, σ_z and σ_y are the horizontal and vertical dispersion coefficients (m), and y_1 and y_2 are the finite line-source endpoints in y-coordinates ($y_2 > y_1$).

7.1.2 ADMS

ADMS is a model developed by Cambridge Environmental Research Consultants (CERC). As per the description provided by the CERC, the source is decomposed into several source elements. The difference in streamwise distance between source elements and each receptor is constrained not to vary too rapidly, subject to the maximum number of source elements. The concentration is then calculated by summing the contributions from each element. In the case of an area source, the contribution from each element is approximated by a crosswind line source of finite length. Roads are modeled as line sources with no plume rise and with modifications to account for traffic-produced turbulence, and street canyons, which is an optional feature. To consider the extra vertical turbulence produced by traffic on busy roads, the vertical plume spread parameter surges. Similarly, an extra component is included in the lateral plume spread parameter to model the effect of lateral turbulence except for the street canyons [55]. The expression for the concentration is given in Equation (7.2).

$$C = \frac{Q}{2\sqrt{2\pi}\sigma_z U} \exp\left(-\frac{(z-z_s)}{2\sigma_z^2}\right)\left[\text{erf}\left(\frac{y+L_s/2}{\sqrt{2}\sigma_y}\right)\text{-erf}\left(\frac{y-L_s/2}{\sqrt{2}\sigma_y}\right)\right]\text{+reflection term} \tag{7.2}$$

where C from a finite crosswind line source of length Ls is given by equation. The source strength Q is in mass/m/s. y is the lateral distance from the plume centerline (m), z_s is the height

of the plume above the ground (m), U is the wind speed at the plume height (m/s) and the reflection term means the surface reflection coefficient [23], [28], [44], [55], [104].

7.1.3 ISC3

The ground-level concentration at a receptor located downwind of the area source is given by the following expression. The σ_z is directly proportional to downwind distance and the plume function is also considered to be infinite for a downwind receptor distance of 0 [23]. ISC3 arbitrarily sets the plume function to 0 when the receptor distance is less than 1 meter [105]. The model estimates the concentration or deposition value for each source and receptor combination for each hour of input meteorology and calculates user-selected short-term averages [52]. The expression for the concentration used for an area source in ISC3 is given in Equation (7.3).

$$C = \frac{Qk}{2\pi u_c} \int_0^x \frac{VD}{\sigma_z \sigma_y} \left(\int_0^y \exp\left[-0.5 \left(\frac{y}{\sigma_y} \right)^2 \right] dy \right) dx \tag{7.3}$$

where, k units scaling coefficient, V is vertical term, D is the decay term as a function of x.

7.1.4 SLSM

SLSM is a simple line-source model used to calculate the concentration of the pollutant from a mobile source using basic meteorological data and source information. The concentration is uniform in the y-direction at any given downwind distance. The wind direction is considered normal to the line of emission. If the wind direction is not normal to the line of emission, then θ (the angle between the wind direction and line source) is considered, and sin θ appears in the equation. The sinθ is not used in the equation if the angle is less than 45 degrees.

$$C_{(x,0)} = \frac{2q}{(2\pi)^{\frac{1}{2}} \sigma_z u \sin\theta} \exp\left[-\frac{1}{2} \left(\frac{H}{\sigma_z} \right)^2 \right] \tag{7.4}$$

Equation (7.4) is taken from the textbook by Wark et al. [3].

7.2 Predicted vs Observed Pollutant Concentrations

Difference measures represent a quantitative estimate of the size of the differences between observed and predicted values. Correlation is the quantitative measure of the association between observed and predicted values. A model's ability to predict air pollution levels under changing conditions can only be tested after field measurements are taken under similarly changing conditions. These requirements cause the calibration of models to be a very expensive and often time-consuming study. The usual way to evaluate the predictions from a model is to draw a scatter diagram using predicted values and observed values. A variation of this approach is by computing the ratio of the predicted to the observed value. Literature in the fields of science and engineering is full of such examples. Typically, the ratio (Co/Cp) of a good model, should not exhibit any trend with variables such as wind speed and stability class, and should not exhibit large deviations from unity (implying a perfect match between the model and observed). The usual way to evaluate predictions from a model is to draw a scatter diagram using Cp and Co [85]. Scatter plots and Cp/Co plots are simulated for SLINE 1.1, SAREA 1.1, and SLINE PM 1.1 after running with the considered datasets. Hereby Cp1- Gaseous model predictions of SLINE 1.1, Cp2- Gaseous model predictions of SAREA 1.1, Cp3- Gaseous model predictions of CLINE4, Cp4- Gaseous model predictions of ADMS, Cp5- Gaseous model predictions of ISC3, Cp6- Gaseous model predictions of SLSM, Cp(SLINE PM 1.1)- PM model predictions of SLINE PM 1.1, and Cp(SLSM)- PM model predictions of SLSM.

7.2.1 Scatter Plots

The scatter plots using Cp and Co values are presented in this section. The graphical analysis gives a qualitative measure of the model performance. The performance of each model can be observed visually and identify the best performing model by observing the trendline of each

model's predictions. The scatter plots are based on a linear scale. Figures from 7-1 to 7-10 represent the scatter plots for the predicted concentrations of gaseous pollutants. Figures from 7-11 to 7-14 represent the scatter plots for the predicted concentrations of PM of different particle size ranges.

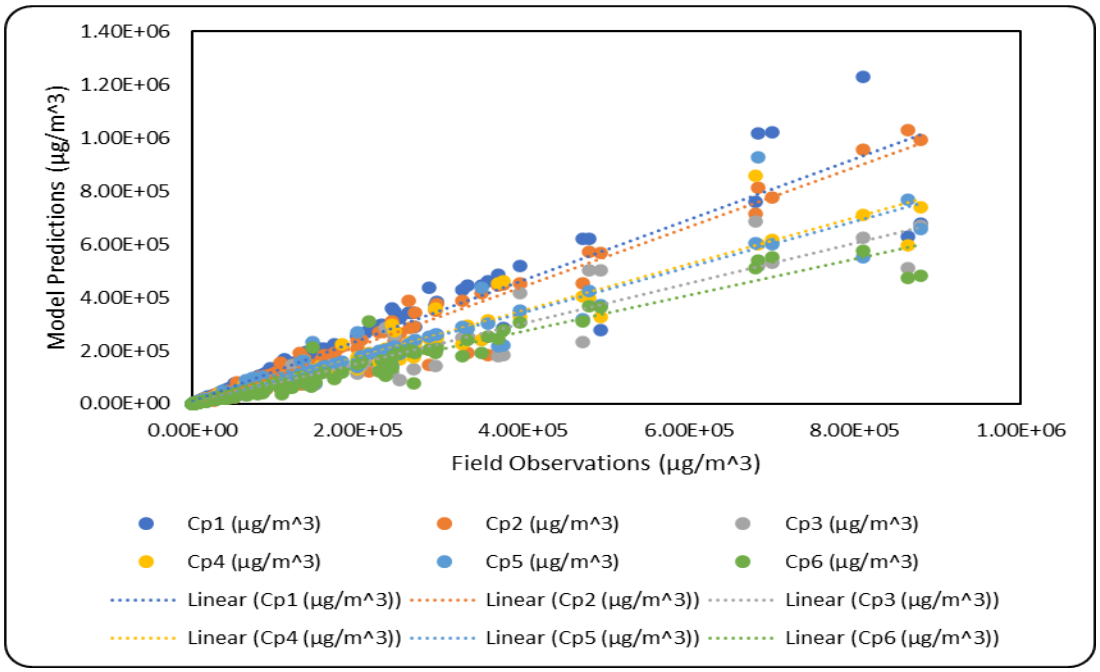

Figure 7-1: Model predictions vs Field Observations with CALTRANS data (SF_6) for stable atmospheric conditions

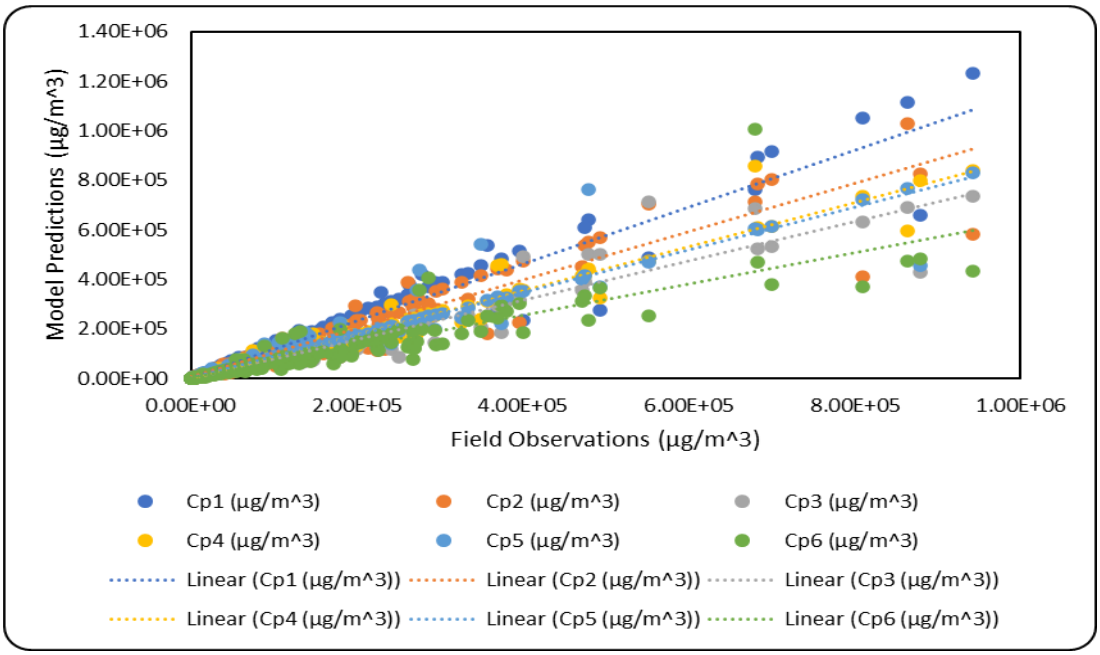

Figure 7-2 Model predictions vs Field Observations with CALTRANS data (SF_6) for unstable atmospheric conditions

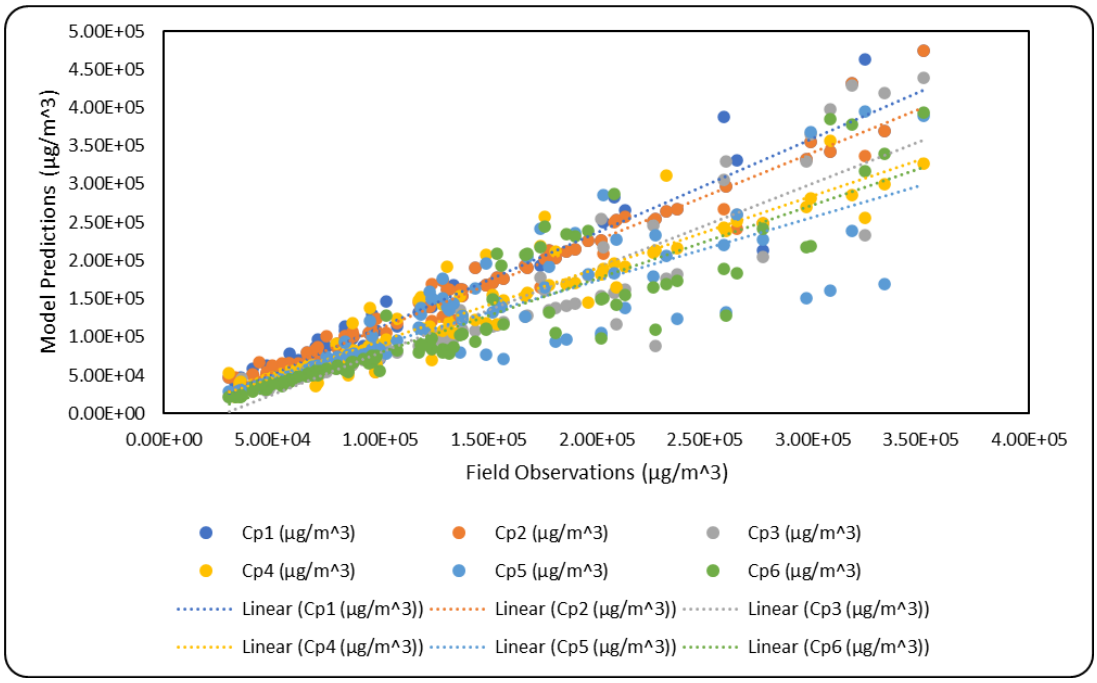

Figure 7-3: Model predictions vs Field Observations with Idaho Falls data (SF_6) for stable atmospheric conditions

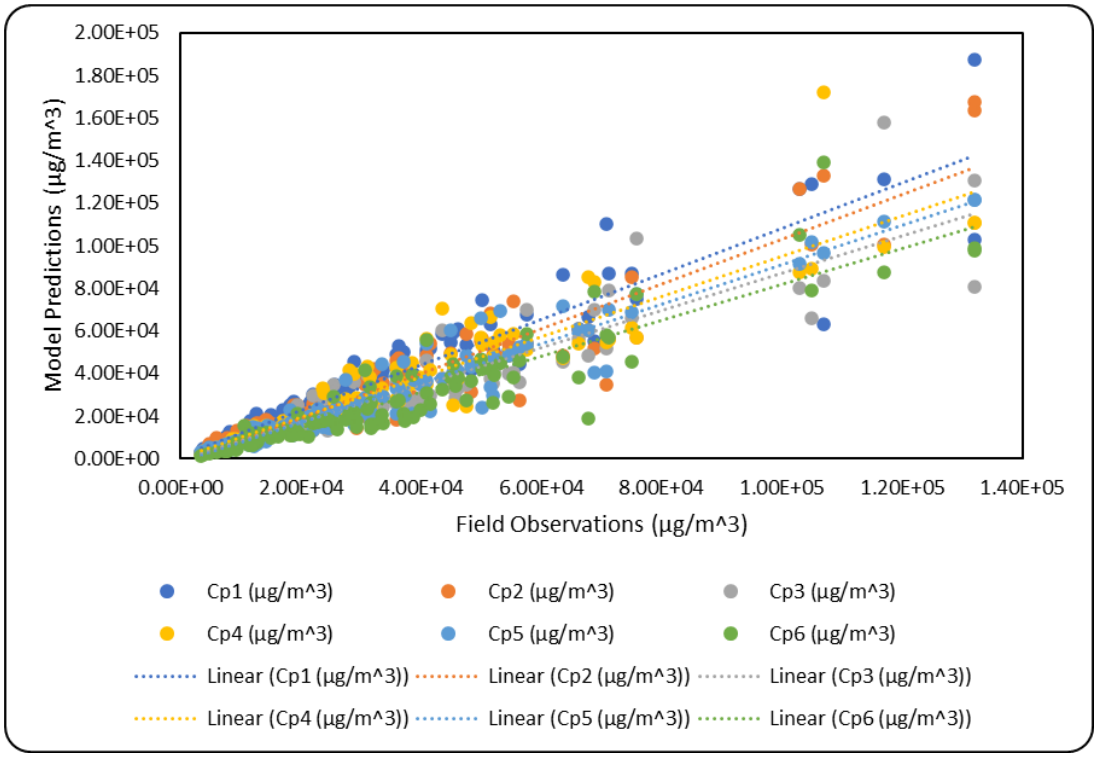

Figure 7-4: Model predictions vs Field Observations with Idaho Falls data (SF_6) for unstable atmospheric conditions

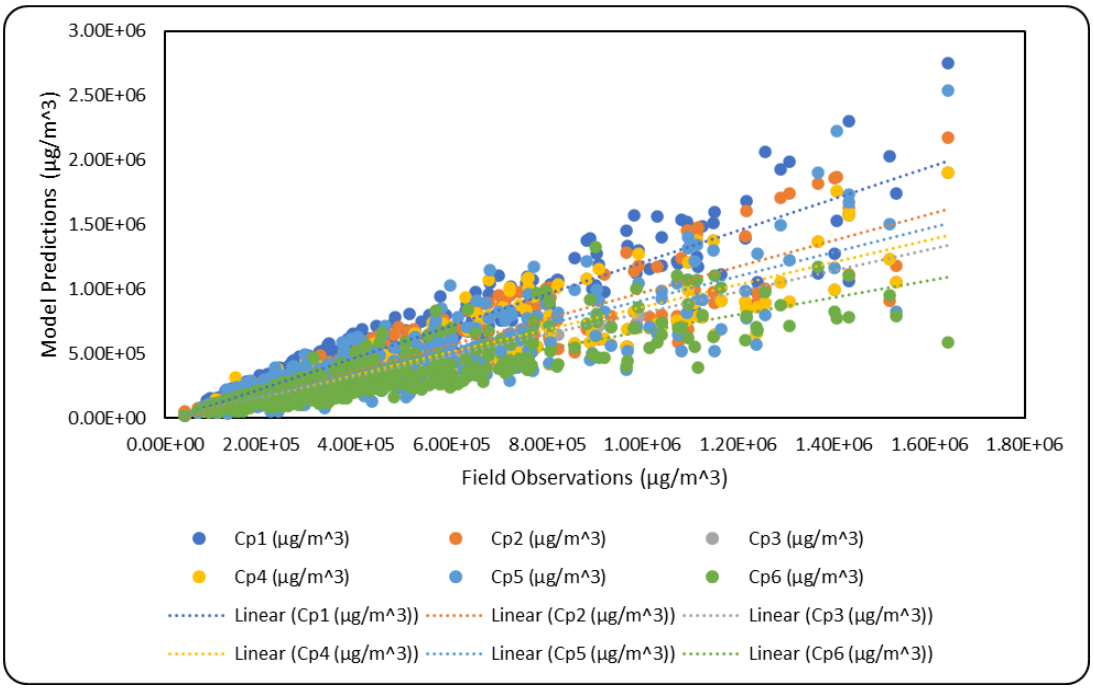

Figure 7-5: Model predictions vs Field Observations with Raleigh data (NO) for stable atmospheric conditions

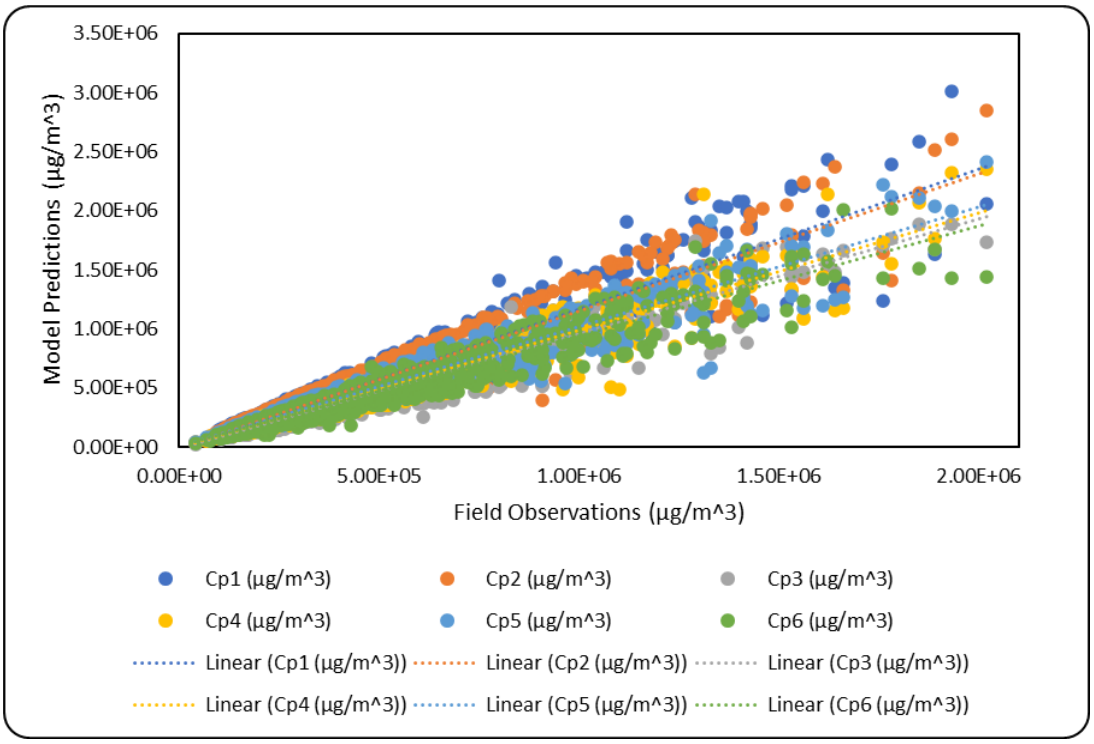

Figure 7-6: Model predictions vs Field Observations with Raleigh data (NO) for unstable atmospheric conditions

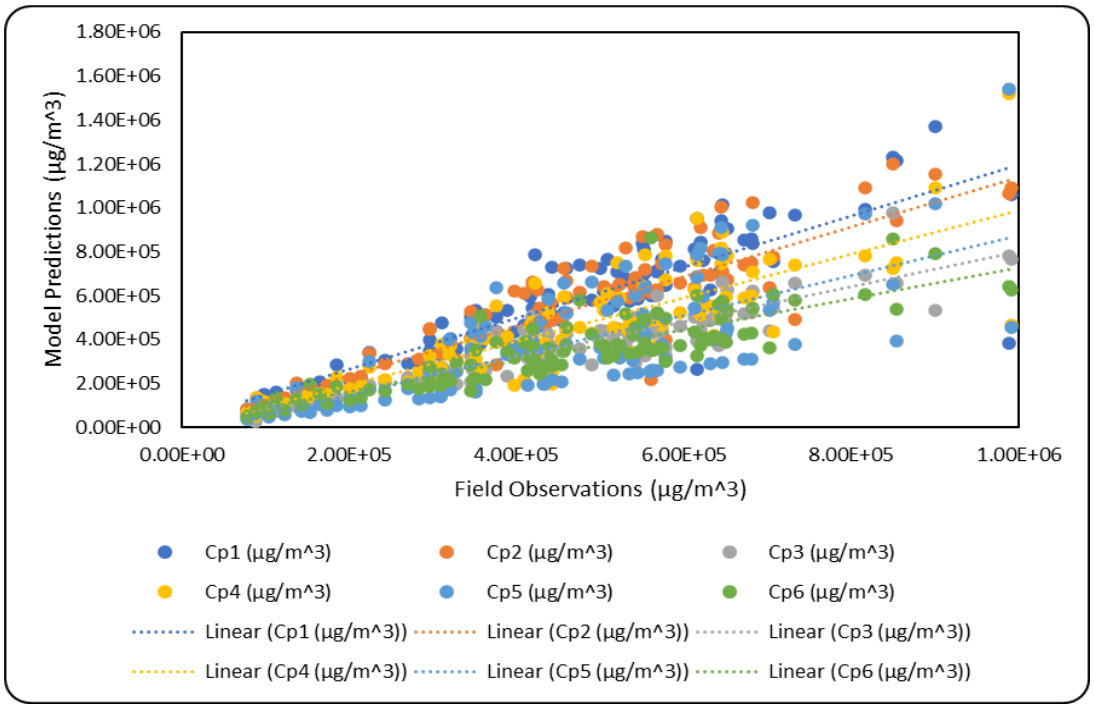

Figure 7-7: Model predictions vs Field Observations with Hyderabad data (CO_2) for stable atmospheric conditions

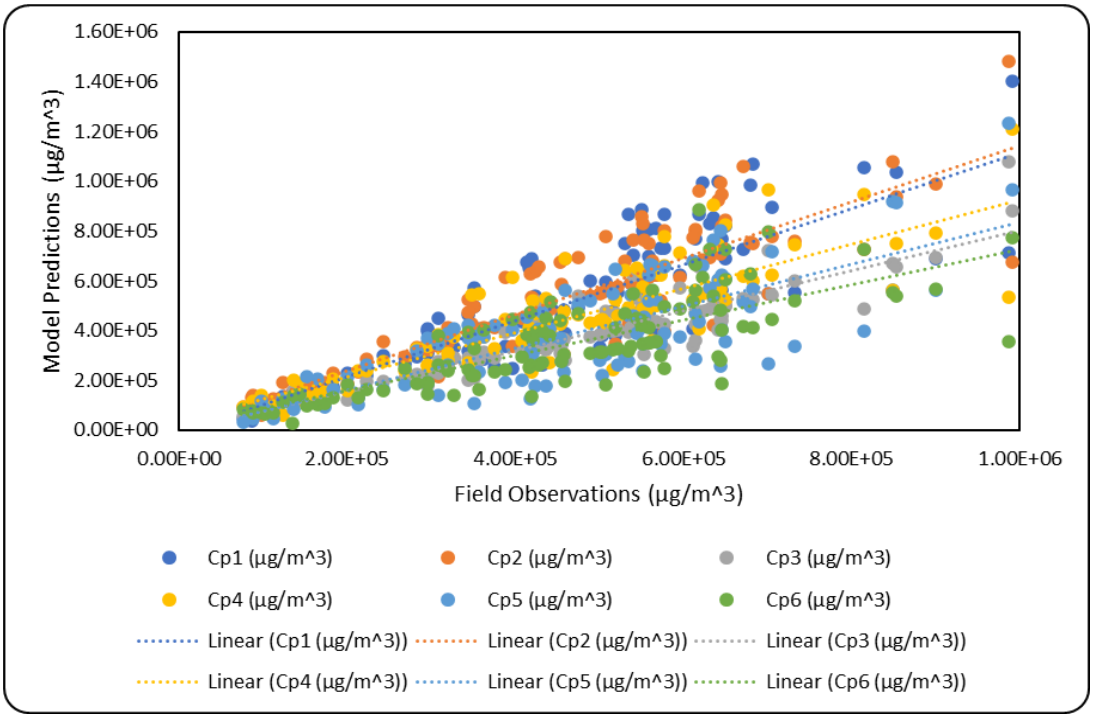

Figure 7-8: Model predictions vs Field Observations with Hyderabad data (CO_2) for unstable atmospheric conditions

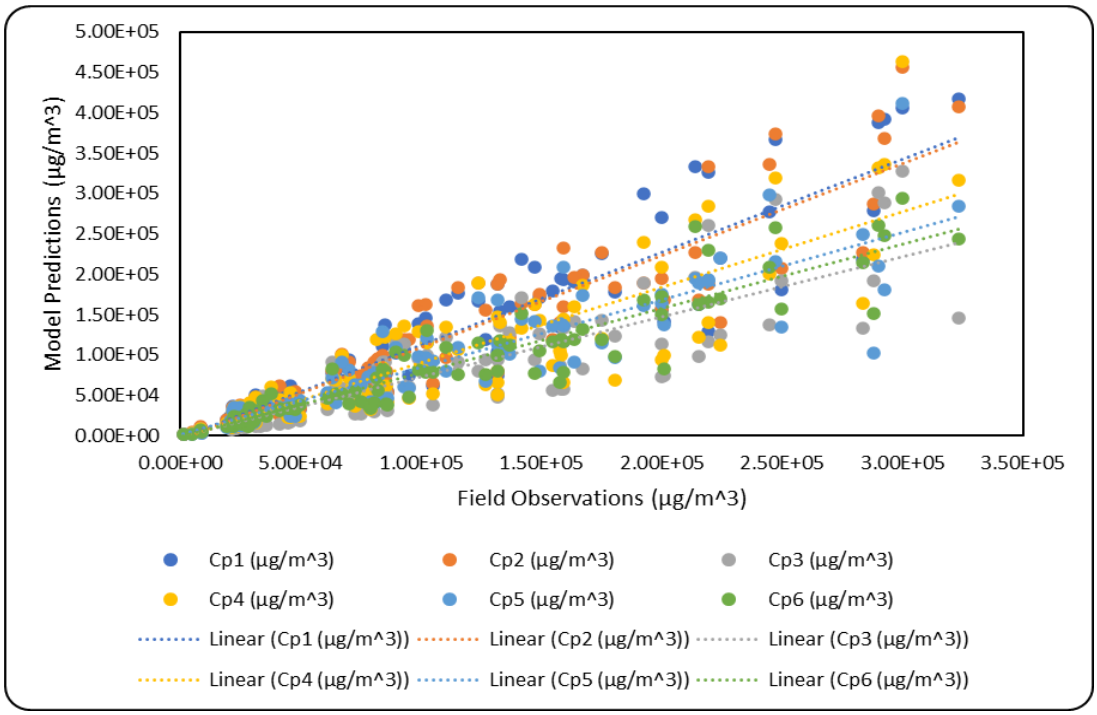

Figure 7-9: Model predictions vs Field Observations with Hyderabad data (NO_2) for stable atmospheric conditions

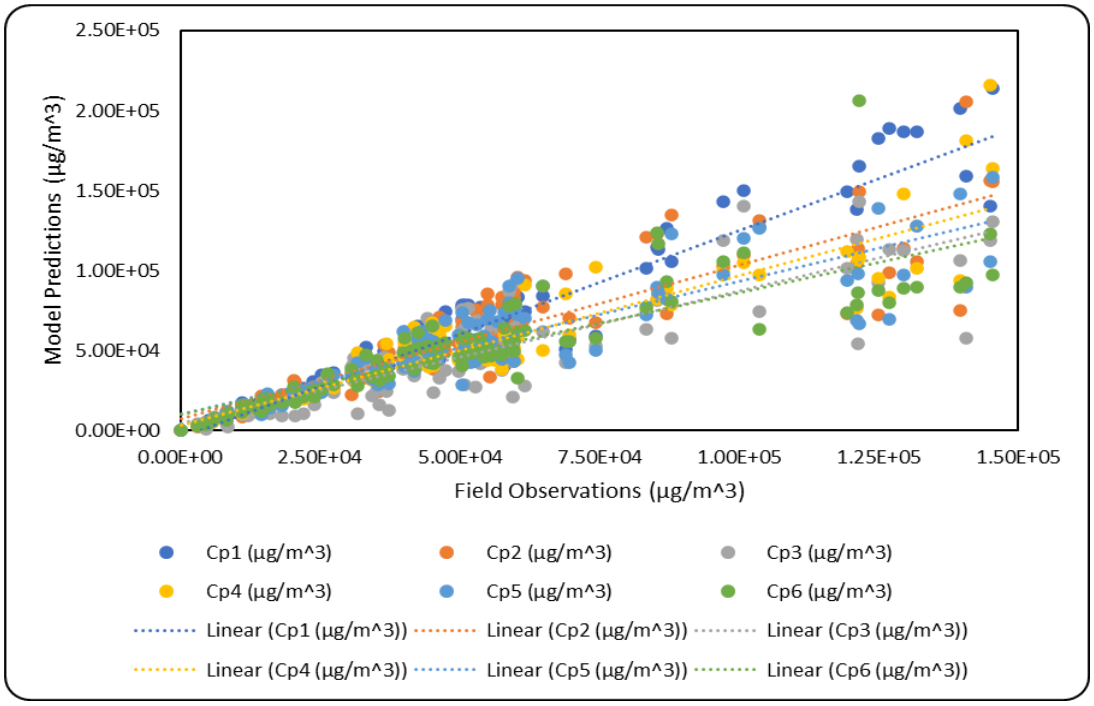

Figure 7-10: Model predictions vs Field Observations with Hyderabad data (NO_2) for unstable atmospheric conditions

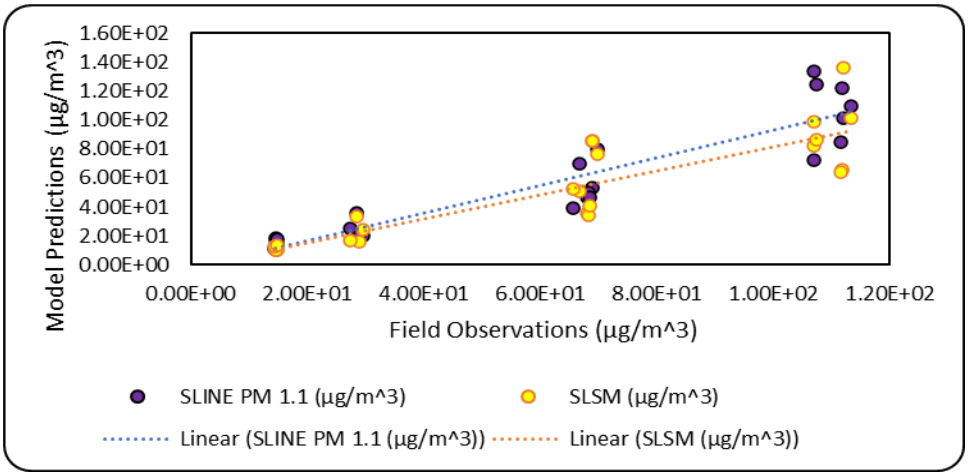

a) For particle size >10 µm

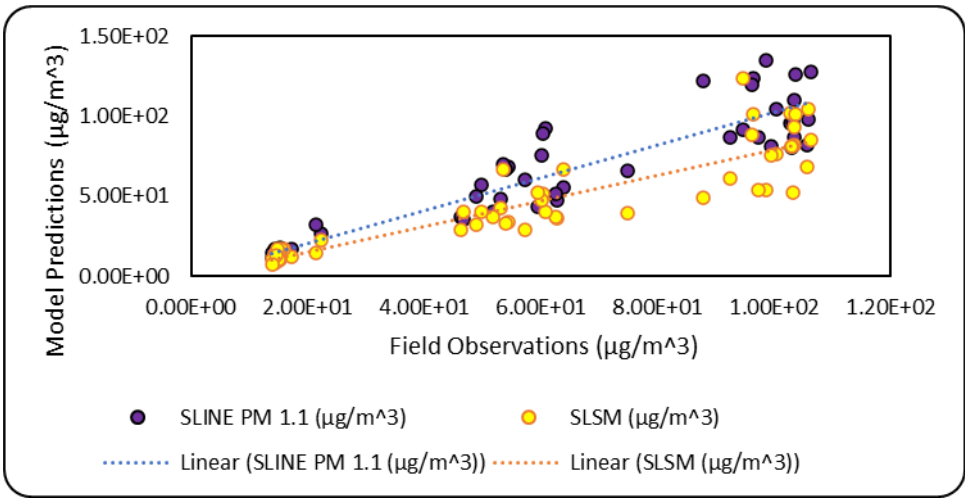

b) For particle sizes between 10 and 2.5 µm

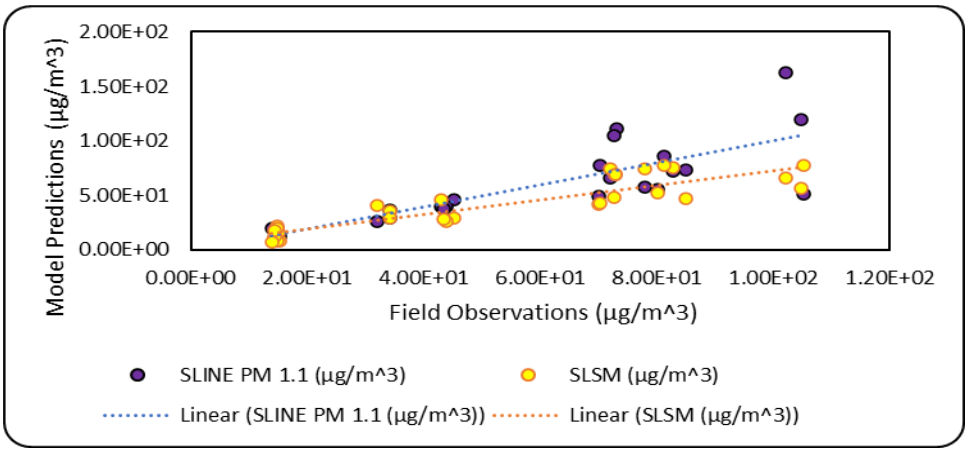

c) For particle size <2.5 µm

Figure 7-11: Model predictions vs Field Observations with Hyderabad data (PM) considering different particle size ranges for stable atmospheric conditions

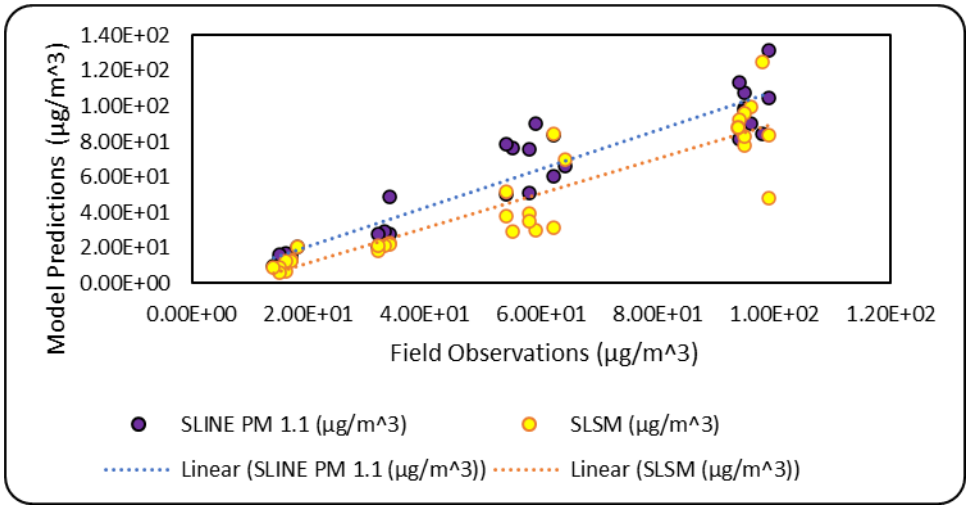

a) For particle size >10 µm

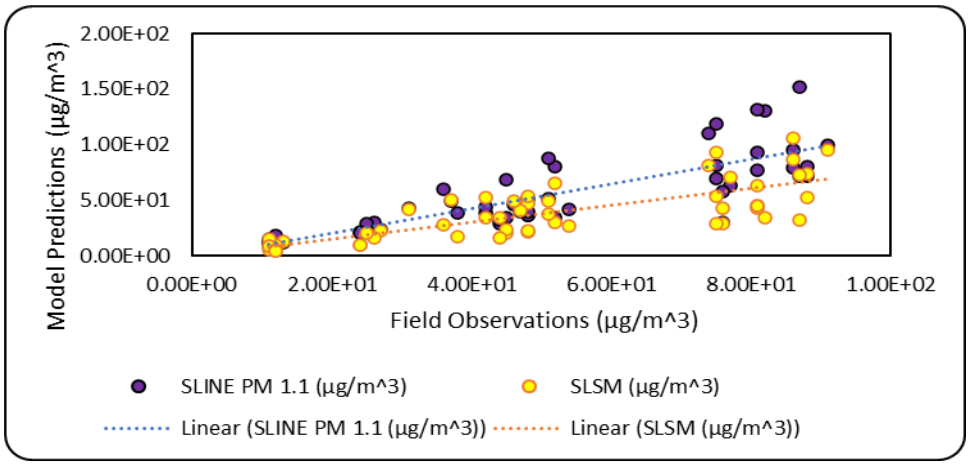

b) For particle sizes between 10 and 2.5 µm

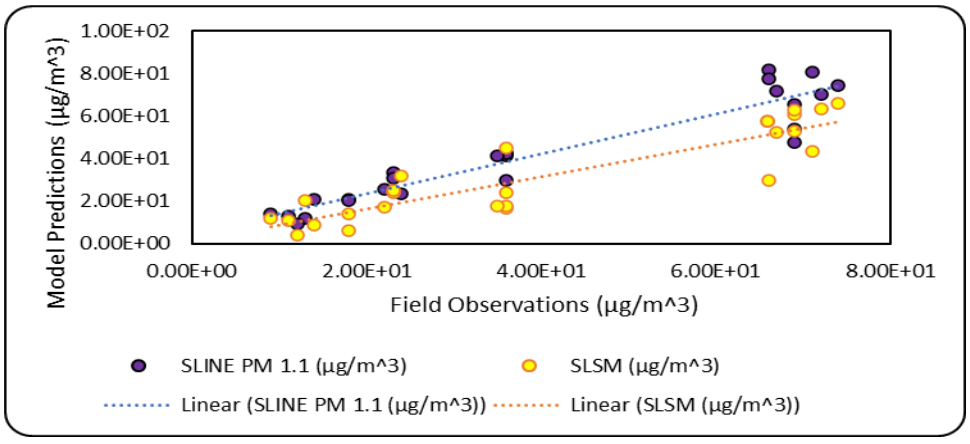

c) For particle size <2.5 µm

Figure 7-12: Model predictions vs Field Observations with Hyderabad data (PM) considering different particle size ranges for unstable atmospheric conditions

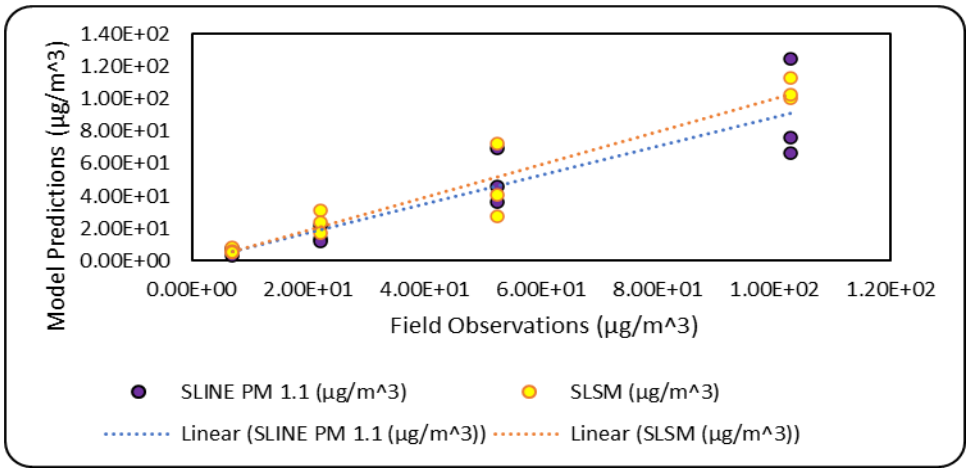

a) For particle sizes between 10 and 2.5 µm

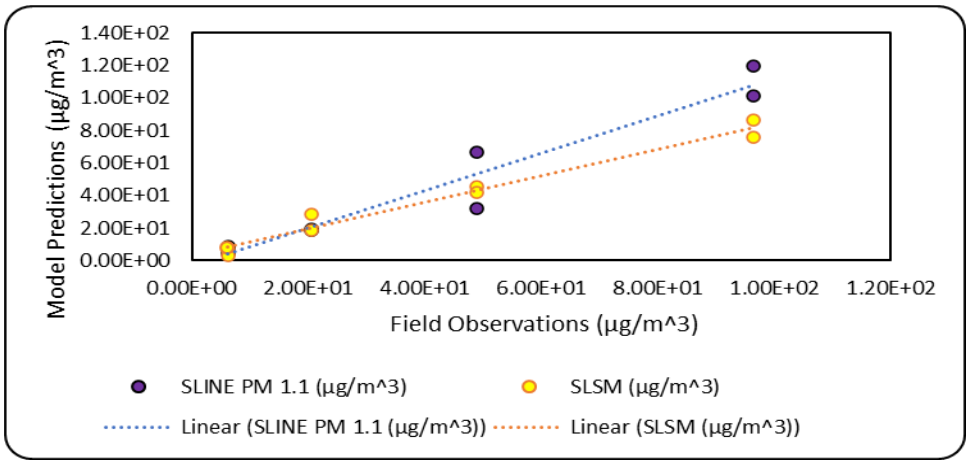

b) For particle sizes between 2.5 and 0.1 µm

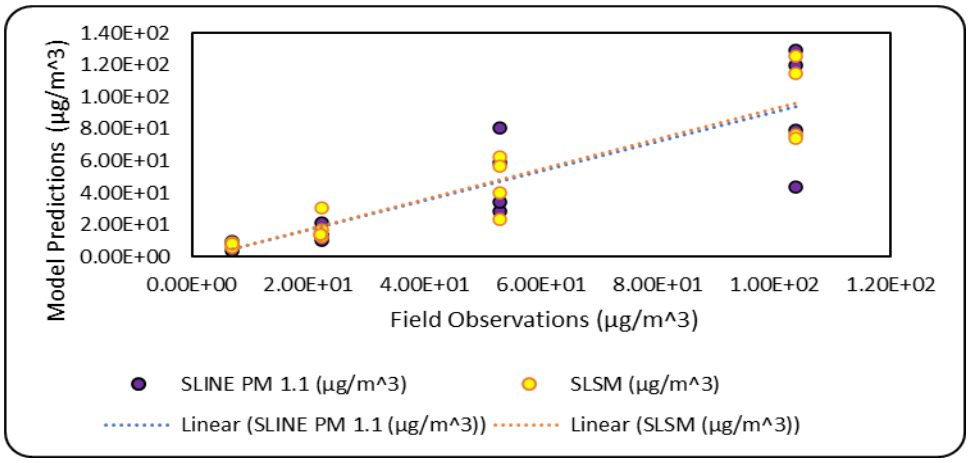

c) For particle size <0.1 µm

Figure 7-13: Model predictions vs Field Observations with Raleigh data (PM) considering different particle size ranges for unstable atmospheric conditions

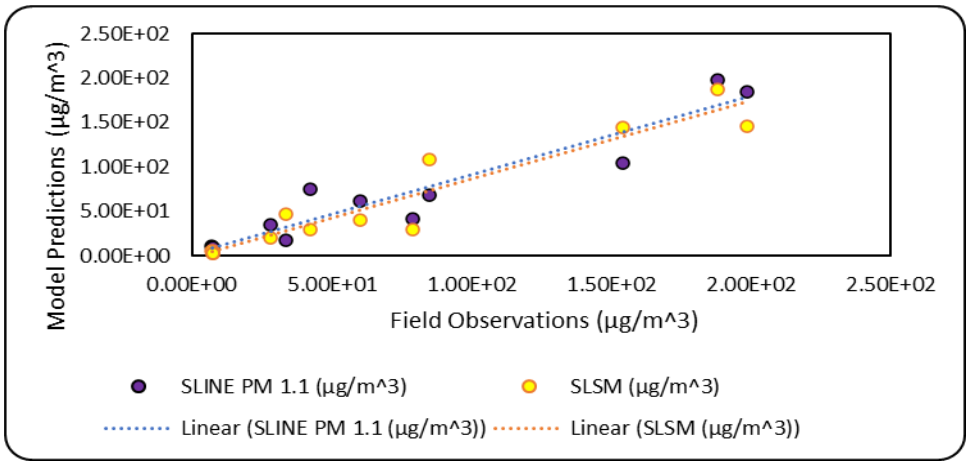

a) For particle sizes between 10 and 2.5 µm

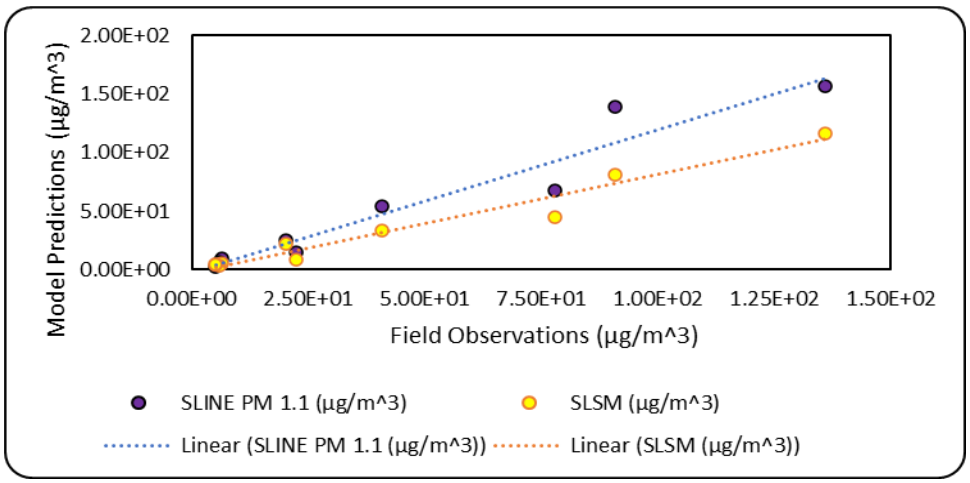

b) For particle sizes between 2.5 and 0.1 µm

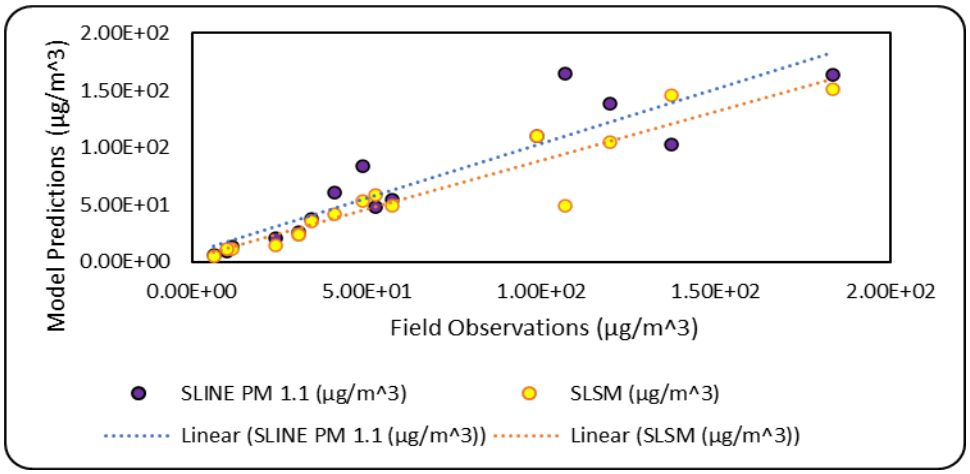

c) For particle size <0.1 µm

Figure 7-14: Model predictions vs Field Observations with Raleigh data (PM) considering different particle size ranges for unstable atmospheric conditions

The trend lines were drawn in every plot to identify the prediction trends of each model. Results with CALTRANS data, it can be observed that SLINE 1.1 has a trendline higher than the other models which means the model is overpredicting other models. SAREA 1.1 predictions are lower than the SLINE 1.1. A similar set of plots were plotted with all the other data sets to observe the performance of all the models. With Idaho Falls data (SF_6) the SLINE 1.1 has the highest trend line for both stability conditions. With Raleigh data for unstable conditions, it can be observed that the predictions of SLINE 1.1 and SAREA 1.1 are close enough and the trend lines are almost overlapping. Using Hyderabad (CO_2) for unstable conditions, it can be observed that the predictions of SAREA 1.1 are a little higher than SLINE 1.1. Using Hyderabad data (NO_2) for stable conditions, it can be observed that the predictions of SLINE 1.1 and SAREA 1.1 are close enough and the trend lines are almost overlapping.

SLINE PM 1.1 is performing better for the Hyderabad PM data set for all the particle size ranges and both the stable conditions. SLINE PM 1.1 is performing better for the Hyderabad PM data set for all the particle size ranges and both the stable conditions.

Overall, for gaseous models, it is observed from scatter plots that SLINE 1.1 is mostly over predicting in all the data sets than all the other models. The trendline of SLINE 1.1 is higher than all the data sets except for Hyderabad data for unstable atmospheric conditions. Overall, for PM models, it is observed from scatter plots that SLINE PM 1.1 is over predicting than SLSM with Hyderabad data set for all the particle sizes. SLSM is over predicting that SLINE PM 1.1 for Particle size between 10 and 2.5 µm and <0.1 µm with Raleigh data set for stable conditions. It can be observed that the predictions of low concentrations of SLINE PM 1.1 and SLSM are close to the larger concentrations.

7.2.2 Cp/Co Plots

Generally, the ratio (Cp/Co) of a good model should not exhibit large deviations from the unity, which implies a perfect match between the model predictions and observed values [46]. The plots in Figures 7-15 to 7-24 (gaseous) and Figures 7-25 to 7-28 (PM) are the plots for the Cp/Co ratio at different downwind distances.

The model predictions for SLINE 1.1, SAREA 1.1, CALINE4, ADMS, ISC3, and SLSM are simulated for the considered data sets. The predicted concentrations were computed using the generic equations and compared with the observed values measured during these real-time field studies. All the computed concentrations were computed at the same height as measured concentrations were taken during the field work. The plots indicate the relativity between the predicted/observed concentrations at measured downwind distances.

The ratio (Cp/Co) of a good model should exhibit values close to unity. If the values are equal to the unity, which implies a perfect match between the model predictions and observed values. Practically it is impossible to achieve for all the data points. If the Cp/Co value is greater than 1 then the model is over-predicting and less than 1 then the model is under-predicting.

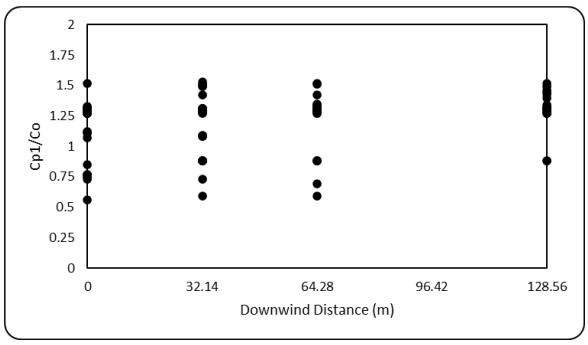

a) Using SLINE 1.1 predictions

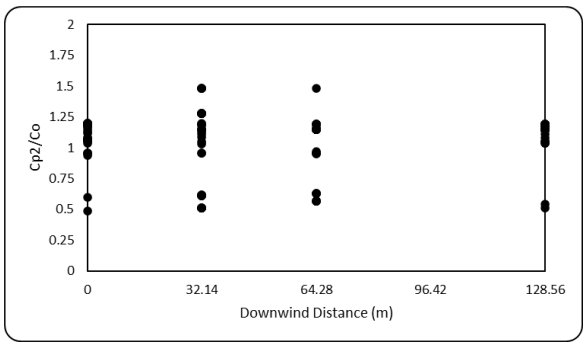

b) Using SAREA 1.1 predictions

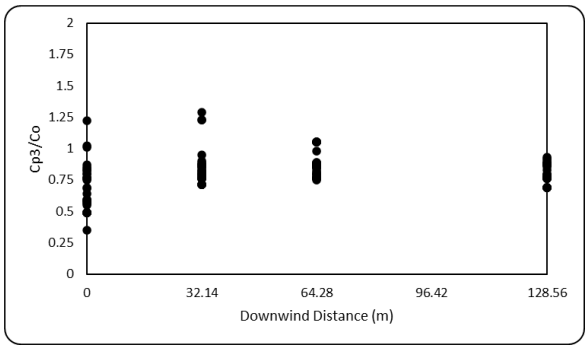

c) Using CALINE 4 predictions

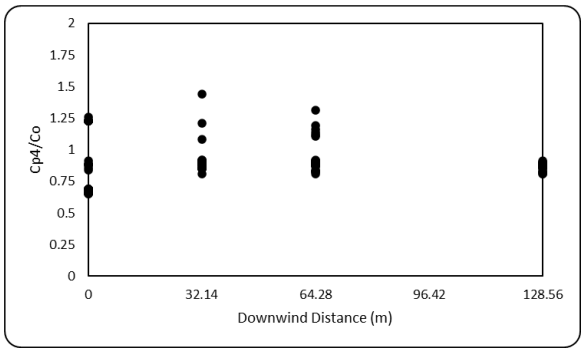

d) Using ADMS predictions

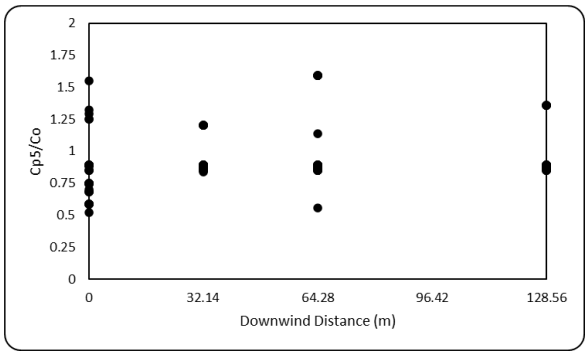

e) Using ISC3 predictions

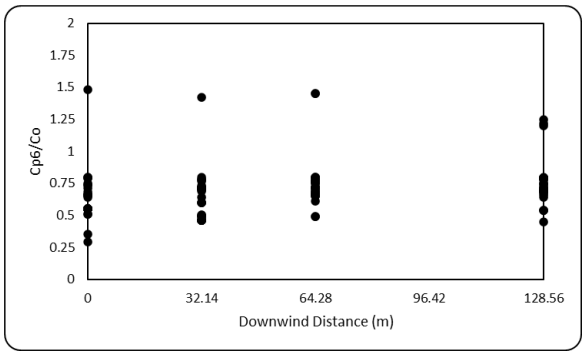

f) Using SLSM predictions

Figure 7-15: Predicted/observed vs downwind distance plots for CALTRANS data (SF_6) for stable atmospheric conditions using

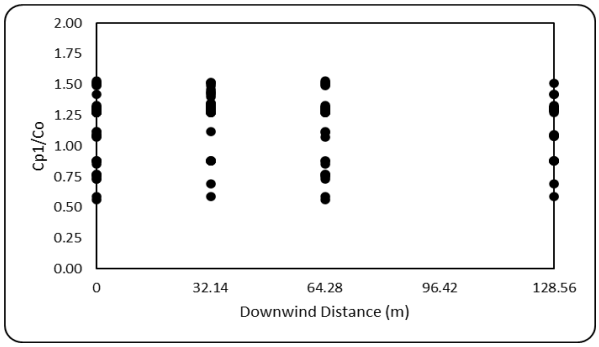

a) Using SLINE 1.1 predictions

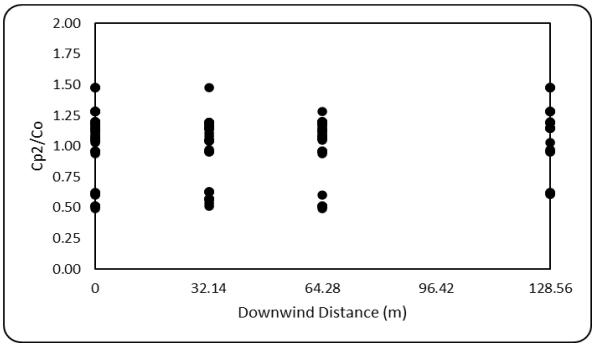

b) Using SAREA 1.1 prediction

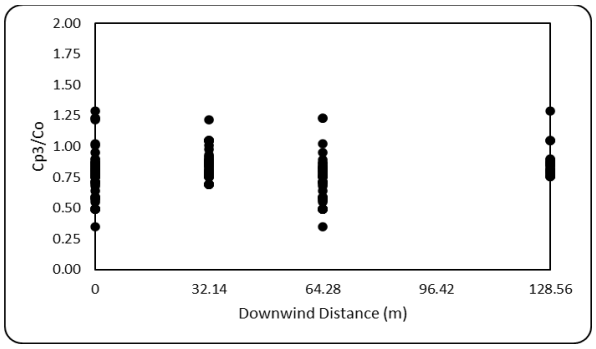

c) Using CALINE 4 predictions

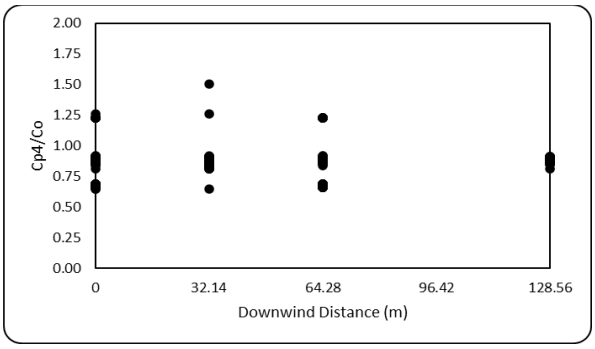

d) Using ADMS predictions

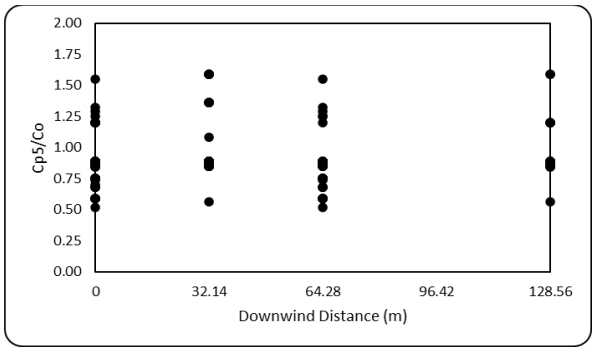

e) Using ISC3 predictions

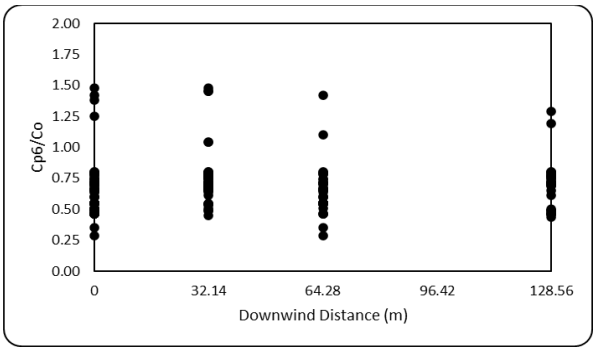

f) Using SLSM predictions

Figure 7-16: Predicted/observed vs downwind distance plots for CALTRANS data (SF_6) for unstable atmospheric conditions

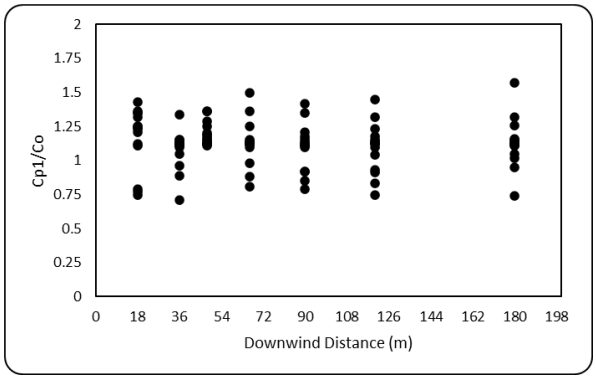

a) Using SLINE 1.1 predictions

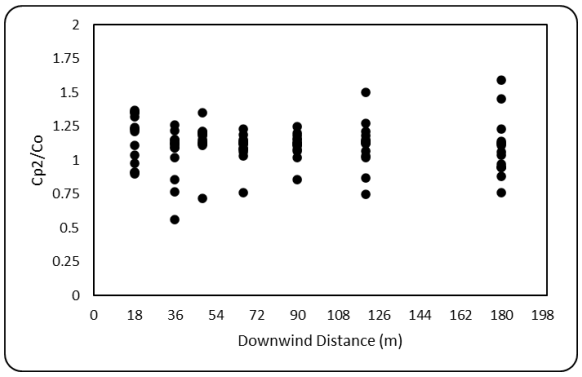

b) Using SAREA 1.1 prediction

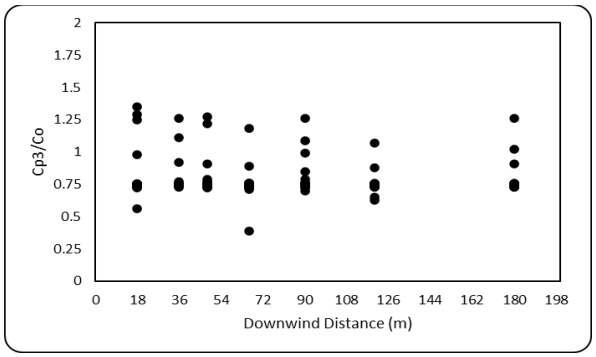

c) Using CALINE 4 predictions

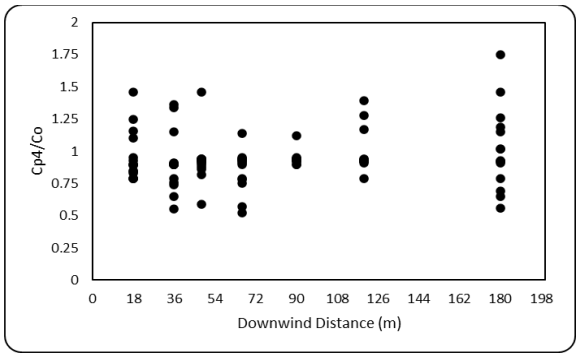

d) Using ADMS predictions

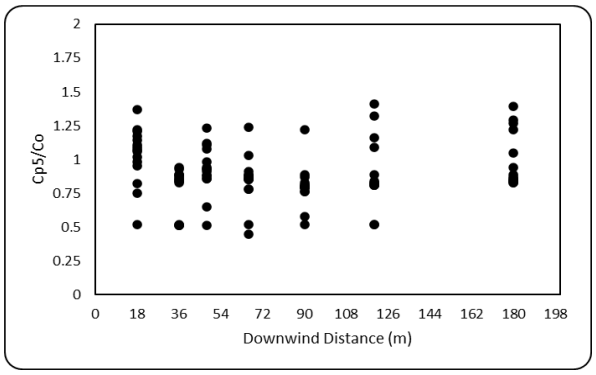

e) Using ISC3 predictions

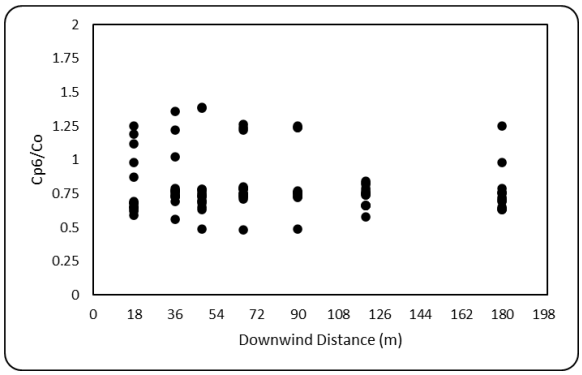

f) Using SLSM predictions

Figure 7-17: Predicted/observed vs downwind distance plots for Idaho Falls data (SF_6) for stable atmospheric conditions

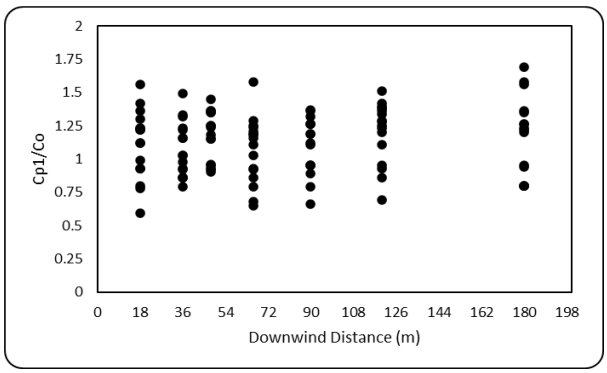

a) Using SLINE 1.1 predictions

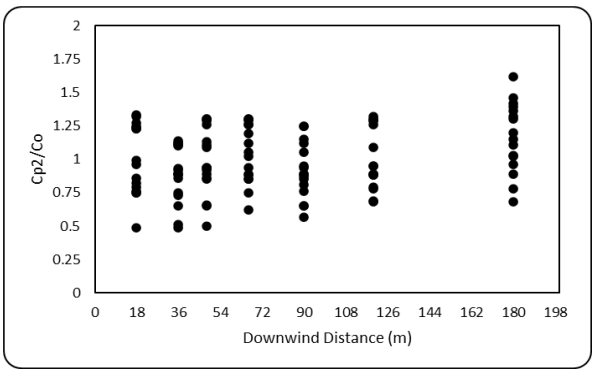

b) Using SAREA 1.1 prediction

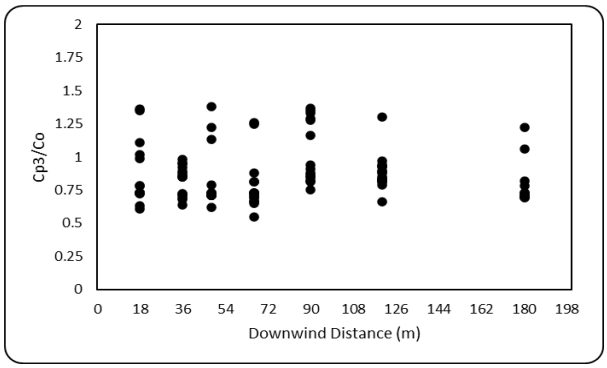

c) Using CALINE 4 predictions

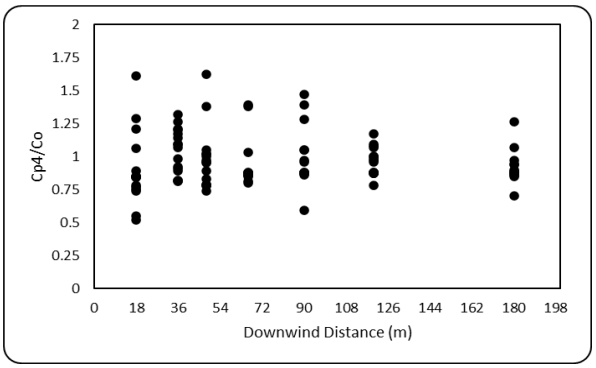

d) Using ADMS predictions

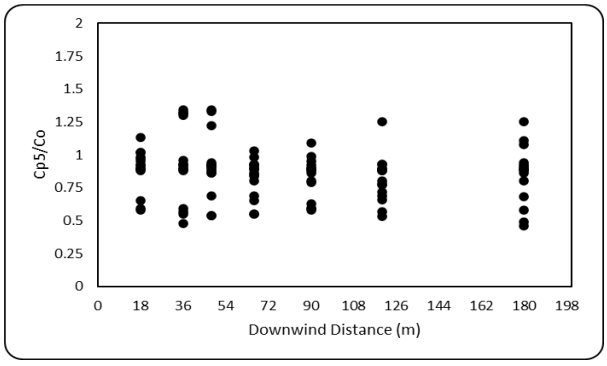

e) Using ISC3 predictions

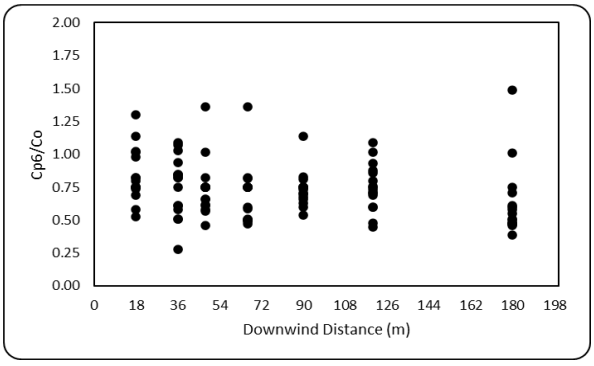

f) Using SLSM predictions

Figure 7-18: Predicted/observed vs downwind distance plots for Idaho Falls data (SF_6) for unstable atmospheric conditions

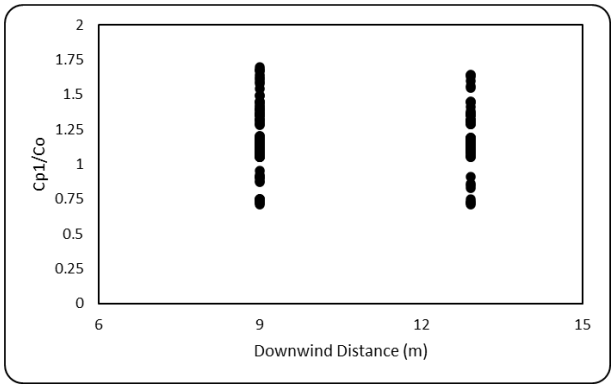

a) Using SLINE 1.1 predictions

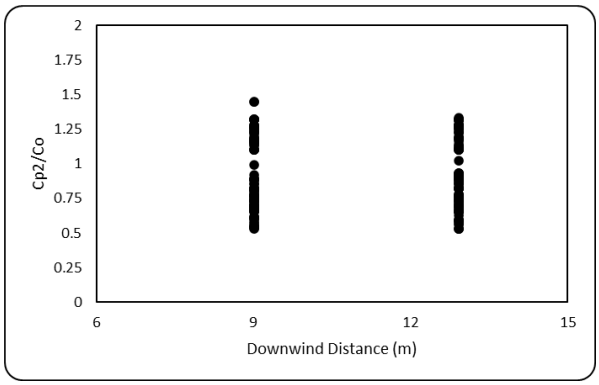

b) Using SAREA 1.1 prediction

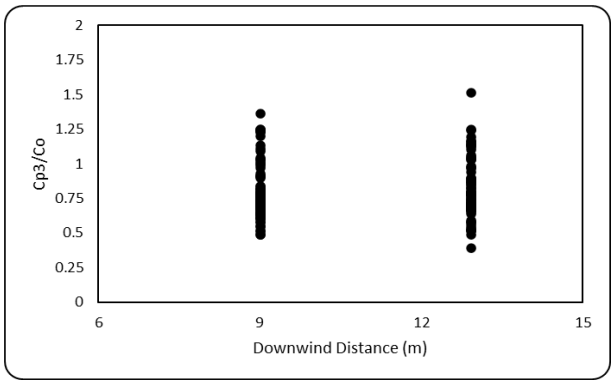

c) Using CALINE 4 predictions

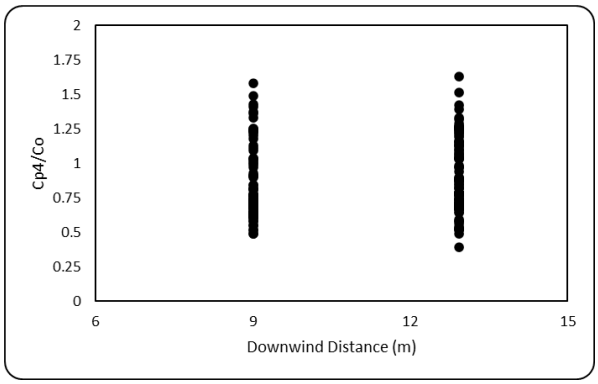

d) Using ADMS predictions

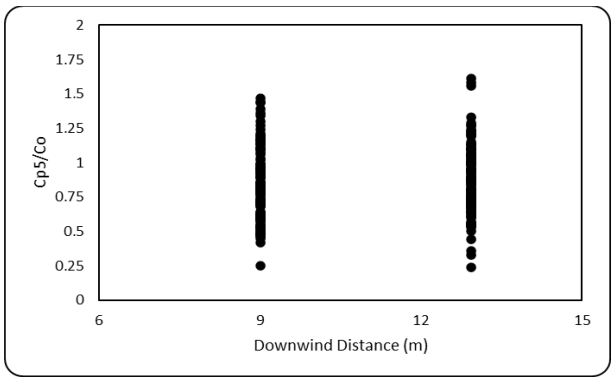

e) Using ISC3 predictions

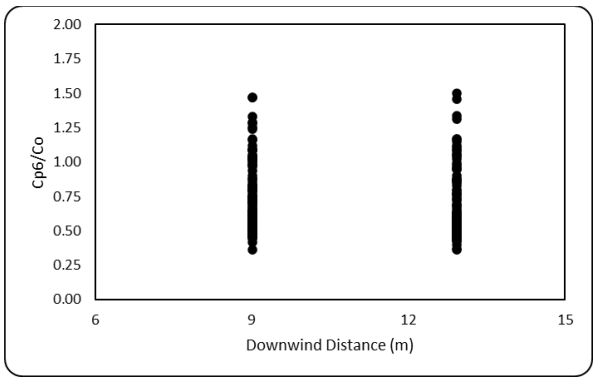

f) Using SLSM predictions

Figure 7-19: Predicted/observed vs downwind distance plots for Raleigh data (NO) for stable atmospheric conditions

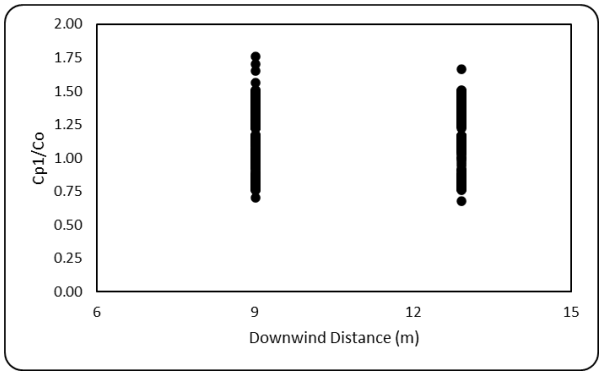

a) Using SLINE 1.1 predictions

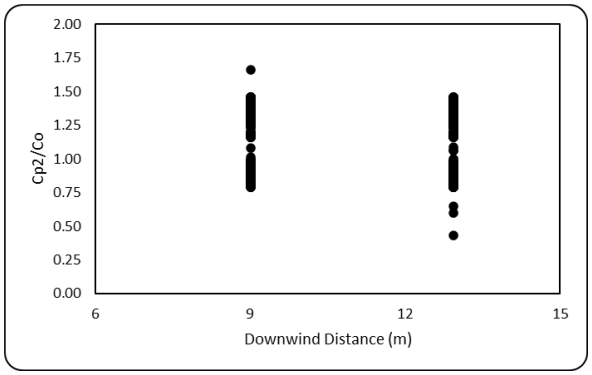

b) Using SAREA 1.1 prediction

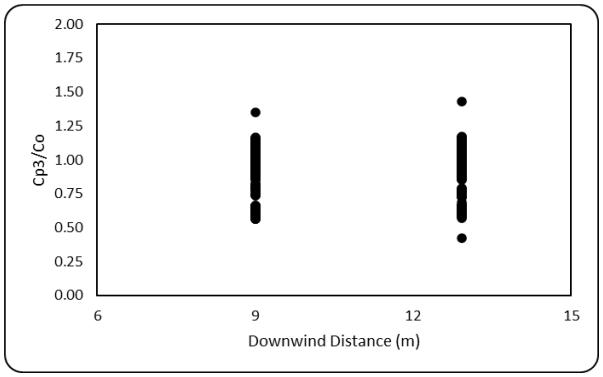

c) Using CALINE 4 predictions

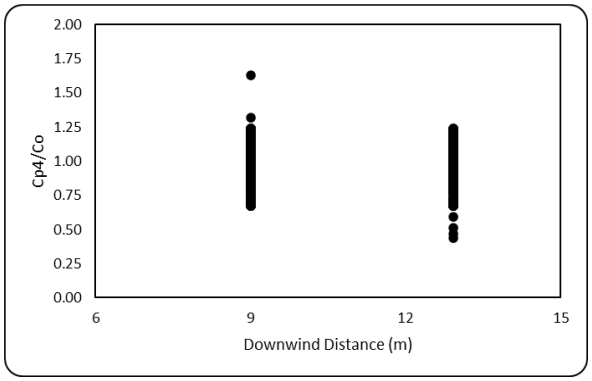

d) Using ADMS predictions

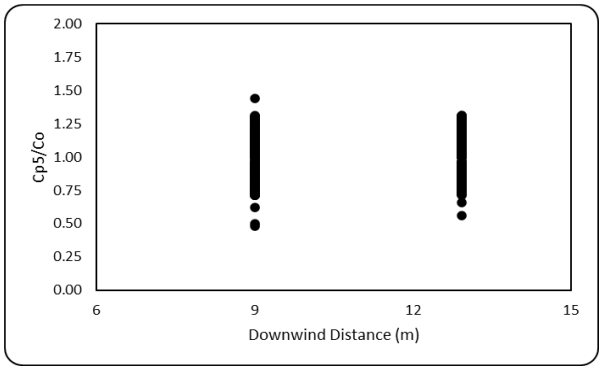

e) Using ISC3 predictions

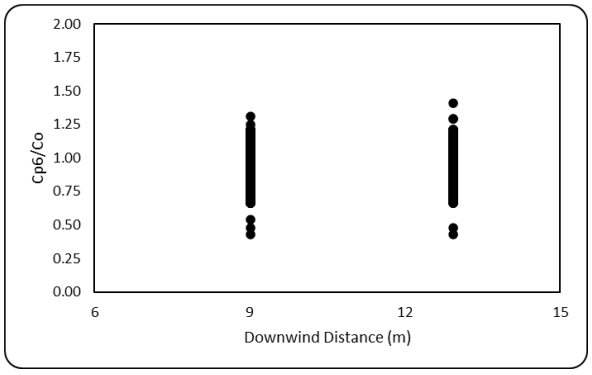

f) Using SLSM predictions

Figure 7-20: Predicted/observed vs downwind distance plots for Raleigh data (NO) for unstable atmospheric conditions

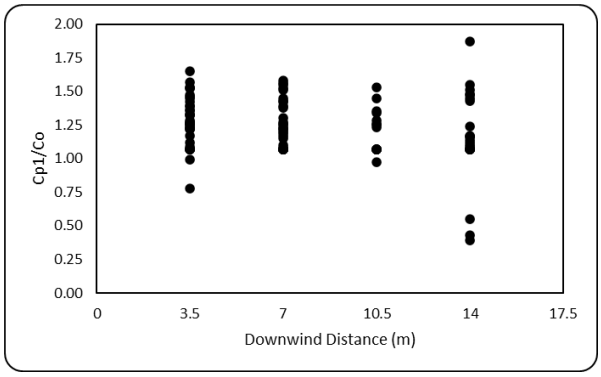

a) Using SLINE 1.1 predictions

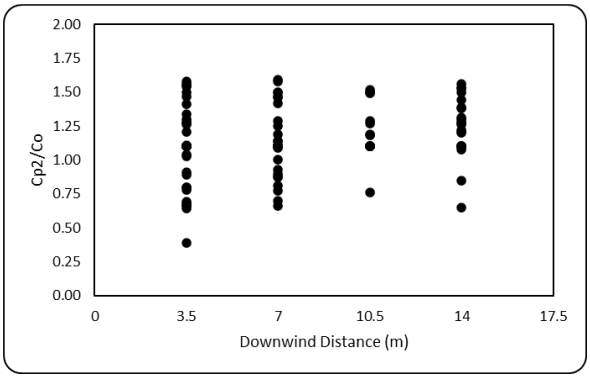

b) Using SAREA 1.1 prediction

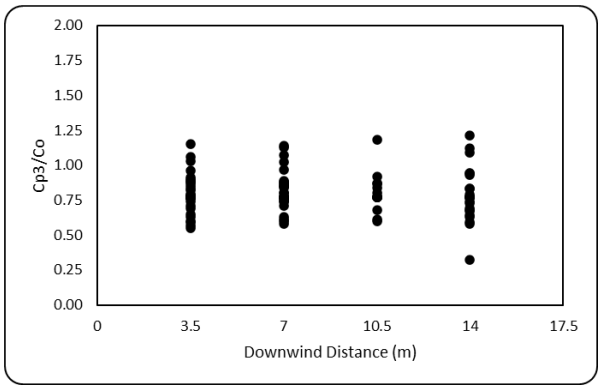

c) Using CALINE 4 predictions

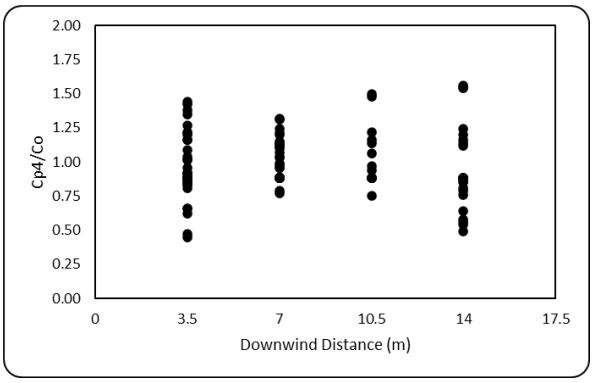

d) Using ADMS predictions

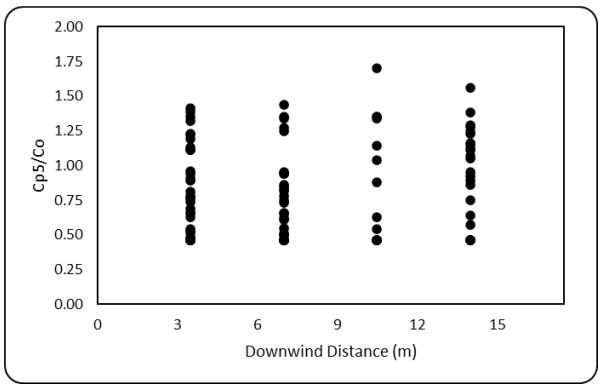

e) Using ISC3 predictions

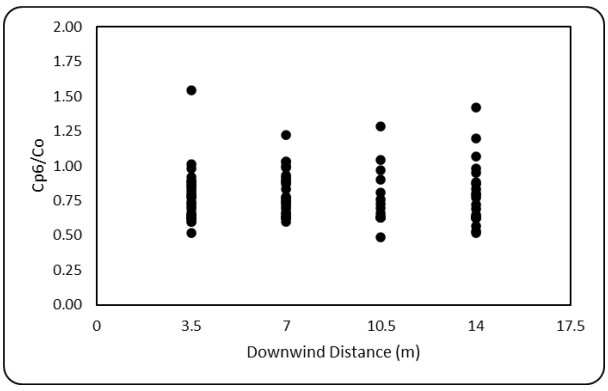

f) Using SLSM predictions

Figure 7-21: Predicted/observed vs downwind distance plots for Hyderabad data (CO_2) for stable atmospheric conditions

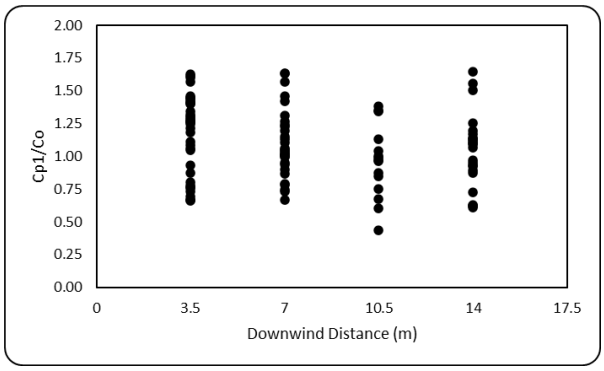

a) Using SLINE 1.1 predictions

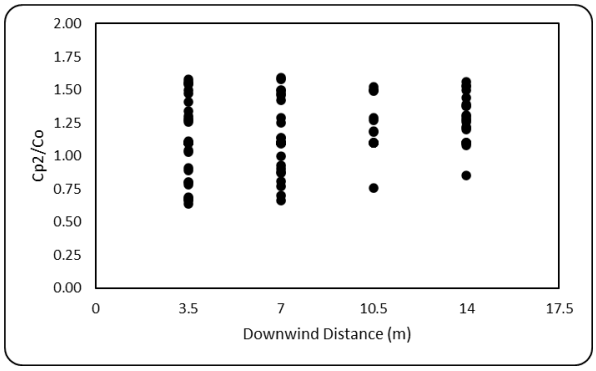

b) Using SAREA 1.1 prediction

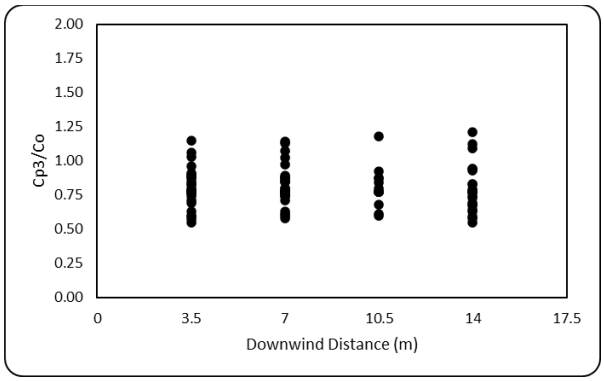

c) Using CALINE 4 predictions

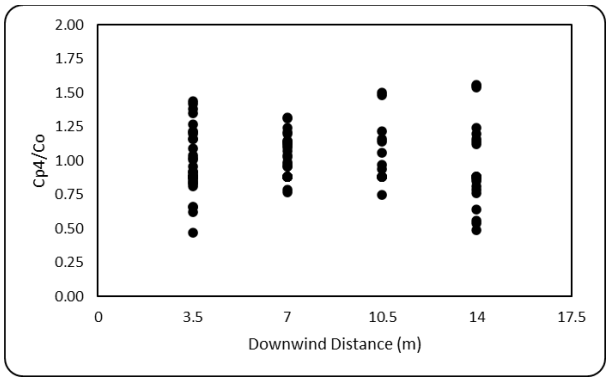

d) Using ADMS predictions

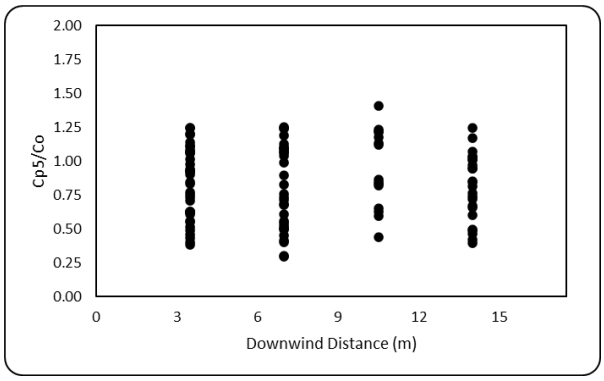

e) Using ISC3 predictions

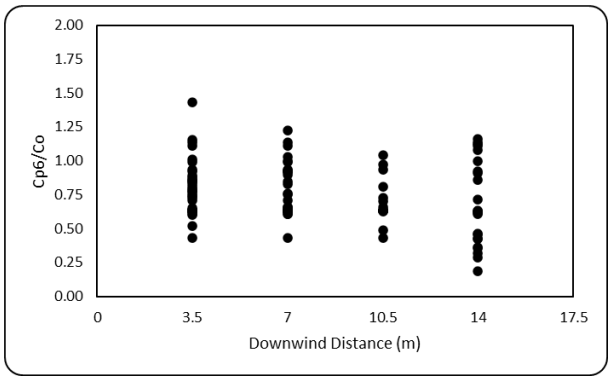

f) Using SLSM predictions

Figure 7-22: Predicted/observed vs downwind distance plots for Hyderabad data (CO_2) for unstable atmospheric conditions

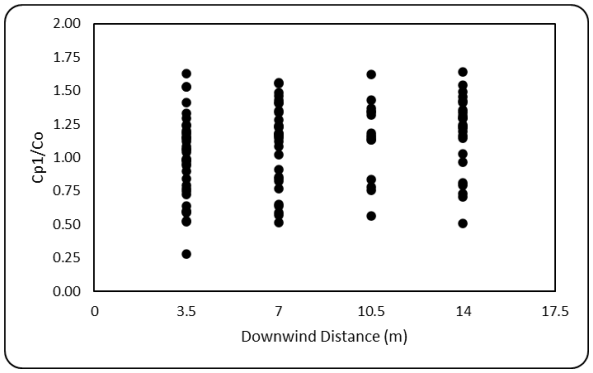

a) Using SLINE 1.1 predictions

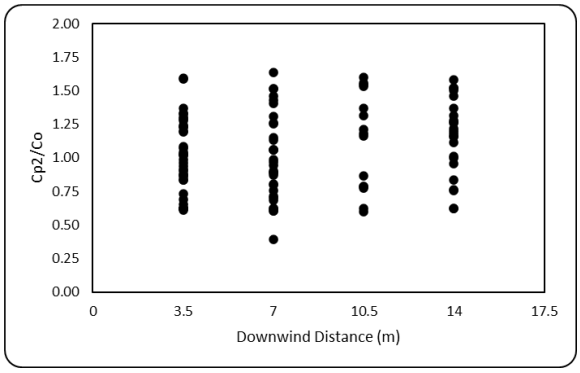

b) Using SAREA 1.1 predictions

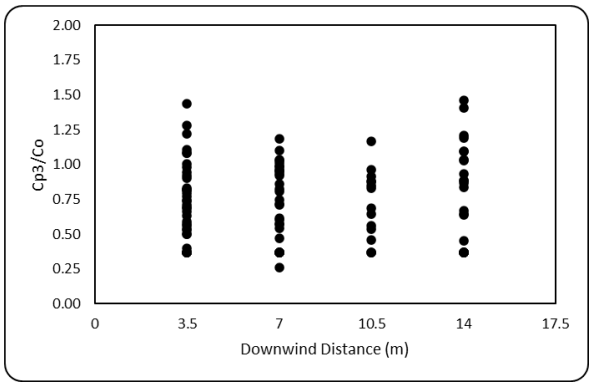

c) Using CALINE 4 predictions

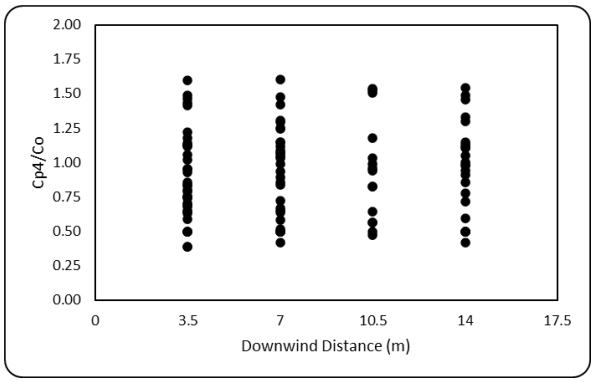

d) Using ADMS predictions

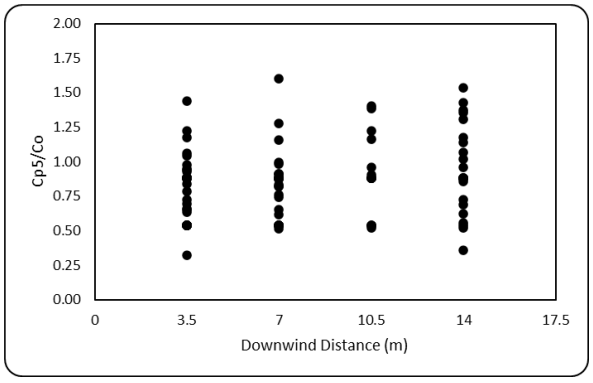

e) Using ISC3 predictions

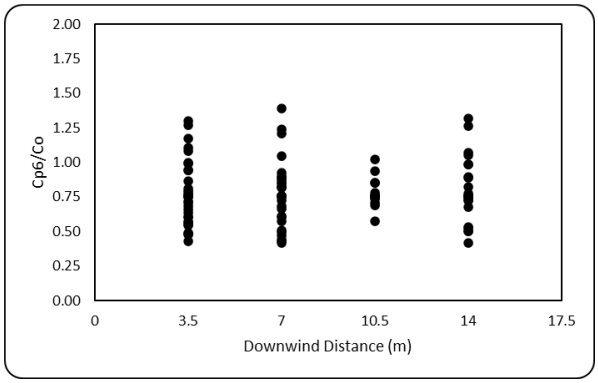

f) Using SLSM predictions

Figure 7-23: Predicted/observed vs downwind distance plots for Hyderabad data (NO_2) for stable atmospheric conditions

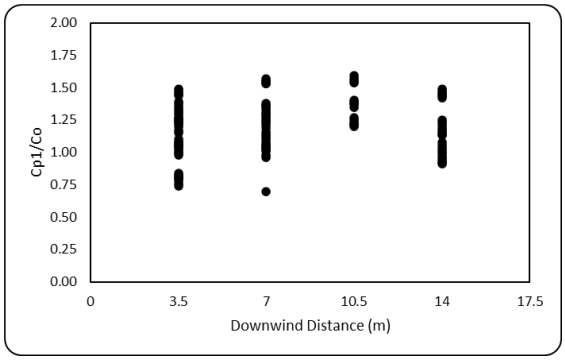

a) Using SLINE 1.1 predictions

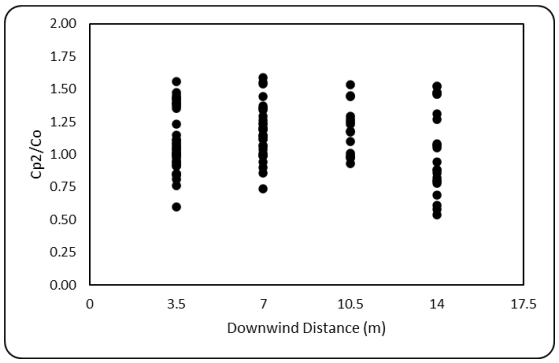

b) Using SAREA 1.1 predictions

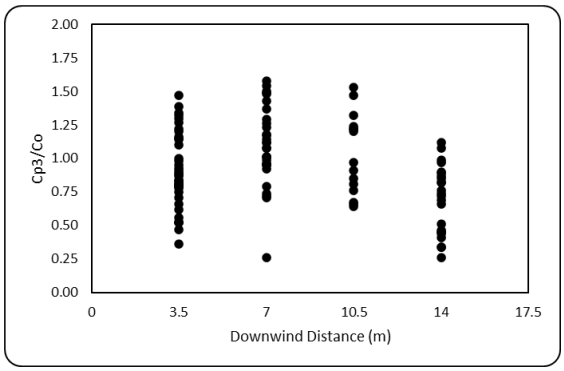

c) Using CALINE 4 predictions

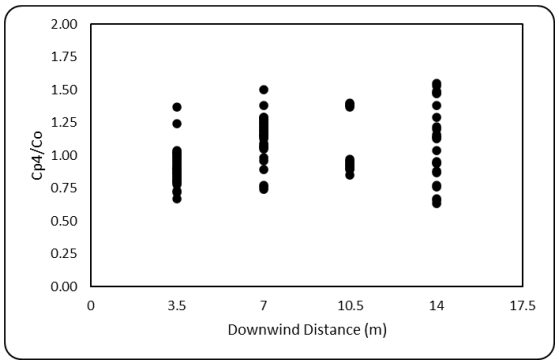

d) Using ADMS predictions

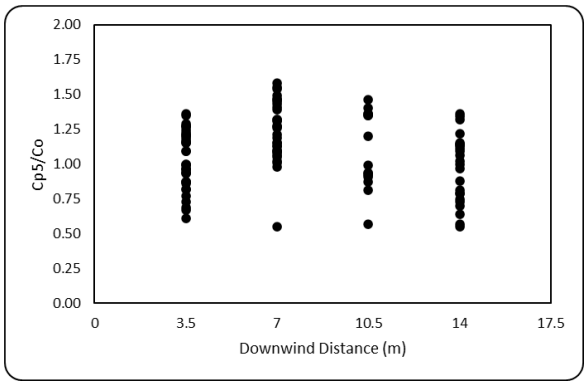

e) Using ISC3 predictions

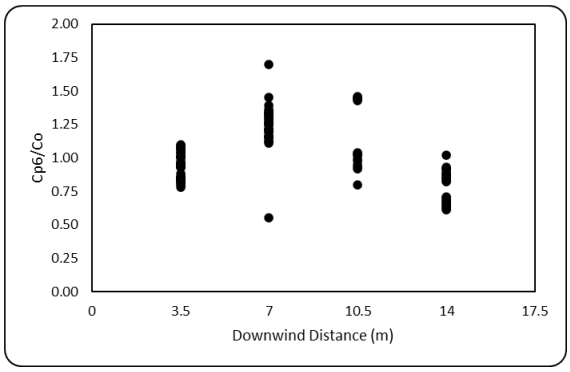

f) Using SLSM predictions

Figure 7-24: Predicted/observed vs downwind distance plots for Hyderabad data (NO_2) for unstable atmospheric conditions

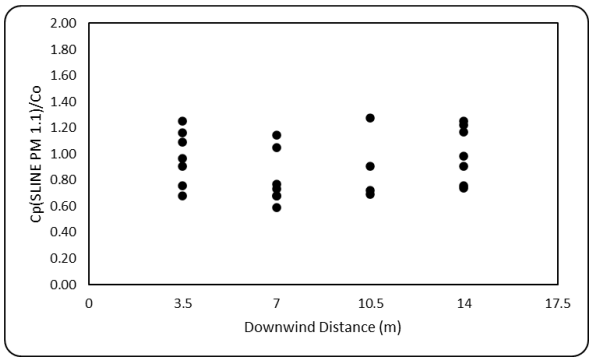

a) Particle size >10 µm

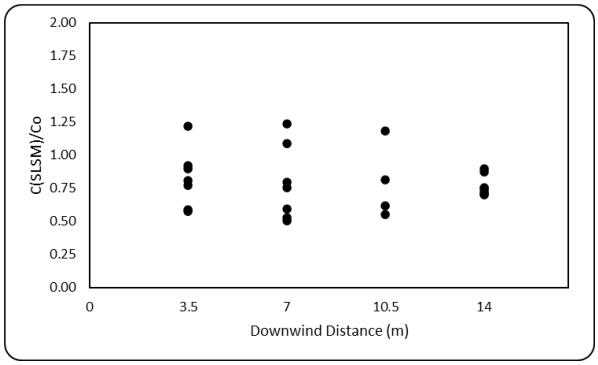

b) Particle size >10 µm

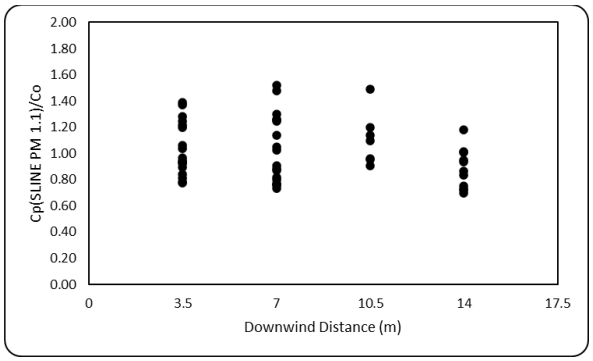

c) Particle size between 10 and 2.5 µm

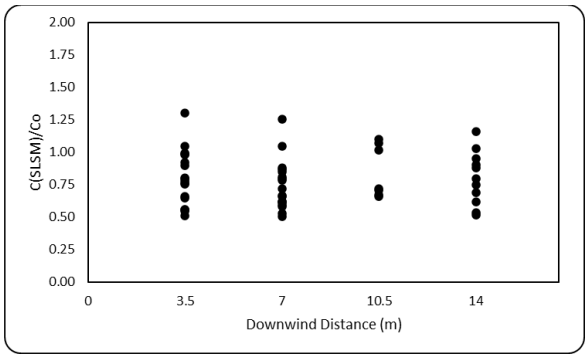

d) Particle size between 10 and 2.5 µm

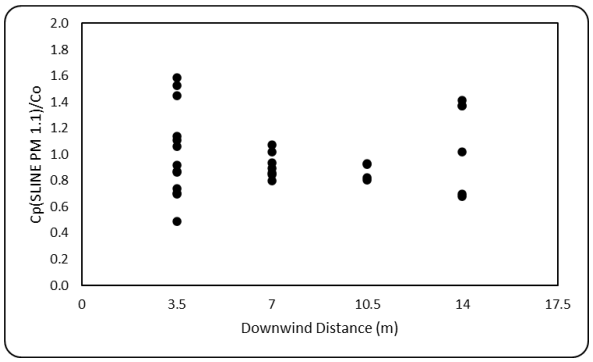

e) Particle size < 2.5 µm

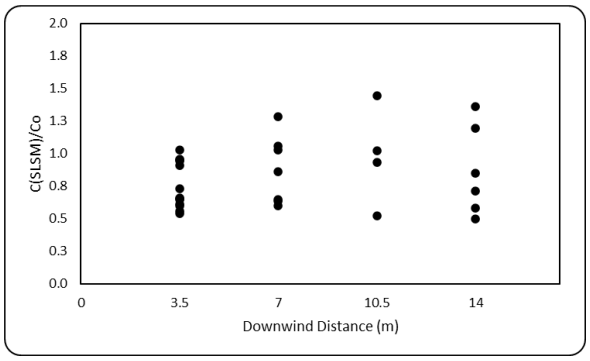

f) Particle size < 2.5 µm

Figure 7-25: Predicted/observed vs downwind distance plots for Hyderabad data (PM) considering different particle ranges for stable atmospheric conditions

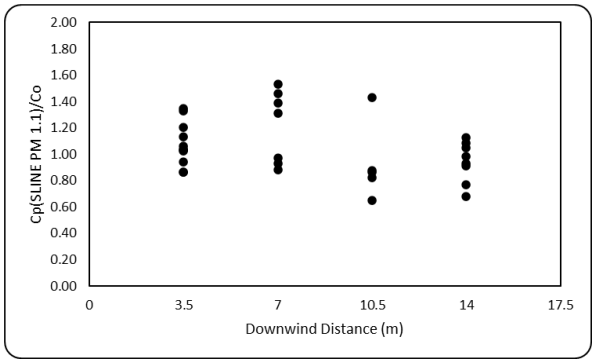

a) Particle size >10 µm

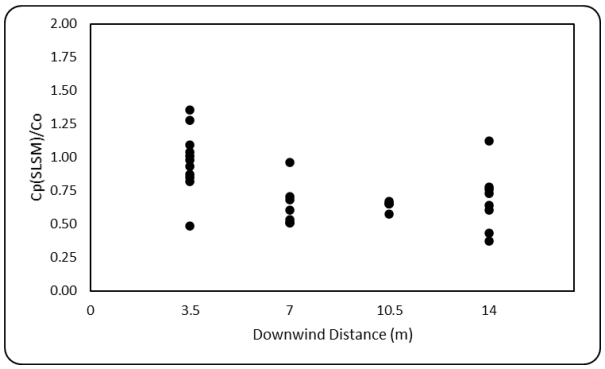

b) Particle size >10 µm

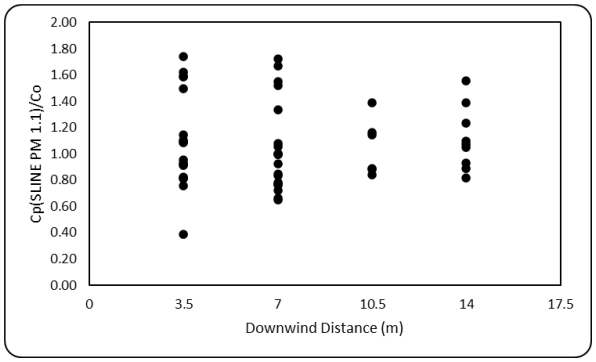

c) Particle size between 10 and 2.5 µm

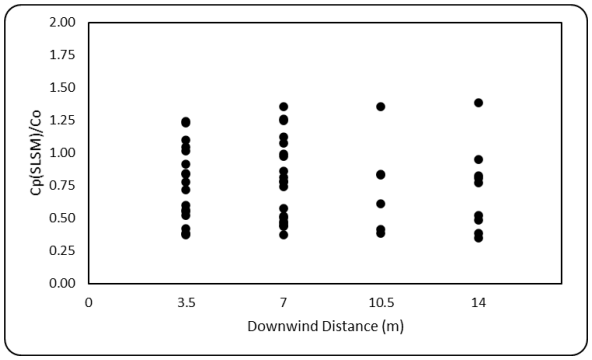

d) Particle size between 10 and 2.5 µm

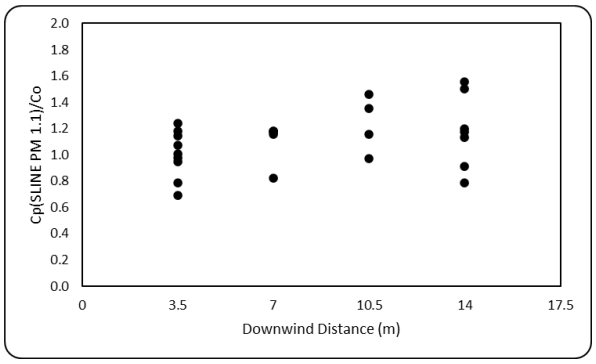

e) Particle size < 2.5 µm

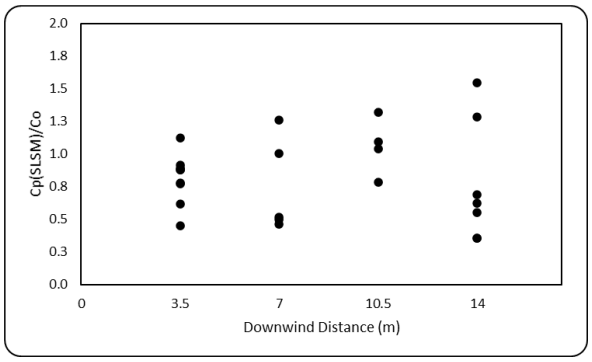

f) Particle size < 2.5 µm

Figure 7-26: Predicted/observed vs downwind distance plots for Hyderabad data (PM) considering different particle ranges for stable atmospheric conditions

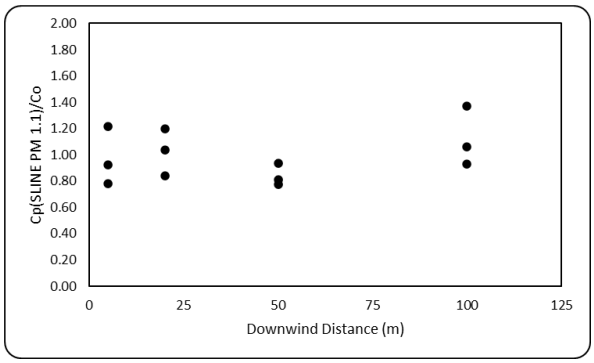

a) Particle size between 10 and 2.5 µm

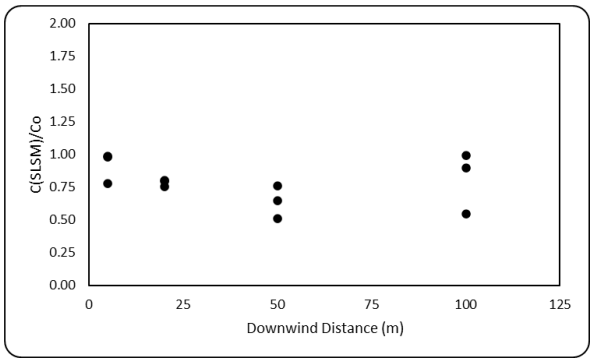

b) Particle size between 10 and 2.5 µm

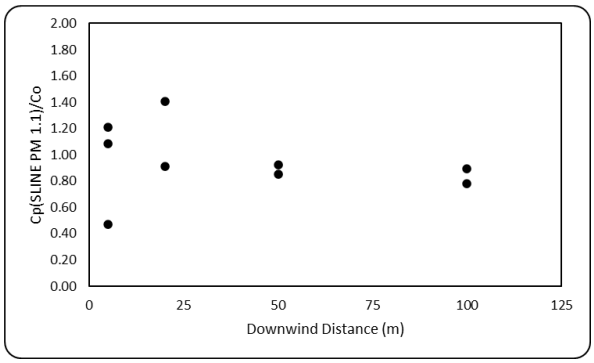

c) Particle size between 2.5 and 0.1 µm

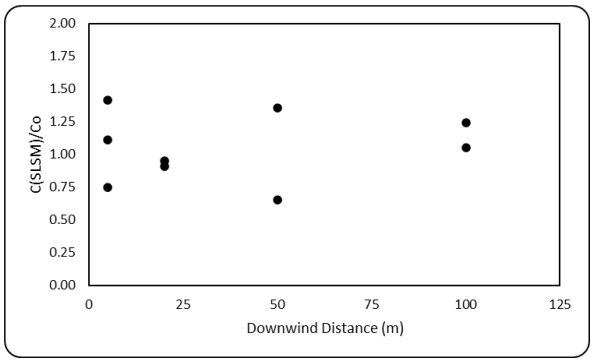

d) Particle size between 2.5 and 0.1 µm

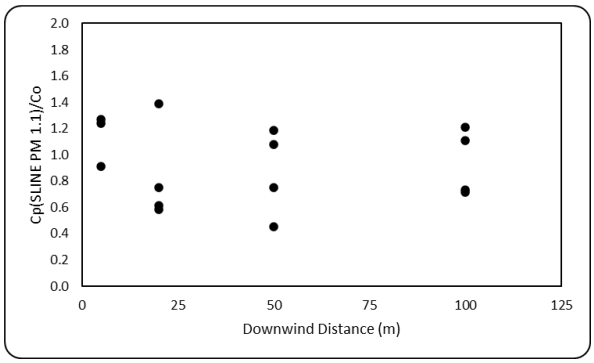

e) Particle size < 0.1 µm

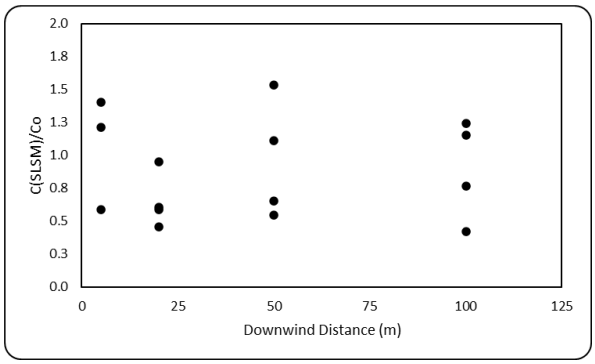

f) Particle size < 0.1 µm

Figure 7-27: Predicted/observed vs downwind distance plots for Raleigh data (PM) considering different particle ranges for stable atmospheric conditions

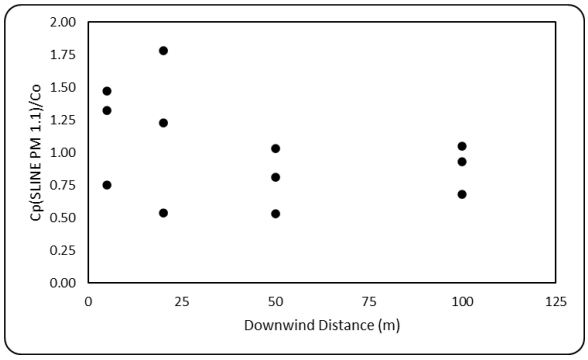

a) Particle size between 10 and 2.5 µm

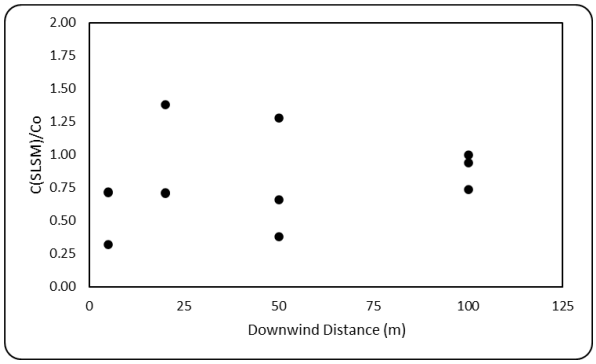

b) Particle size between 10 and 2.5 µm

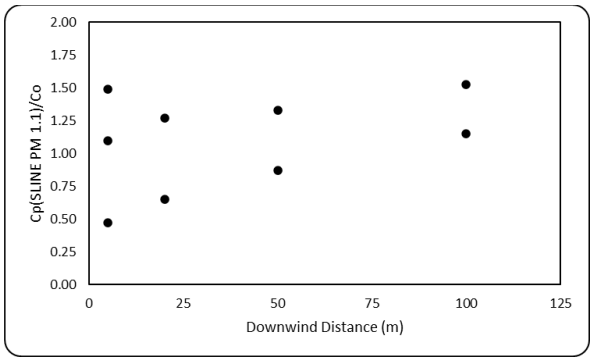

c) Particle size between 2.5 and 0.1 µm

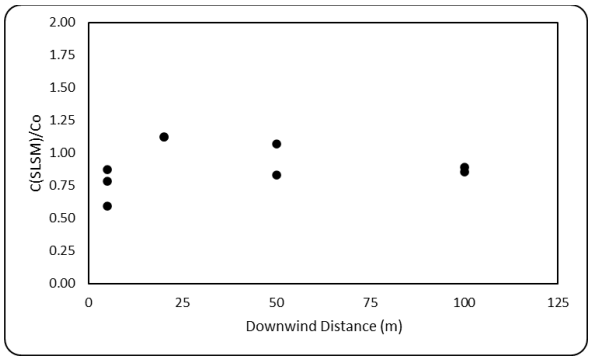

d) Particle size between 2.5 and 0.1 µm

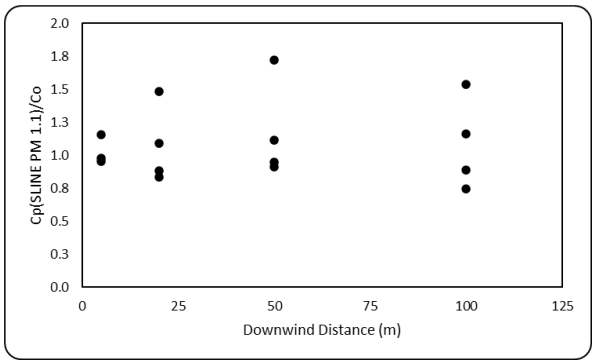

e) Particle size < 0.1 µm

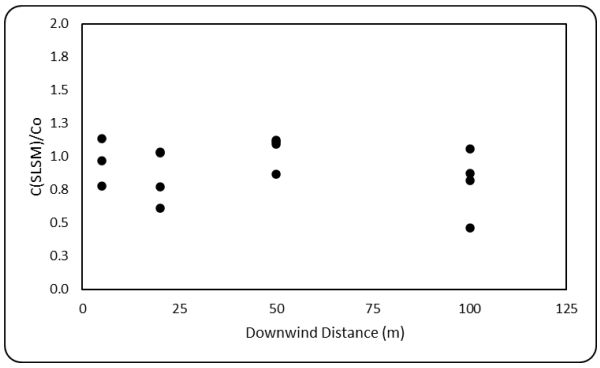

f) Particle size < 0.1 µm

Figure 7-28: Predicted/observed vs downwind distance plots for Raleigh data (PM) considering different particle ranges for unstable atmospheric conditions

Predicted/observed vs downwind distance plots indicate that with CALTRANS data (SF_6) for both atmospheric conditions SLINE 1.1 have both under and over predictions at lower downwind distances, but mostly over predictions at higher downwind distance. SAREA 1.1 have both under and over predictions at all the downwind distances. Both SLINE 1.1 and SAREA 1.1 have more over predictions than the other models. Using Idaho Falls data (SF_6) for both atmospheric conditions, though other models also have the over predictions, the SLINE 1.1 have the highest number of over predictions at all the downwind distances. The trend observed is similar to Hyderabad data (CO_2 and NO_2) for unstable atmospheric conditions. SLINE 1.1 and SAREA 1.1 have mixed predictions (under and over) even more values closer to the ideal value (1) are observed. Overall, from Cp/Co plots of gaseous models, it can be observed that more than 50% of the Cp/Co values of all the data sets are >1 except for the Hyderabad dataset.

From Cp/Co plots of PM models, it can be observed that most of the SLINE PM 1.1 are SLINE PM 1.1 is over predicting larger sized particles at lower downwind distances and small sized particles at larger downwind distances. This can be due to the lower-sized particle can travel larger downwind distances when compared with larger-sized particles.

7.2.3 Q-Q Plots

The predicted and observed concentrations are to be further assessed to see whether a model can generate a concentration distribution that is like the observed, especially at different concentration ranges. The Cp/Co values help to identify if the model is under-predicting or over-predicting. The statistical indicator indicates the accuracy of the model performance. The Q-Q plots represent the similarity between the distribution of observed and predicted values [49]. If the highest observed concentrations and model-predicted concentrations have similar magnitude then the model overpredicts overall, and maybe correctly predicts the values of the highest few observed

concentrations but for the wrong reasons and at wrong downwind distances [49]. Q-Q plots provide a visual characterization of the spread of model-predicted concentrations and observed concentrations concerning the central value [50].

Quantile-Quantile (Q-Q) plots were used in this study to visually assess the similarity in distribution between the observed concentrations and the concentrations predicted using developed and available models. The observed and simulated concentrations using each data set were considered when drawing each plot. They were initially sorted in ascending order and plotted against the quantiles calculated from the theoretical distribution. The standardized residuals (y-axis) were the measure of the strength of the difference between the observed and predicted simulations, and the theoretical quantiles (x-axis) were the theoretically calculated percentiles [86]. The Q-Q plots for the observed data and each model's simulated data were plotted. The plots also indicate the relation between the distribution to the observed concentrations and model predicted concentrations.

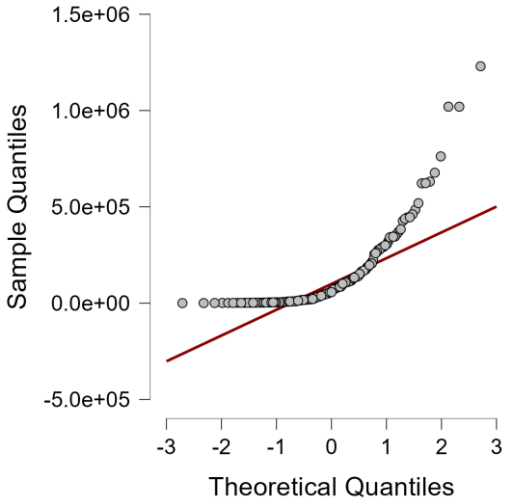

a) SLINE 1.1 predictions

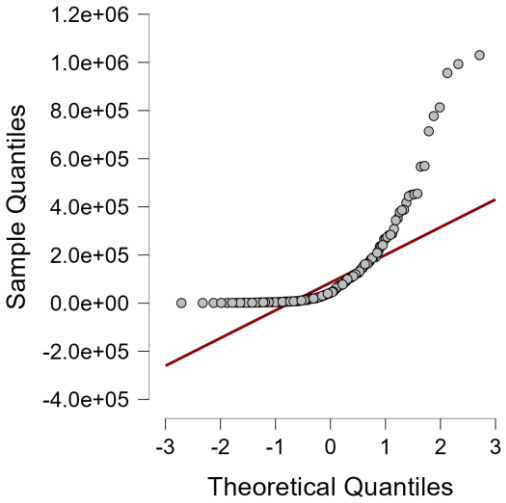

b) SAREA 1.1 predictions

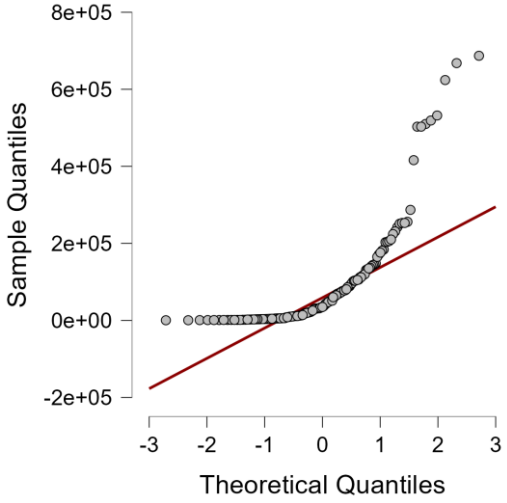

c) CALINE 4 predictions

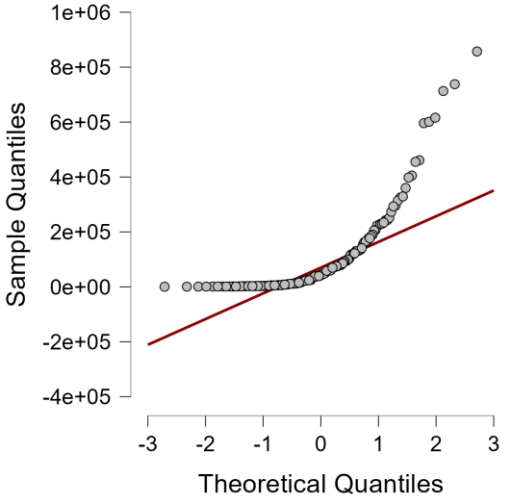

d) ADMS predictions

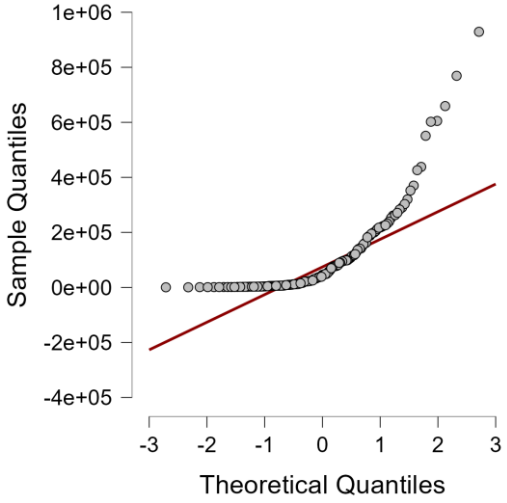

e) ISC3 predictions

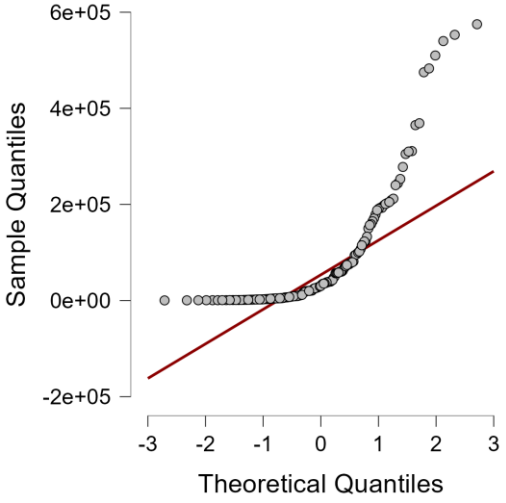

f) SLSM predictions

Figure 7-29: Predictions of CALTRANS data (SF_6) using available models for stable atmospheric conditions

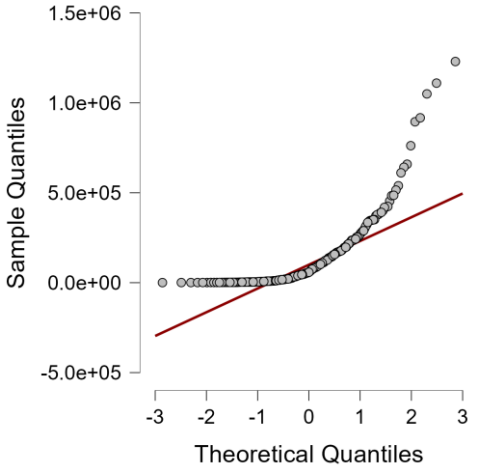

a) SLINE 1.1 predictions

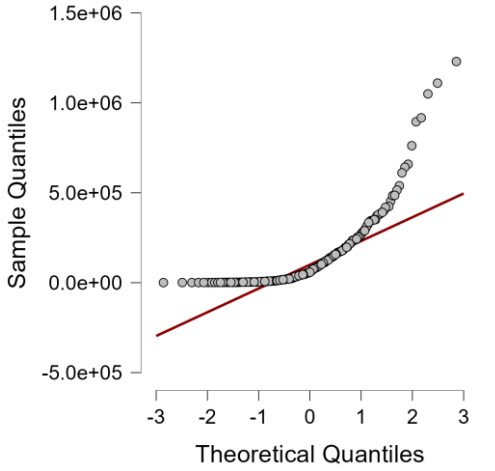

b) SAREA 1.1 predictions

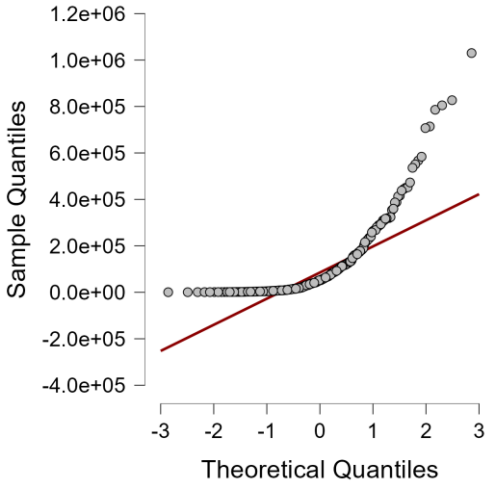

c) CALINE 4 predictions

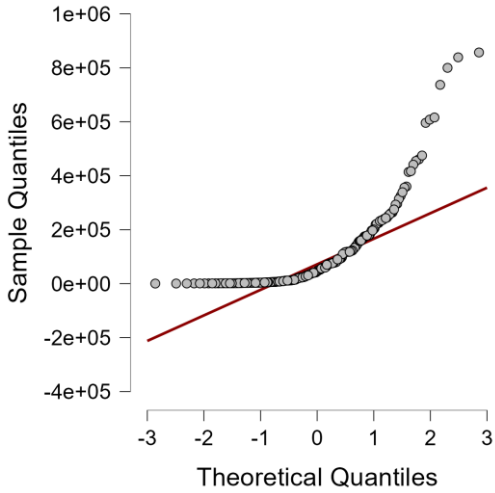

d) ADMS predictions

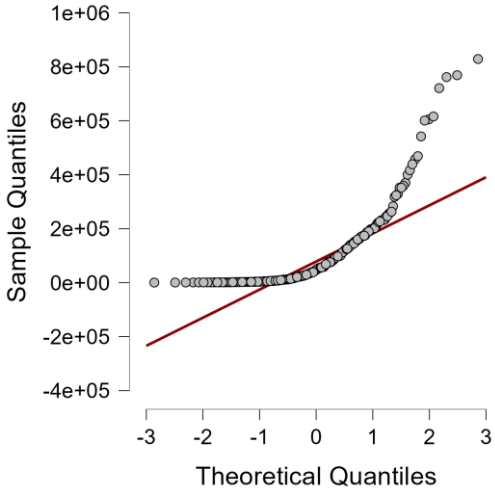

e) ISC3 predictions

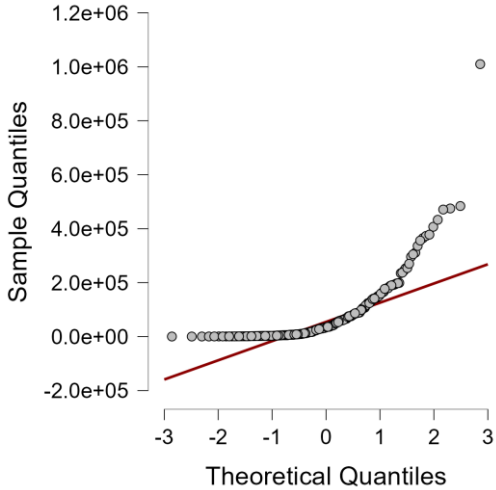

f) SLSM predictions

Figure 7-30: Predictions of CALTRANS data (SF_6) using available models for unstable atmospheric conditions

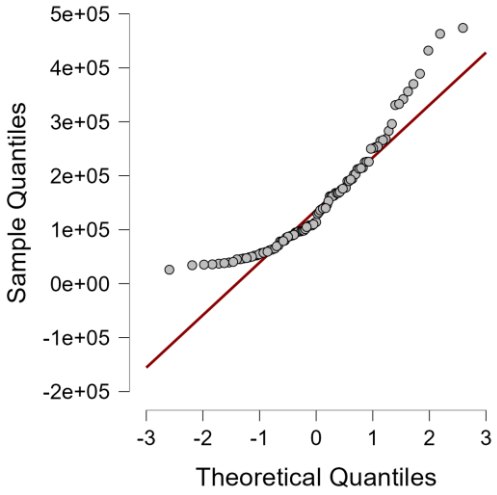

a) SLINE 1.1 predictions

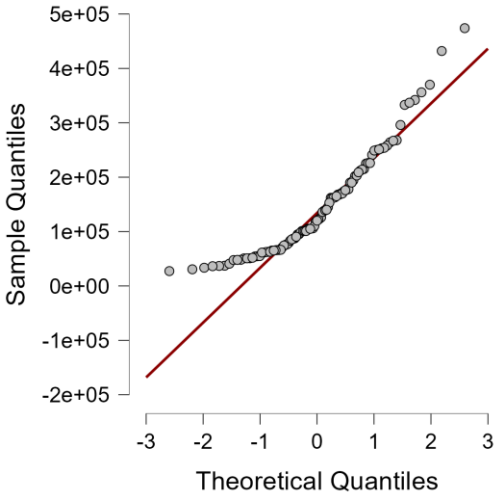

b) SAREA 1.1 predictions

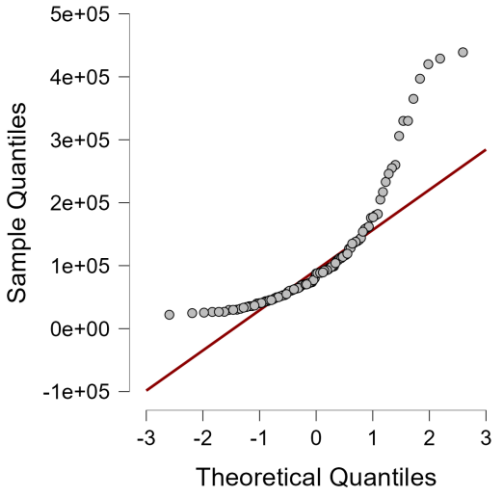

c) CALINE 4 predictions

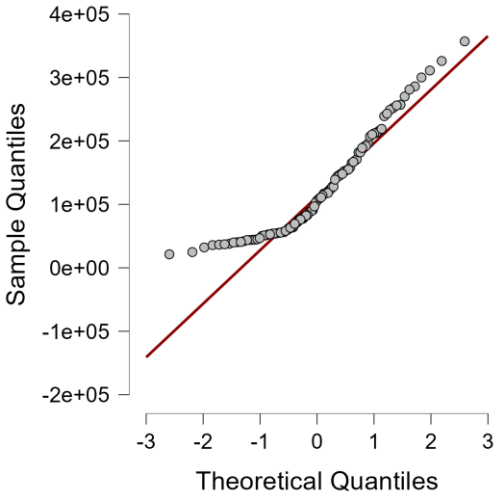

d) ADMS predictions

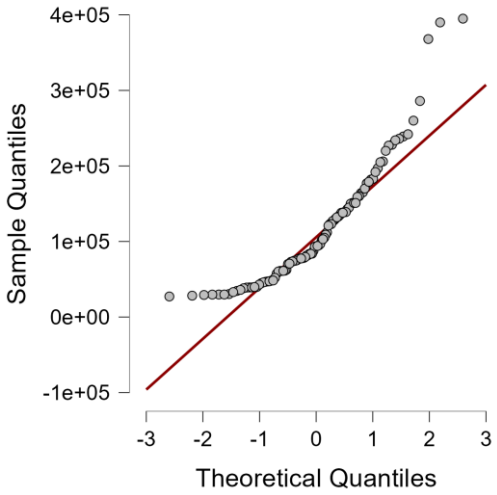

e) ISC3 predictions

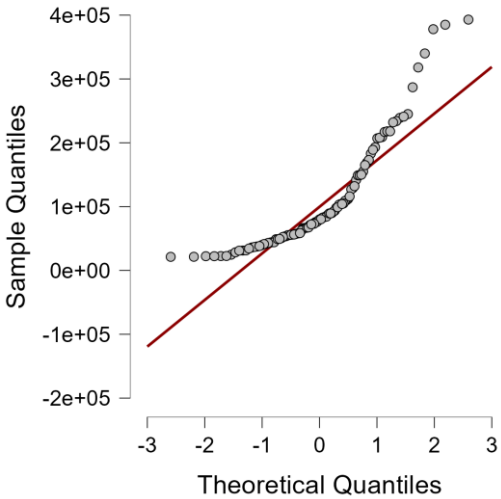

f) SLSM predictions

Figure 7-31: Predictions of Idaho Falls data (SF_6) using available models for stable atmospheric conditions

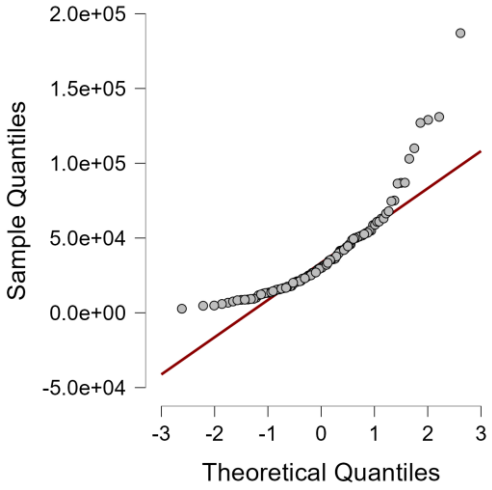

a) SLINE 1.1 predictions

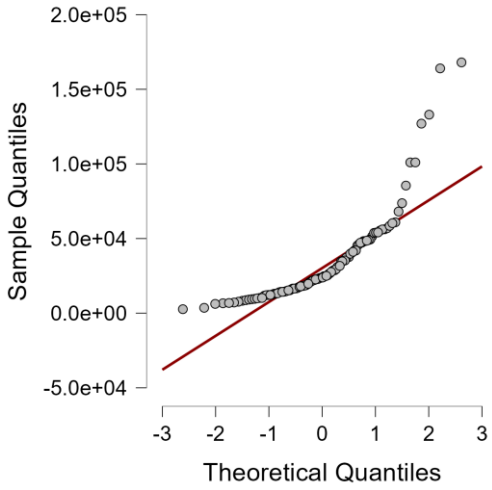

b) SAREA 1.1 predictions

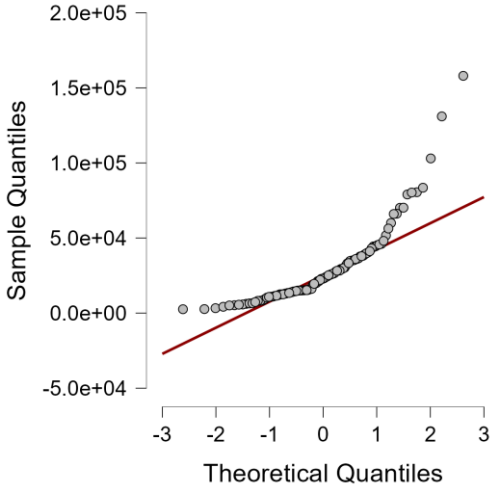

c) CALINE 4 predictions

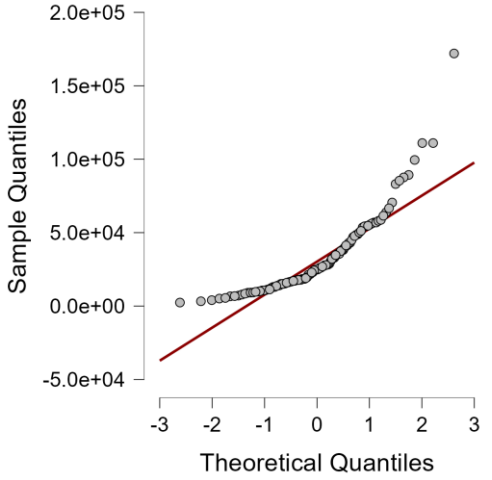

d) ADMS predictions

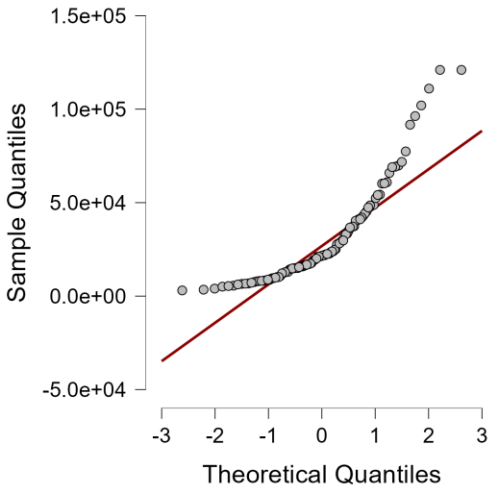

e) ISC3 predictions

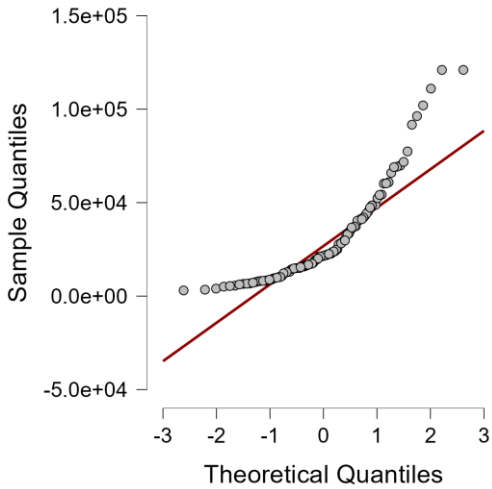

f) SLSM predictions

Figure 7-32: Predictions of Idaho Falls data (SF_6) using available models for unstable atmospheric conditions

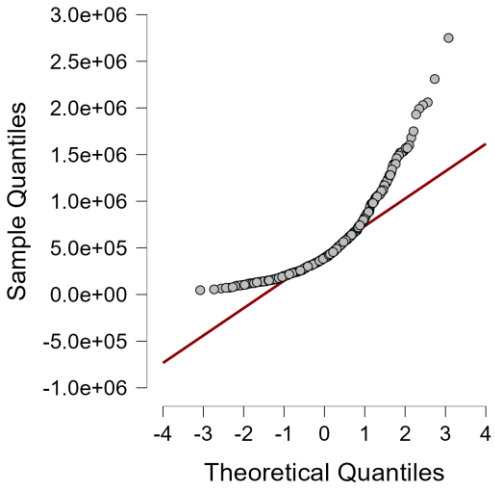

a) SLINE 1.1 predictions

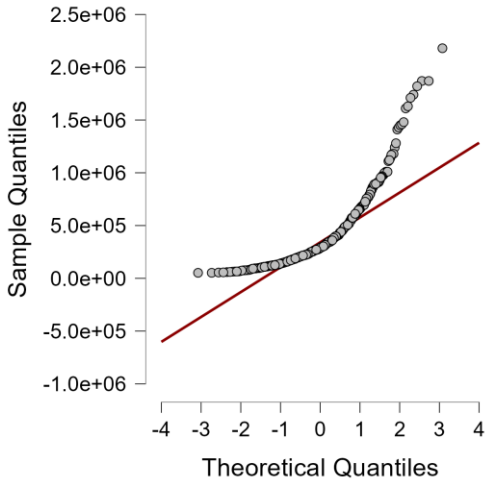

b) SAREA 1.1 predictions

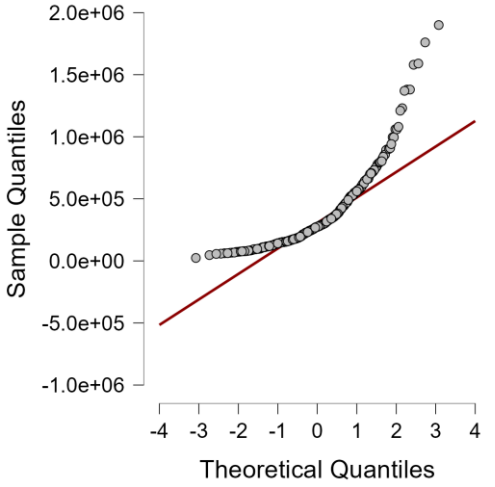

c) CALINE 4 predictions

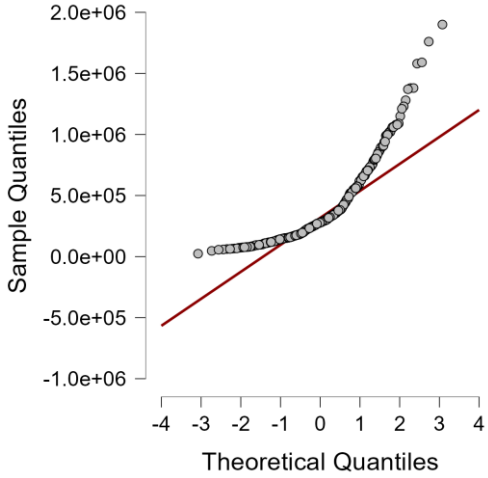

d) ADMS predictions

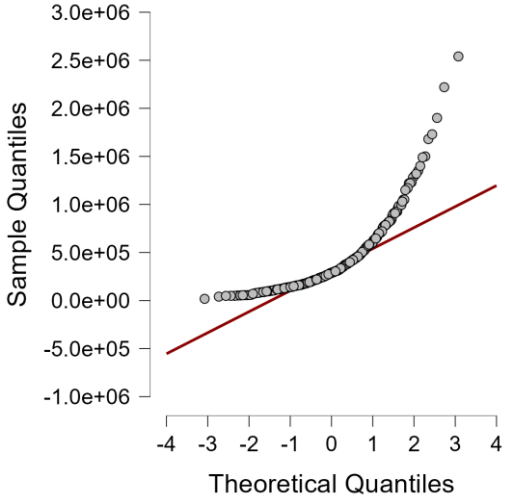

e) ISC3 predictions

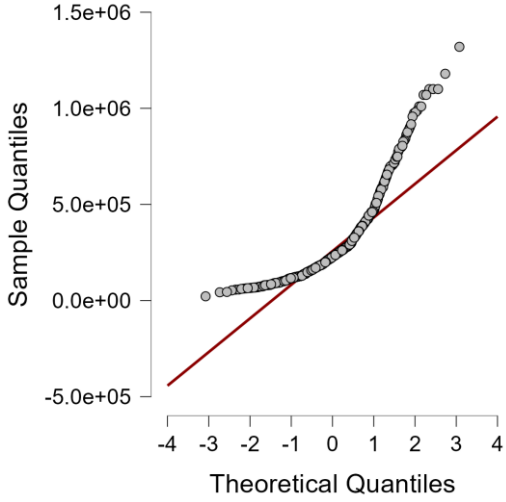

f) SLSM predictions

Figure 7-33: Predictions of Raleigh data (NO) using available models for stable atmospheric conditions

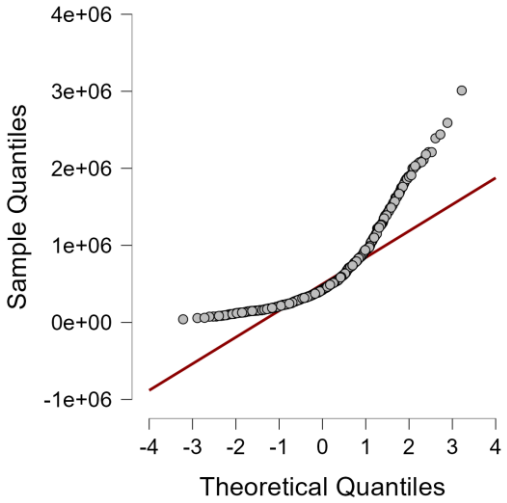

a) SLINE 1.1 predictions

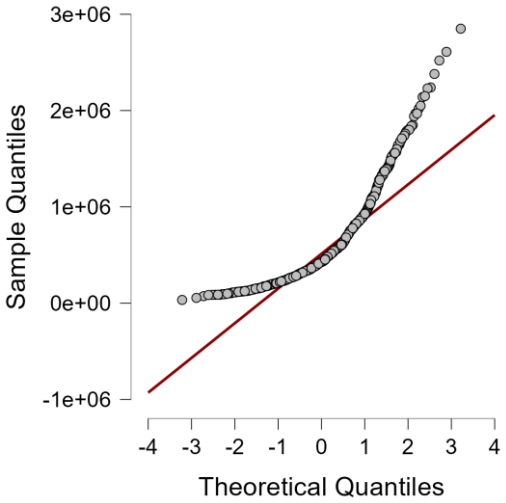

b) SAREA 1.1 predictions

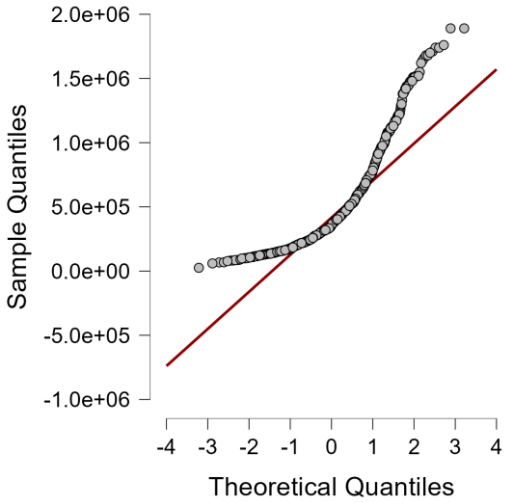

c) CALINE 4 predictions

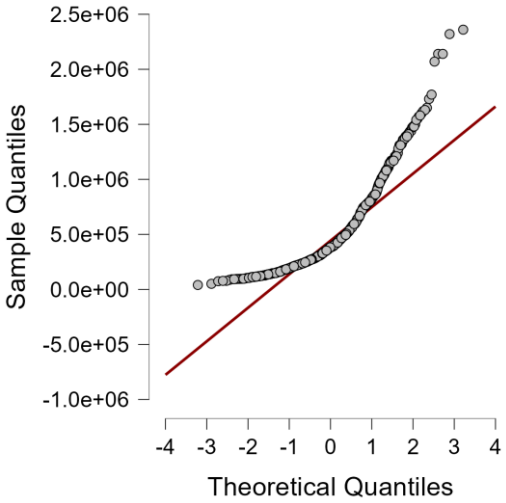

d) ADMS predictions

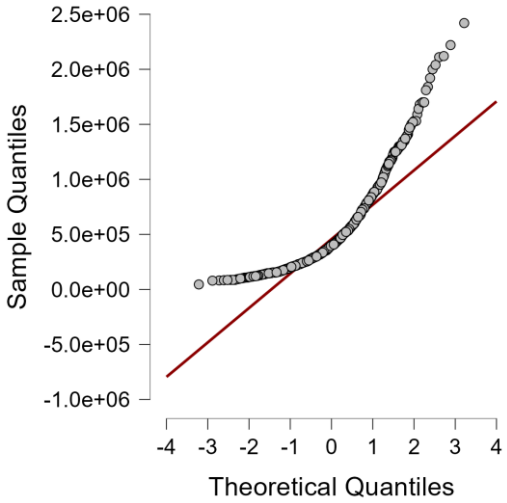

e) ISC3 predictions

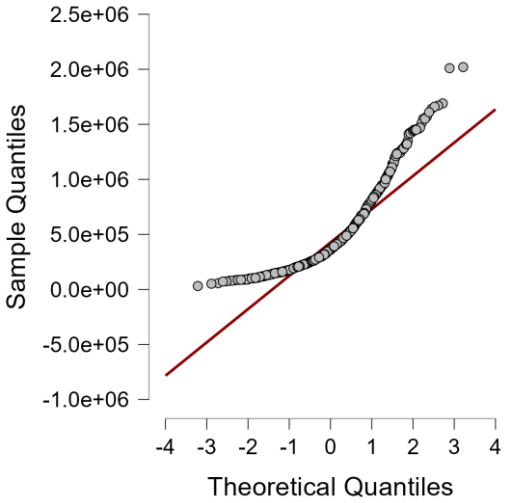

f) SLSM predictions

Figure 7-34: Predictions of Raleigh data (NO) using available models for unstable atmospheric conditions

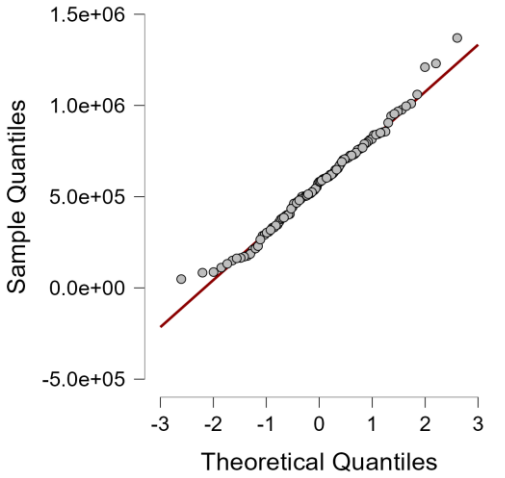

a) SLINE 1.1 predictions

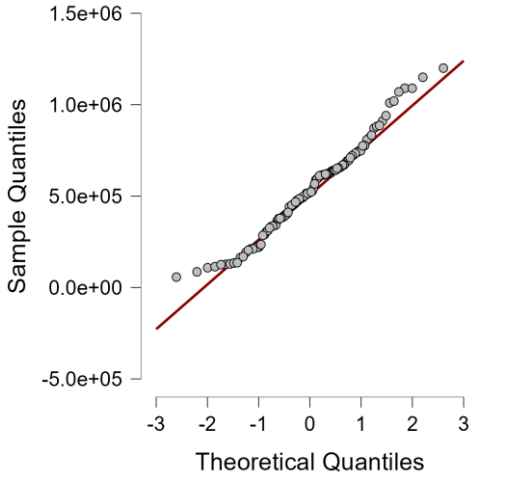

b) SAREA 1.1 predictions

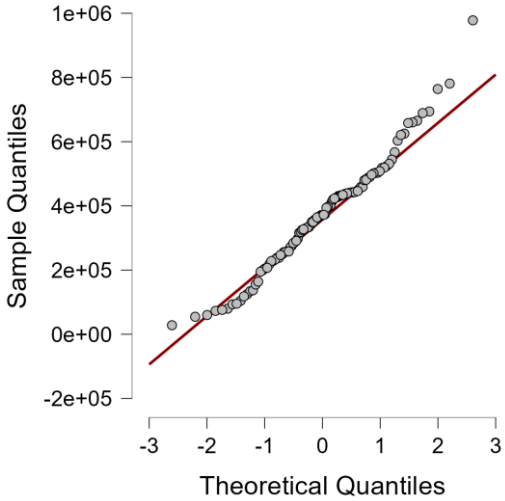

c) CALINE 4 predictions

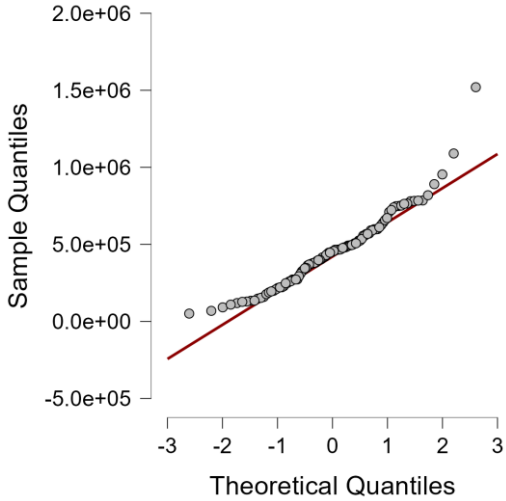

d) ADMS predictions

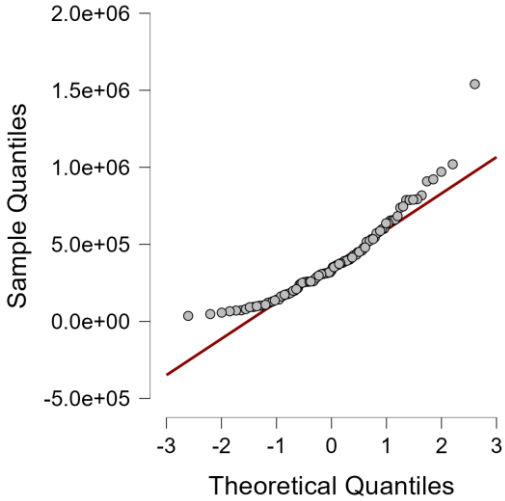

e) ISC3 predictions

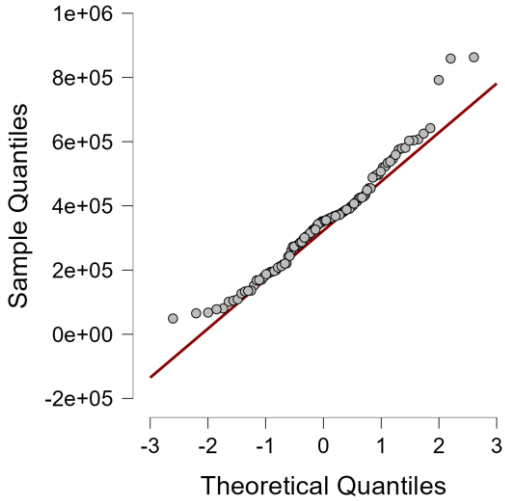

f) SLSM predictions

Figure 7-35: Predictions of Hyderabad data (CO_2) using available models for stable atmospheric conditions

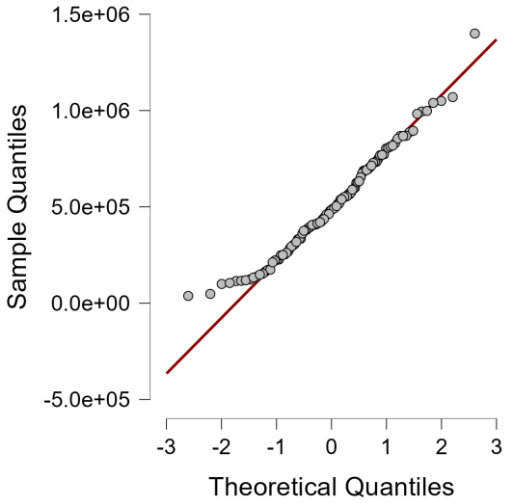

a) SLINE 1.1 predictions

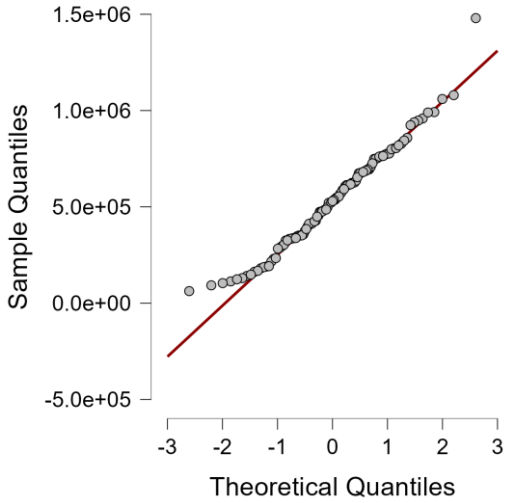

b) SAREA 1.1 predictions

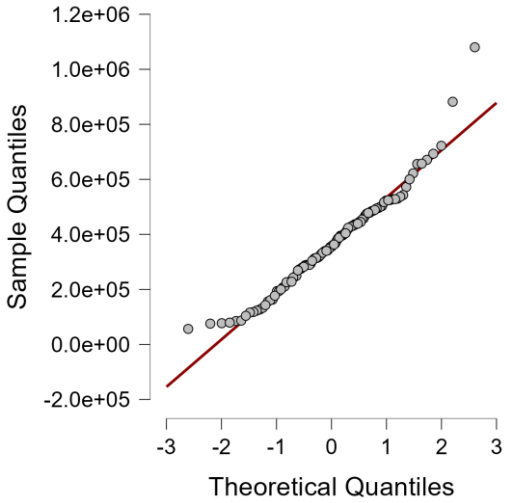

c) CALINE 4 predictions

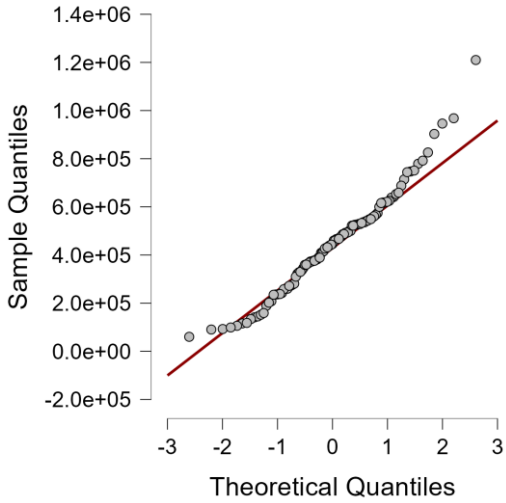

d) ADMS predictions

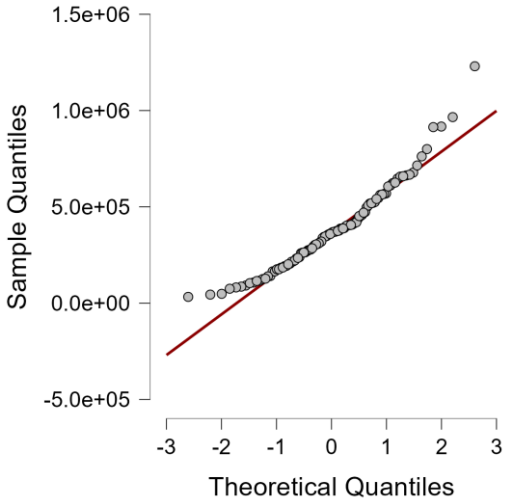

e) ISC3 predictions

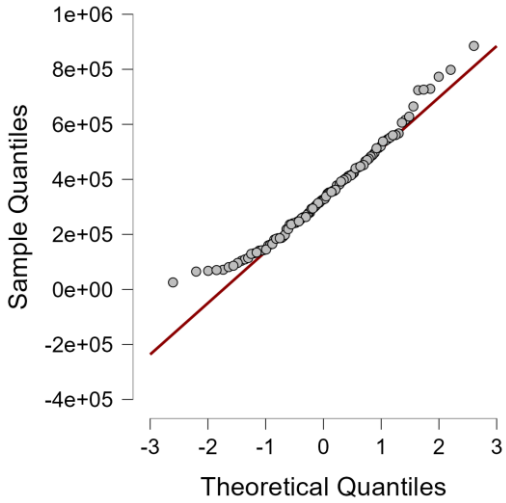

f) SLSM predictions

Figure 7-36: Predictions of Hyderabad data (CO_2) using available models for unstable atmospheric conditions

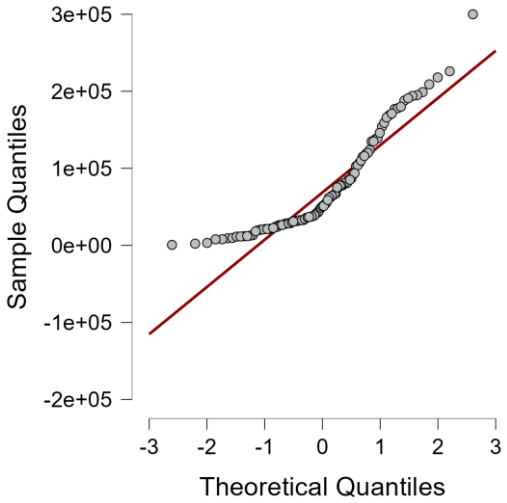

a) SLINE 1.1 predictions

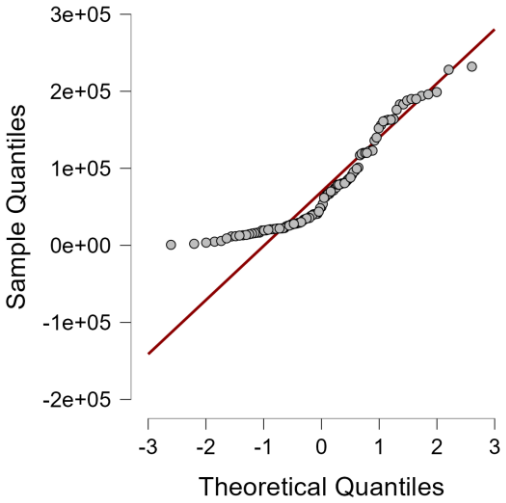

b) SAREA 1.1 predictions

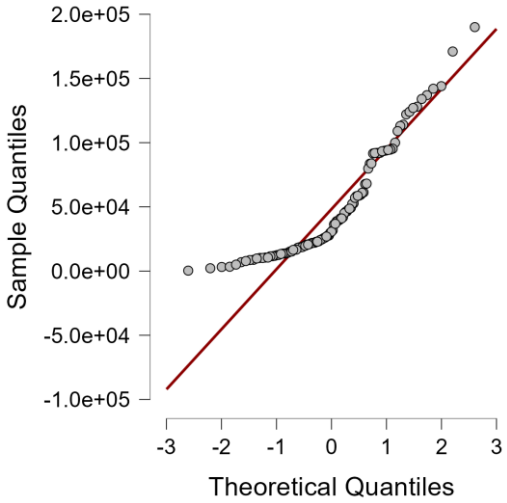

c) CALINE 4 predictions

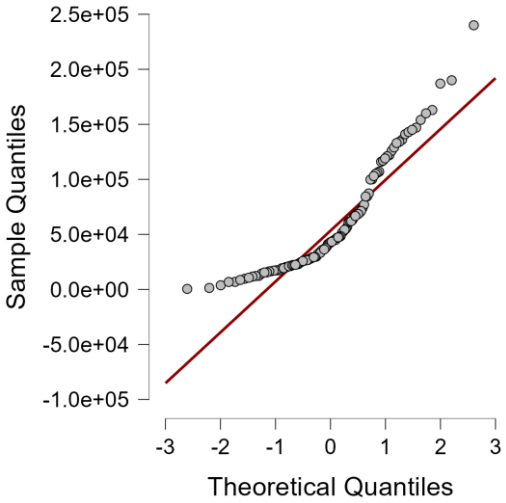

d) ADMS predictions

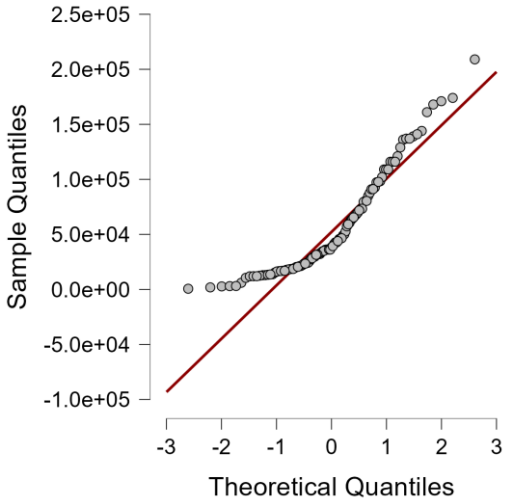

e) ISC3 predictions

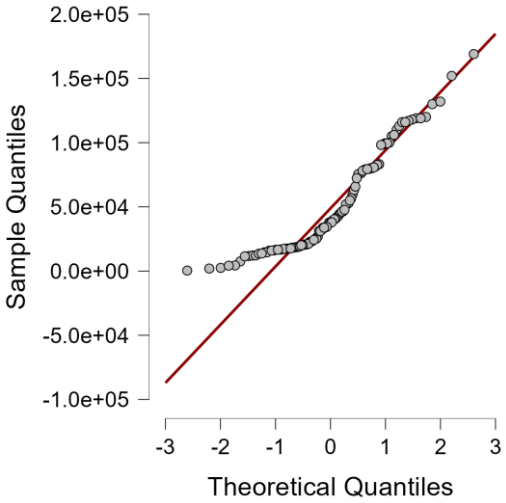

f) SLSM predictions

Figure 7-37: Predictions of Hyderabad data (NO_2) using available models for stable atmospheric conditions

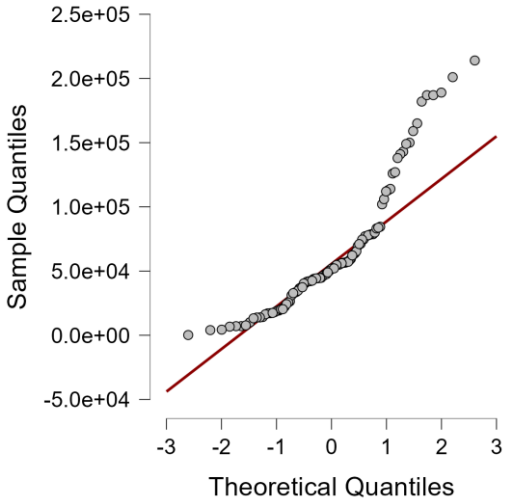

a) SLINE 1.1 predictions

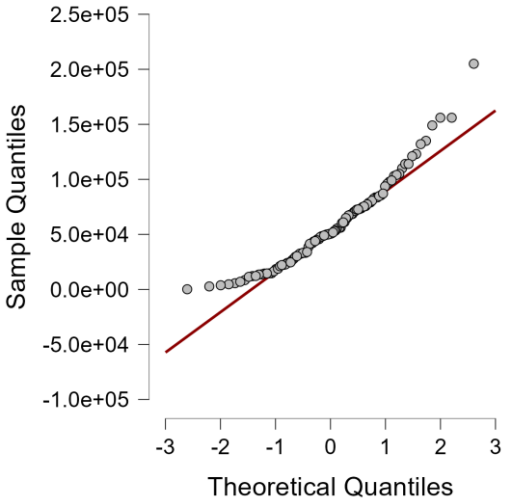

b) SAREA 1.1 predictions

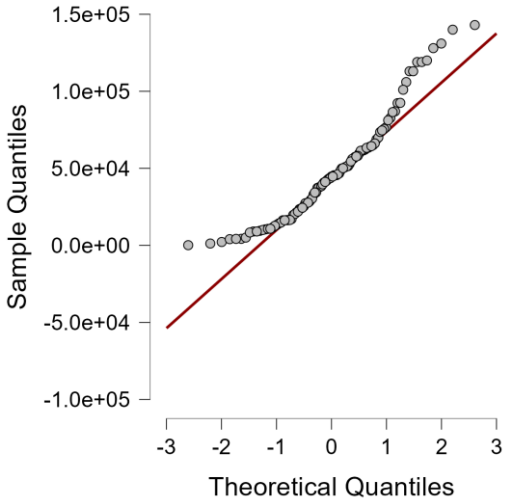

c) CALINE 4 predictions

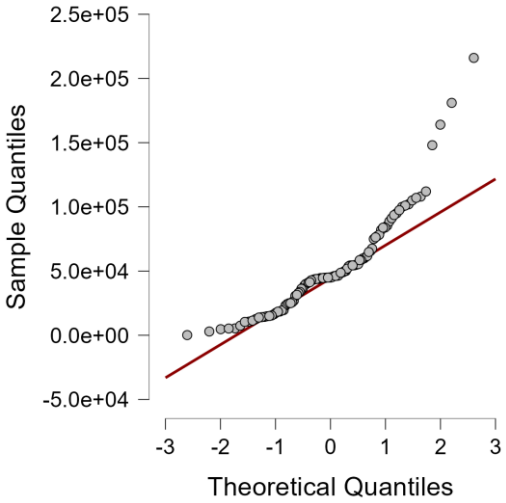

d) ADMS predictions

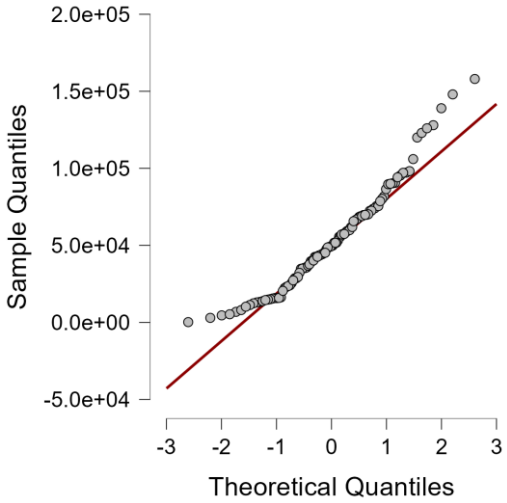

e) ISC3 predictions

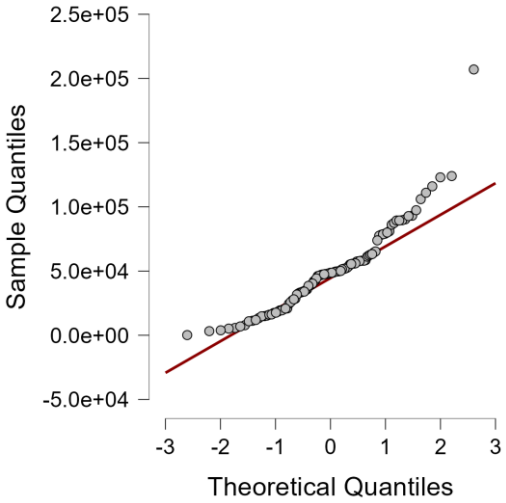

f) SLSM predictions

Figure 7-38: Predictions of Hyderabad data (NO_2) using available models for unstable atmospheric conditions

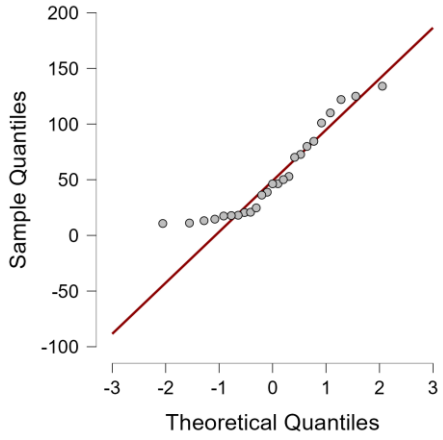

a) SLINE PM 1.1 predictions for particle size >10 µm

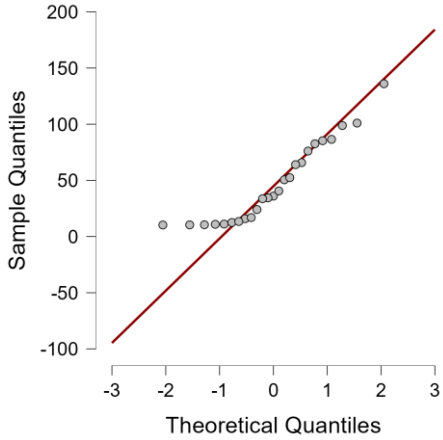

b) SLSM predictions for particle size >10 µm

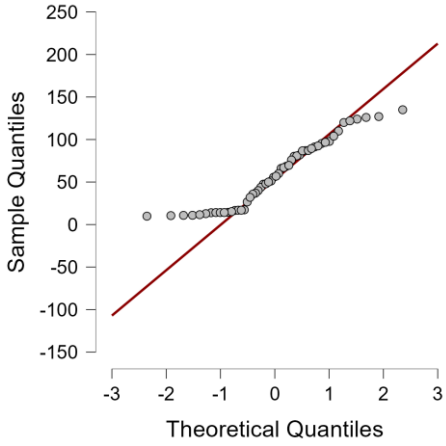

c) SLINE PM 1.1 predictions for particle size between 10 and 2.5 µm

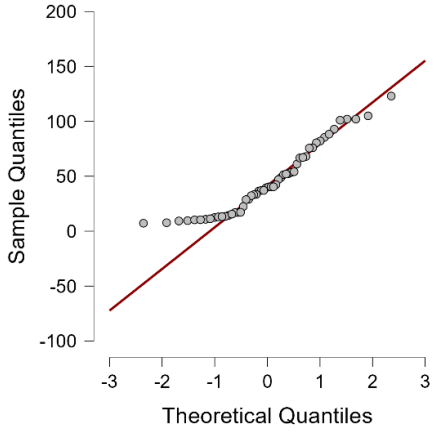

d) SLSM predictions for particle size between 10 and 2.5 µm

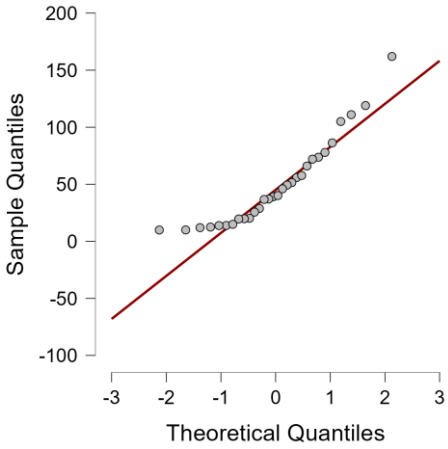

e) SLINE PM 1.1 predictions for particle size between <2.5 µm

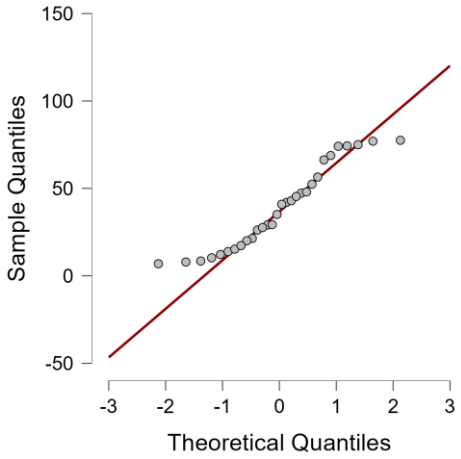

f) SLSM predictions for particle size between <2.5 µm

Figure 7-39: Predictions of Hyderabad data (PM) with different particle size ranges using SLINE PM 1.1 and SLSM for stable atmospheric conditions

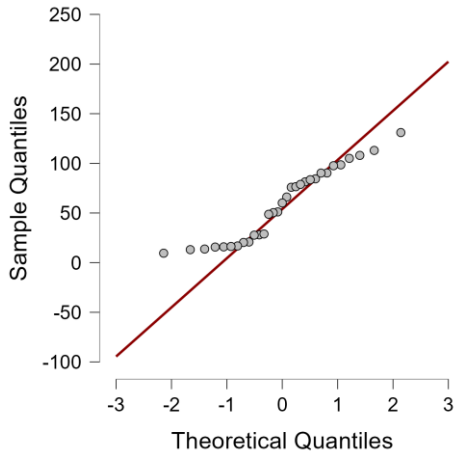

a) SLINE PM 1.1 predictions for particle size >10 µm

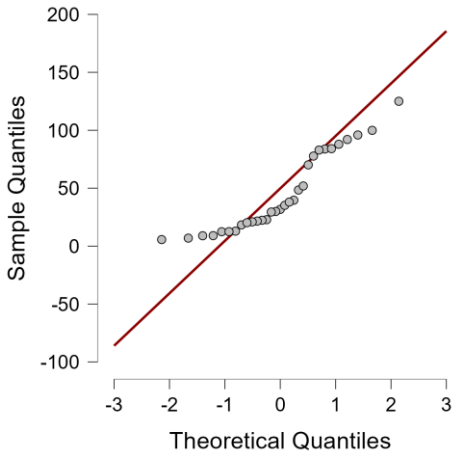

b) SLSM predictions for particle size >10 µm

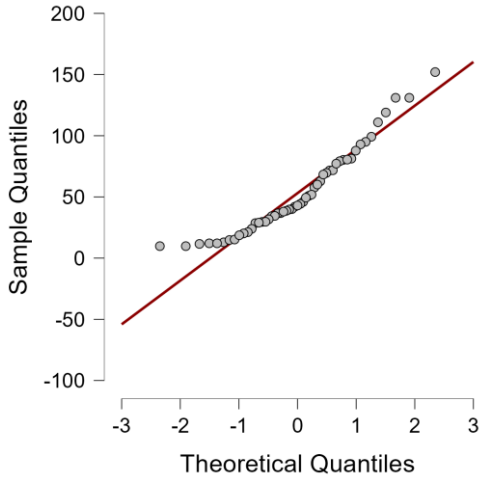

c) SLINE PM 1.1 predictions for particle size between 10 and 2.5 µm

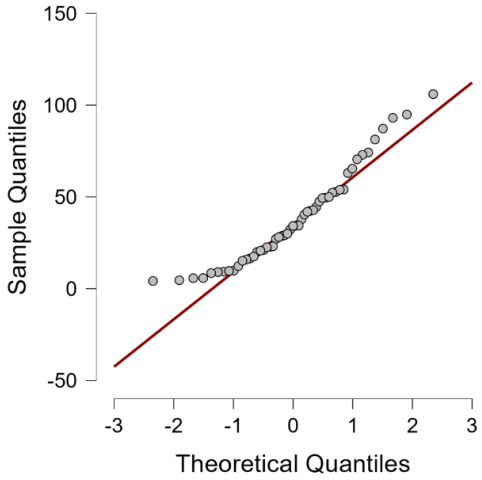

d) SLSM predictions for particle size between 10 and 2.5 µm

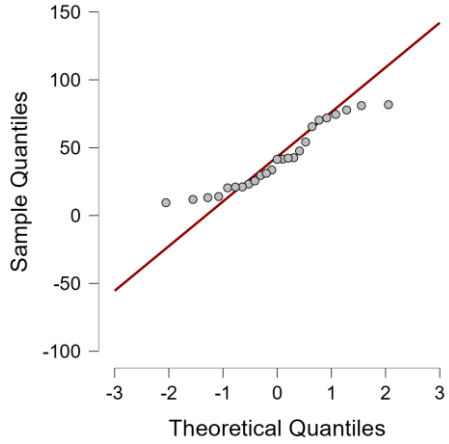

e) SLINE PM 1.1 predictions for particle size between <2.5 µm

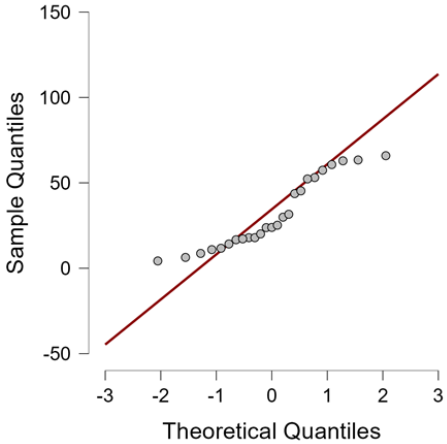

f) SLSM predictions for particle size between <2.5 µm

Figure 7-40: Predictions of Hyderabad data (PM) with different particle size ranges using SLINE PM 1.1 and SLSM for unstable atmospheric conditions

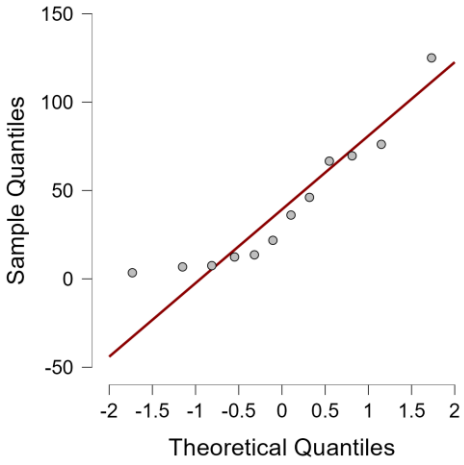

a) Particle size between 10 and 2.5 µm

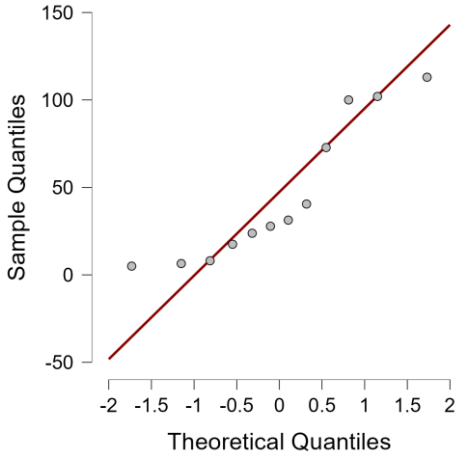

b) Particle size between 10 and 2.5 µm

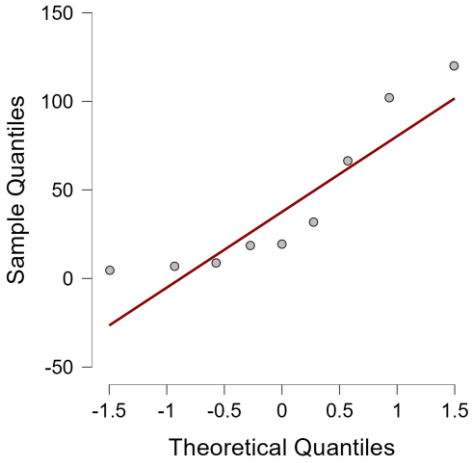

c) Particle size between 2.5 and 0.1 µm

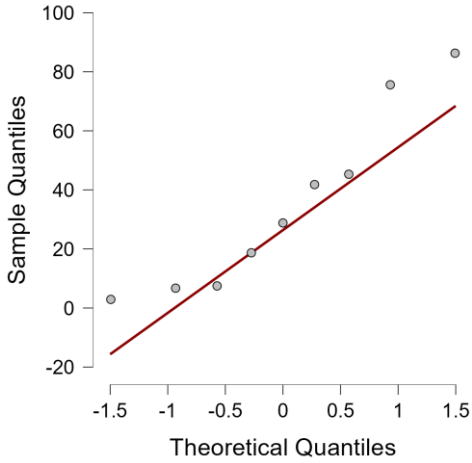

d) Particle size between 2.5 and 0.1 µm

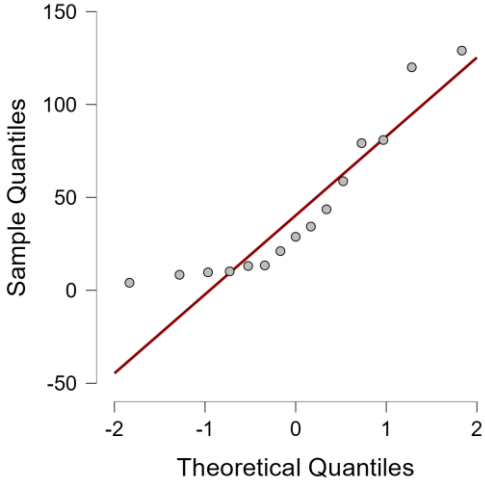

e) Particle size between <0.1 µm

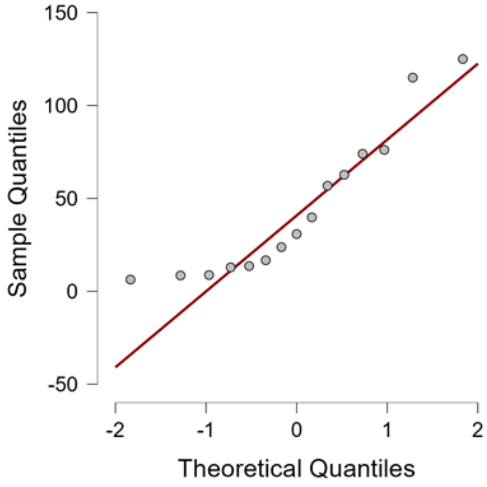

f) Particle size between <0.1 µm

Figure 7-41: Predictions of Raleigh data (PM) with different particle size ranges using SLINE PM 1.1 and SLSM for stable atmospheric conditions

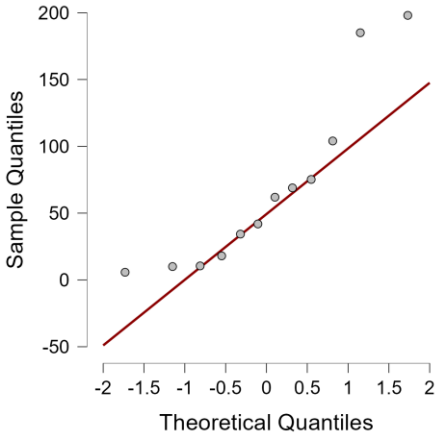

a) Particle size between 10 and 2.5 µm

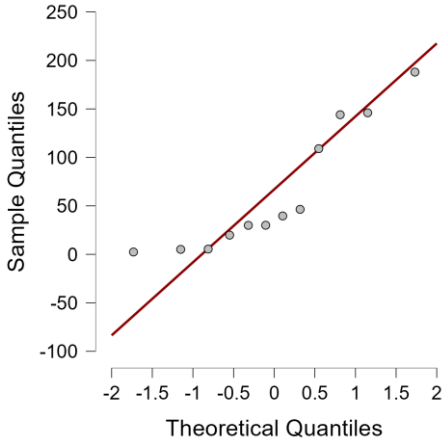

b) Particle size between 10 and 2.5 µm

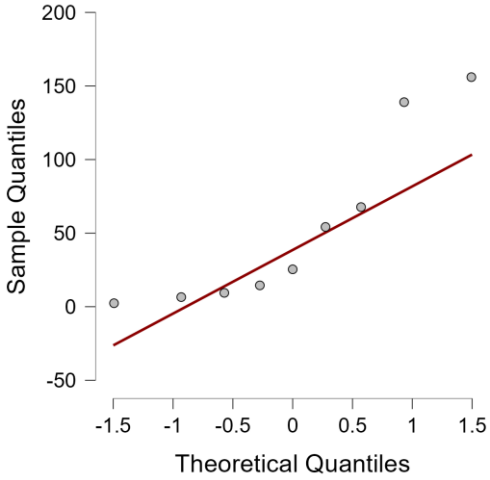

c) Particle size between 2.5 and 0.1 µm

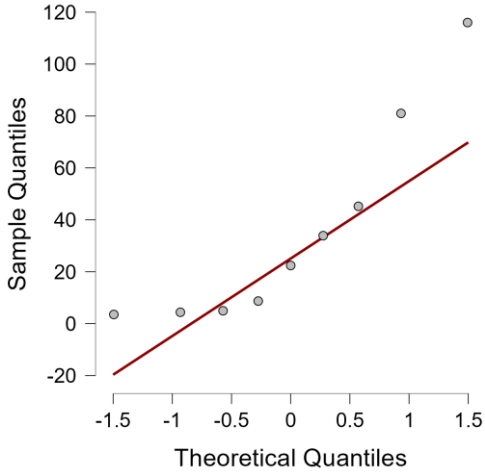

d) Particle size between 2.5 and 0.1 µm

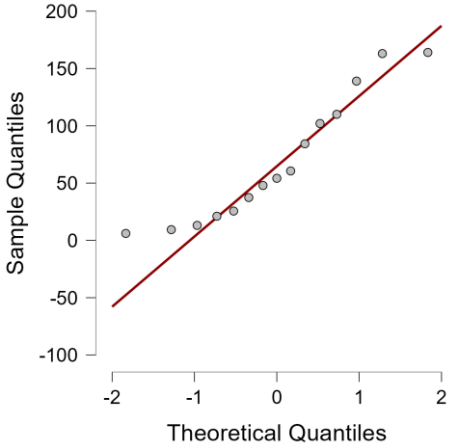

e) Particle size between <0.1 µm

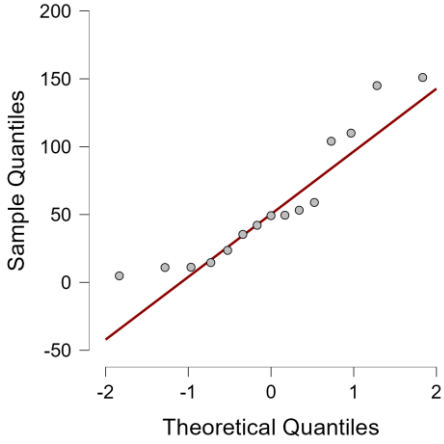

f) Particle size between <0.1 µm

Figure 7-42: Predictions of Raleigh data (PM) with different particle size ranges using SLINE PM 1.1 and SLSM for unstable atmospheric conditions

The Q-Q plots help to see whether a model can generate a concentration distribution that is like the observed, especially at different concentration ranges. For Gaseous models, it can be observed from the Q-Q plots that the trend followed by model predictions is similar to that of observed values however a variation is observed at higher concentrations using CALTRANS data (SF_6) for stable atmospheric conditions. It can also be observed that SLINE 1.1 has a high Y-axis range than the other models and the second-highest range is for SAREA 1.1. Using CALTRANS data (SF_6) for unstable atmospheric conditions, it can be observed that SLINE 1.1 and SAREA 1.1 both have a high Y-axis range than the other models. For Idaho Falls data (SF_6) for both atmospheric conditions, varying trends can be observed from mid-range concentrations to high concentrations. Also varying trends in higher concentrations. A significant variation in prediction trends can be observed with Hyderabad (CO_2) for stable atmospheric conditions. The large variation in trends for all the models can be observed for Hyderabad data (NO_2) for both atmospheric conditions. From Q-Q plots, the upper limit range of model predictions of SLINE 1.1 are always higher than all the other models. For PM models, from Q-Q plots, it can be observed that more deviation in prediction trends can be observed for both Hyderabad and Raleigh data sets. The upper limit range of model predictions of SLINE PM 1.1 is always higher or equal to the SLSM.

7.3 Comparison of Models using Statistical Indicators

The quantitative performance of the models (SLINE 1.1, SAREA 1.1) and comparison with the available models (CALINE4, ADMS, ISC3, and SLSM) are studied by computing the statistical indicators that include MB, FB, NMSE, r, MG, VG, and Fa2 (See Table 7-1). These statistical performance measures are based on the suggestions given in the literature [85].

Table 7-1: Comparison of developed models with available models using statistical indicators

	Statistical Indicator	MB(μg/m^3)	FB	NMSE	r	MG	VG	Fa2
CALTRANS Stable Conditions	**SLINE 1.1**	12.34	0.11✓	0.05✓	0.88✓	0.89✓	1.20✓	0.84✓
	SAREA 1.1	15.86	0.34✓	1.61✓	0.81✓	1.32	1.20✓	0.82✓
	CALINE4	17.11	−0.26✓	0.37✓	0.75✓	1.44	1.35	0.79
	ADMS	11.43	−0.14✓	0.10✓	0.86✓	1.24✓	1.22✓	0.83✓
	ISC3	15.45	0.39✓	1.57✓	0.78✓	1.36	1.23✓	0.82✓
	SLSM	15.12	−0.26✓	0.35✓	0.73	1.41	1.48	0.76
CALTRANS Unstable Conditions	**SLINE 1.1**	-14.97	−0.16✓	0.14✓	0.87✓	1.28	1.13✓	0.85✓
	SAREA 1.1	23.12	0.35✓	1.73✓	0.78✓	1.37	1.26	0.86✓
	CALINE4	20.61	−0.31✓	0.54✓	0.71	1.48	1.41	0.74
	ADMS	13.90	−0.19✓	0.21✓	0.86✓	1.33	1.24✓	0.84✓
	ISC3	19.87	0.32✓	1.86✓	0.76✓	1.42	1.30✓	0.79
	SLSM	15.96	−0.28✓	0.47✓	0.72	1.44	1.49	0.70
Idaho Falls Stable Conditions	**SLINE 1.1**	6.75✓	0.15✓	0.05✓	0.75✓	0.88✓	1.22✓	0.81✓
	SAREA 1.1	11.32	0.31✓	1.25✓	0.84✓	1.19✓	1.11✓	0.83✓
	CALINE4	15.05	−0.29✓	0.12✓	0.65	1.45	1.49	0.72
	ADMS	14.95	−0.10✓	0.02✓	0.76✓	1.20✓	1.27	0.79
	ISC3	12.47	0.34✓	0.99✓	0.83✓	1.21✓	1.16✓	0.80✓
	SLSM	18.51	−0.33✓	0.17✓	0.58	1.49	1.51	0.63
Idaho Falls Unstable Conditions	**SLINE 1.1**	-3.64✓	−0.11✓	0.02✓	0.87✓	1.11✓	1.11✓	0.92✓
	SAREA 1.1	23.09	0.46✓	1.18✓	0.79✓	1.20✓	1.18✓	0.81✓
	CALINE4	11.17	−0.23✓	0.09✓	0.68	1.46	1.46	0.71
	ADMS	10.16	−0.14✓	0.03✓	0.86✓	1.25✓	1.22✓	0.89✓
	ISC3	20.11	0.43✓	2.04	0.76✓	1.22✓	1.21✓	0.74
	SLSM	16.72	−0.25✓	0.11✓	0.66	1.49	1.47	0.68
Raleigh 2006 Stable Conditions	**SLINE 1.1**	15.02	0.14✓	0.04✓	0.80✓	0.86✓	1.22✓	0.83✓
	SAREA 1.1	8.01✓	0.18✓	0.89✓	0.83✓	1.05✓	1.07✓	0.86✓
	CALINE4	18.51	−0.32✓	0.18✓	0.73	1.48	1.51	0.75
	ADMS	10.70✓	−0.22✓	0.07✓	0.87✓	1.24✓	1.25✓	0.88✓
	ISC3	9.95✓	0.19✓	0.95✓	0.82✓	1.07✓	1.09✓	0.87✓
	SLSM	20.34	−0.26✓	0.11✓	0.69	1.48	1.47	0.72
Raleigh 2006 Unstable Conditions	**SLINE 1.1**	-15.72	−0.12✓	0.03✓	0.85✓	1.13✓	1.24✓	0.87✓
	SAREA 1.1	16.07	0.20✓	1.10✓	0.85✓	1.10✓	1.03✓	0.89✓
	CALINE4	17.30	−0.26✓	0.11✓	0.74	1.42	1.48	0.77
	ADMS	10.11	0.17✓	0.04✓	0.83✓	1.29	1.33	0.86✓
	ISC3	12.71	0.23✓	1.07✓	0.83✓	1.15✓	1.06✓	0.86✓
	SLSM	15.61	−0.26✓	0.11✓	0.74	1.41	1.49	0.76

Hyderabad Stable Conditions	**SLINE 1.1**	13.02	0.13✓	0.32✓	0.81✓	1.26	1.32	0.84✓
	SAREA 1.1	14.94	-0.07✓	0.28✓	0.79✓	1.12✓	1.17✓	0.81✓
	CALINE4	15.31	0.02✓	0.59✓	0.73	1.53	1.59	0.74
	ADMS	19.78	0.17✓	0.13✓	0.78✓	1.36	1.38	0.80✓
	ISC3	20.92	-0.18✓	0.53✓	0.71	1.40	1.43	0.76
	SLSM	20.77	0.09✓	0.64✓	0.72	1.31	1.34	0.73
Hyderabad Unstable Conditions	**SLINE 1.1**	-13.56	-0.19✓	0.17✓	0.82✓	1.21✓	1.24✓	0.88✓
	SAREA 1.1	13.03	0.10✓	0.14✓	0.81✓	1.23✓	1.25✓	0.84✓
	CALINE4	10.35	-0.22✓	0.7✓	0.75✓	1.35	1.38	0.78✓
	ADMS	11.98	0.22✓	0.52✓	0.81✓	1.26	1.29	0.81✓
	ISC3	18.92	0.44✓	1.56✓	0.77✓	1.31	1.35	0.78
	SLSM	11.86	0.12✓	0.71✓	0.72	1.48	1.41	0.74

The statistical evaluation results for the inter-comparison of developed models with available models are presented in Table 7-1. The numerical result gives a quantitative relationship between observed and predicted values. The values with '✓' denote the interpretation of statistical criteria which were satisfied by the suggested range from the literature for a better performing model. The average statistical indicator values of all models for all the datasets are presented in Figures 7-43.

The results from Figures 7-43 indicate that SLINE 1.1 has the least mean error of 11.88 $\mu g/m^3$ and SAREA 1.1 (Similar to CALINE4) has the 3rd least error of 15.68 within considered models. SLINE 1.1 has the 1st best FB value of 0.14 and SAREA 1.1 is the 5th best FB value of 0.25. The SLINE 1.1 has the 1st best NMSE value of 0.1 and SAREA 1.1 has the 5th best NMSE of 1.02. SLINE 1.1 (Similar to ADMS) has the highest correlation of 0.83 between predicted and observed values and SAREA 1.1 has the 2nd highest correlation of 0.81. For MG, SLINE 1.1 has the 1st best value of 1.08 and SAREA 1.1 has the 2nd best value of 1.20. For VG, SAREA 1.1 has the 1st best value of 1.16 and SLINE 1.1 has the 2nd best value of 1.21. For Fa2, SLINE 1.1 has highest value of 0.86 and SAREA 1.1 (Similar to ADMS) has the 2nd best value of 0.84. The results indicate that SLINE 1.1 is performing better than other models including SAREA 1.1.

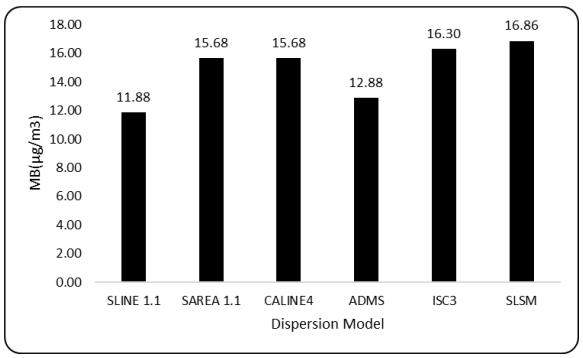

a) Comparison of average MB

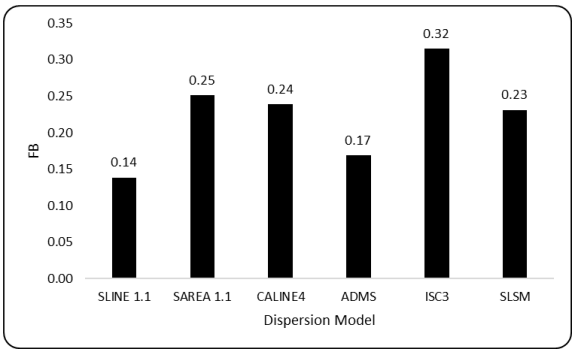

b) Comparison of average FB

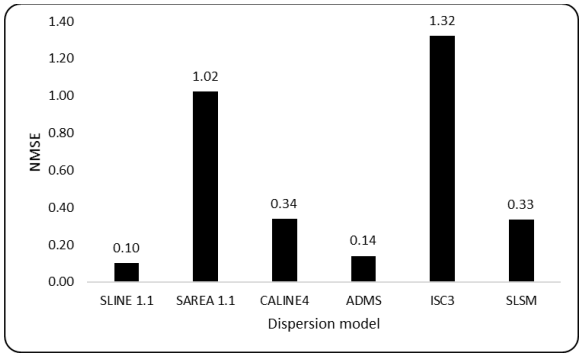

c) Comparison of average NMSE

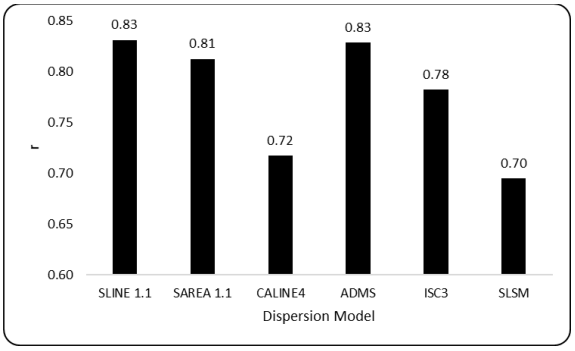

d) Comparison of average r

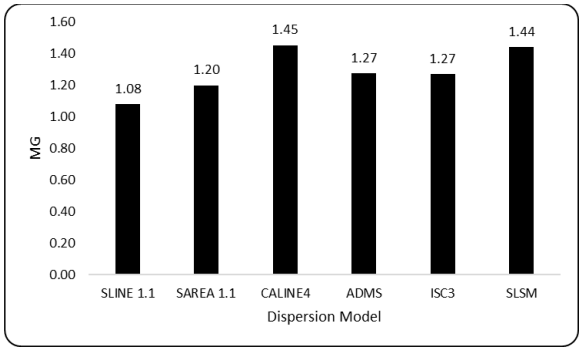

e) Comparison of average MG

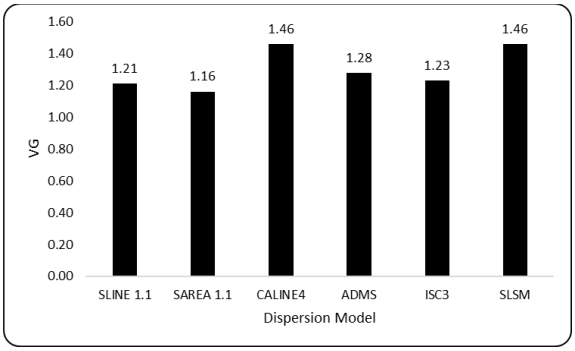

f) Comparison of average VG

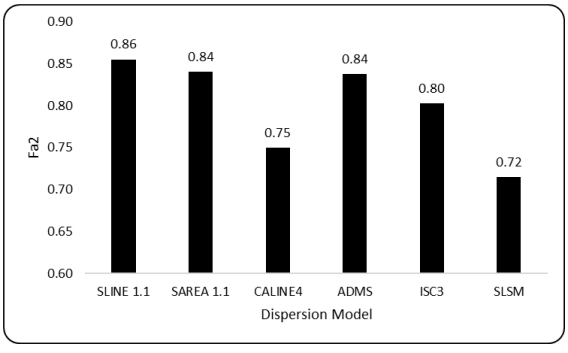

g) Comparison of average Fa2

Figure 7-43: Comparison of average statistical indicator values of gaseous models for 4 datasets

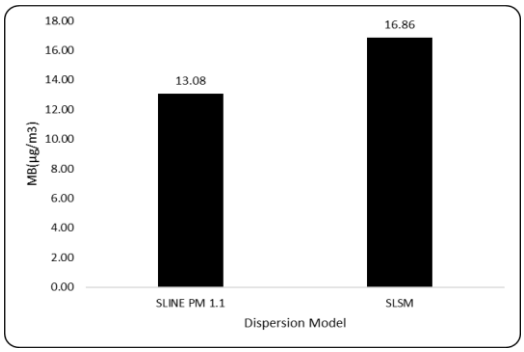

a) Comparison of average MB

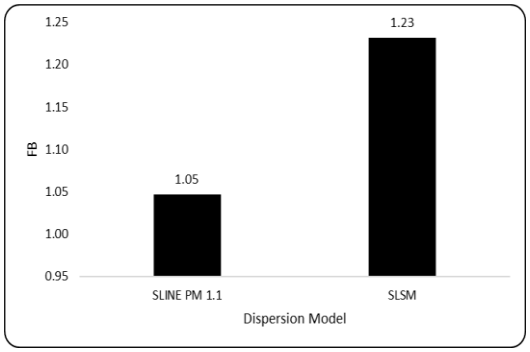

b) Comparison of average FB

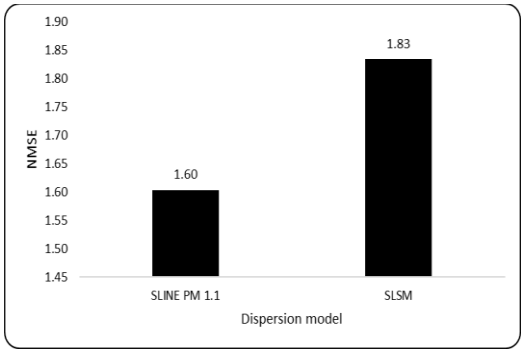

c) Comparison of average NMSE

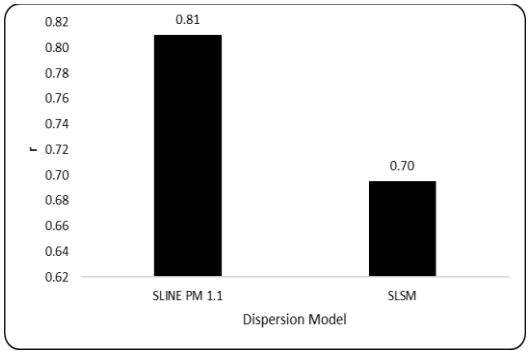

d) Comparison of average r

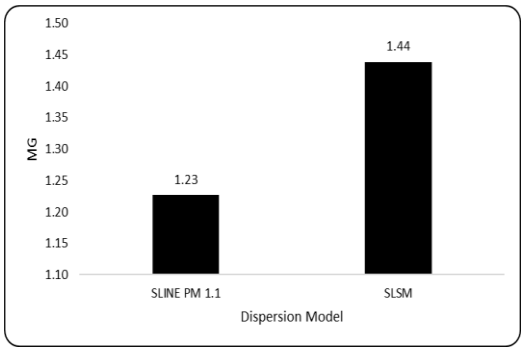

e) Comparison of average MG

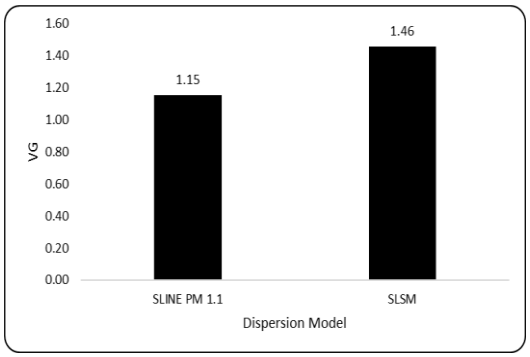

f) Comparison of average VG

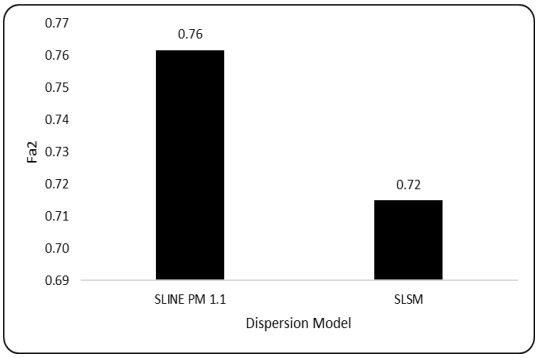

a) Comparison of average Fa2

Figure 7-44: Comparison of average statistical indicator values of PM models for 2 datasets.

SLINE PM 1.1 has mean error of 13.08 µg/m^3, which is better than SLSM. The results indicate that almost all the FB and NMSE values at are in the satisfactory range reported in the literature. Other parameters shows that the model needs improvement. The SLINE PM 1.1 model predictions correlate up to 81% with the field observations and SLSM predictions correlate up to 70% with the field observations.

Overall, the statistical indicator results indicate that SLINE 1.1 is performing better in terms of all the statistical indicators than the other models including SAREA 1.1 for gaseous pollutants. SLINE PM 1.1 is performing better in terms of all statistical indicators except Fa2 for PM.

The question that has not been answered yet: Is SLINE 1.1 significantly different from other models used in this dissertation? This is discussed in the following section.

7.4 Inter-comparison of Models using BOOT software (Version 2.0)

BOOT has been primarily used to evaluate the performance of air dispersion models. It provides concise information on model performance [106]. The current study uses Version 2.0 of the BOOT software. This software is significant in providing the summary of confidence limit analyses based on percentile confidence limits. It also provides a summary of performance measures for the considered dispersion models, which is necessary to perform inter-comparison analysis. SLINE 1.1, SAREA 1.1, CALINE4, ADMS, ISC3, and SLSM models are intercompared to identify the significantly different models. The results are presented in Table 7-2. SLINE PM 1.1 and SLSM are inter compared using BOOT software to identify if they are significantly different. The results are presented in Table 7-3.

The BOOT results indicate that for gaseous models, SLINE 1.1, SAREA 1.1, ADMS, and SLSM are significantly different from each other. However, the relation (significantly different or

not) between CALINE4 and ISC3 with the other models could not be determined using the current field data. Therefore, the comparison should be continued in the future with more datasets to determine if SLINE 1.1, SAREA 1.1, ADMS, and SLSM are significantly different from CALINE4 and ISC3. For PM models, the relation between SLINE PM 1.1 and SLSM could not be determined using the current field data. Therefore, the comparison should be continued in the future with more datasets to determine if SLINE PM 1.1 is significantly different from SLSM.

Table 7-2: Inter-comparison results of the gaseous models using BOOT software with 95% confidence limits

	SLINE 1.1	**SAREA 1.1**	**CALINE4**	**ADMS**	**ISC3**	**SLSM**
SLINE 1.1		X		X		X
SAREA 1.1	X			X		X
CALINE4						
ADMS	X	X				X
ISC3						
SLSM	X	X		X		

Table 7-3: Inter-comparison results of the PM models using BOOT software with 95% confidence limits

	SLINE PM 1.1	**SLSM**
SLINE PM 1.1		
SLSM		

Chapter 8

Conclusions

8.1 Concluding Remarks

8.1.1 Gaseous Models

SLINE 1.1 and SAREA 1.1 are the dispersion model developed for gaseous pollutants associated with highway mobile sources. These models incorporate wind shear near the ground and use a TPT model based on the physics associated with mobile source dispersion. SLINE 1.1 and SAREA 1.1 models are based on an analytical solution of the convective-diffusion equation after incorporating wind shear near the ground. The models used in the study incorporate improved physics, known at the time of development, related to the dispersion of effluents from mobile sources. The simulation schemes are being constantly improved over time. However, the updated three-phase atmospheric turbulence parametrization uses the current physics of mobile source dispersion and empirical coefficients based on mobile source field studies.

The sensitivity analysis is performed on SLINE 1.1 and SAREA 1.1 using SI method. Overall results indicate that the SLINE 1.1 and SAREA 1.1 models are highly sensitive to the emission rate, moderately sensitive to wind velocity, and sensitive to the vertical spread of the

mobile plume. But the magnitude of sensitivity is high in SLINE 1.1 model than in the SAREA 1.1.

A comparative analysis is performed between developed models (SLINE 1.1, SAREA 1.1) and the available models (CALINE4, ADMS, ISC3, SLSM) for gaseous pollutants using CALTRANS, Idaho Falls, Raleigh, Hyderabad data sets. The comparison analysis included identifying the relationship between the observed and predicted concentrations using Scatter Plots, Cp/Co plots, Q-Q plots, and statistical indicators (MB, FB, NMSE, r, MG, VG, and Fa2). The scatter plots show that the trendline of model predictions of SLINE 1.1 is higher than all the other models except for Hyderabad data (CO_2) for unstable atmospheric conditions. From scatter plots, SLINE 1.1 is mostly predicted in all the data sets. The trendline of SLINE 1.1 is higher than all the data sets except for Hyderabad data for unstable atmospheric conditions. From Cp/Co plots, more than 50% of the Cp/Co values of all the data sets are >1 except for the Hyderabad dataset. The Cp/Co plots indicate that SLINE 1.1 is over-predicting than other models including SAREA 1.1. From Q-Q plots, the upper limit range of model predictions of SLINE 1.1 are always higher than all the other models. The results from this evaluation indicate that the SLINE 1.1 is performing better than all the other models. Overall plots indicate that SAREA 1.1 and ADMS are performing similarly better after SLINE 1.1. Note that the other models in the study are showing mixed results (both under and over-predicting). All the statistical indicators of SLINE 1.1 are close to ideal values or better than or equal to the compared models except for MG values. These statistical indicator results also indicate that SLINE 1.1 is performing better than all the other models including SAREA 1.1. The model predictions of SLINE 1.1 and SAREA 1.1 are up to 83% and 82% correlated respectively with the observed data. Generally, a model that is over-predicting is preferred for the regulatory purpose of compliance with the air quality standards.

The Inter-comparison analysis is performed using BOOT (Version 2.0) software. The BOOT results indicate that SLINE 1.1, SAREA 1.1, ADMS, and SLSM are significantly different from each other. However, it is difficult to say whether these four models are significantly different or not from CALINE4 and ISC3. Additional field datasets should be used to determine this point.

Based on the findings of this study, it is encouraged to use the updated turbulence parametrization along with the empirical coefficients given in Tables 2-3 with other line-source models.

8.1.2 Particulate model

This study presents the development of SLINE PM 1.1, an analytical line source dispersion model to predict ground-level concentrations for PM for different particle size ranges. Separate dispersion equations are presented for the infinite as well as finite-length mobile sources. The application of the SLINE PM 1.1 model for emission data with a given particle size profile and emission data with no particle size distribution is provided.

The sensitivity of the model is tested using the SI method. The results indicate that SLINE PM 1.1 is highly sensitive to emission rate, moderately sensitive to wind velocity, and coefficient a, and slightly sensitive to vertical plume spread.

The model performance is evaluated using the Hyderabad and Raleigh data sets. The total concentrations computed using the developed equations were compared with a simple line source model SLSM available in the textbook for a test case. Similar to the gaseous models, the model evaluation includes performance estimation using scatter plots, Cp/Co plots, and statistical indicators (MB, FB, NMSE, r, MG, VG, and Fa2).

From scatter plots, SLINE PM 1.1 is over predicting than SLSM with Hyderabad data set for all the particle sizes. SLSM is over predicting that SLINE PM 1.1 for Particle size between 10

and 2.5 µm and <0.1 µm with Raleigh data set for stable conditions. From Cp/Co plots, SLINE PM 1.1 is over predicting larger-sized particles at lower downwind distances and small-sized particles at larger downwind distances. From Q-Q plots, the upper limit range of model predictions of SLINE PM 1.1 is always higher or equal to the SLSM. It can be observed that the predictions of low concentrations of both models (SLINE PM 1.1 and SLSM) are close to the larger concentrations. Overall, the results from the test case indicate that the simple line source model (SLSM) under-predicts PM concentrations at different downwind distances relatively with SLINE PM 1.1. The results indicate that all the FB and NMSE values are in the satisfactory range reported in the literature and show that the SLINE PM 1.1 model is a better-performing model than SLSM. The model predictions of SLINE PM 1.1 are correlated from 72 to 89% with the observed data. The BOOT results indicate that for PM models, the relation between SLINE PM 1.1 and SLSM could not be determined using the current field data.

Additionally, the performance of the basic line-source SLSM model is improved when the proposed TPT model is used for dispersion calculations (See Appendix A for a complete analysis) [107].

8.2 Recommendations and Future Work

- Future work needs to be done for the evaluation and comparison of area-source models with line-source dispersion models for highway mobile sources using more data sets to understand their performance.
- It will be important to update the turbulence parametrization based on new findings reported in the field in future years.
- The SLINE PM 1.1 should be evaluated with more data sets to improve the deposition velocity for different particle size should be indicated.

- The accuracy of the SLINE PM 1.1 model may be improved by determining the best empirical coefficients from field studies at different downwind distances and various particle size distributions.
- The use of the concepts of artificial intelligence (AI), including regression trees and sensitivity analysis (using analysis of variance) to identify the statistically significant input variables. The identified variables can be used as inputs to develop multilayer perceptron models for mobile source dispersion as suggested by Kadiyala et al. [108].

References

[1] A. Y. Watson, R. R. Bates, and D. Kennedy, "Atmospheric transport and dispersion of air pollutants associated with vehicular emissions," in *Air Pollution, the Automobile, and Public Health*, National Academies Press (US), 1988.

[2] "Air Pollution and Your Health," *National Institute of Environmental Health Sciences*. https://www.niehs.nih.gov/health/topics/agents/air-pollution/index.cfm (accessed Feb. 17, 2022).

[3] K. Wark and C. F. Warner, *Air pollution: its origin and control*. New York: Addison-Wesley, 1981.

[4] "68% of the world population projected to live in urban areas by 2050, says UN | UN DESA | United Nations Department of Economic and Social Affairs," May 16, 2018. https://www.un.org/development/desa/en/news/population/2018-revision-of-world-urbanization-prospects.html (accessed Nov. 07, 2020).

[5] S. Timothy, "Guidelines for Developing an Air Quality (Ozone and PM2.5) Forecasting Program, EPA-456/R-03-002 June 2003."

[6] US EPA, "Smog, Soot, and Other Air Pollution from Transportation," *US EPA*, Sep. 10, 2015. https://www.epa.gov/transportation-air-pollution-and-climate-change/smog-soot-and-local-air-pollution (accessed Nov. 07, 2020).

[7] K. Karroum *et al.*, "A Review of Air Quality Modeling," *MAPAN*, pp. 1–14, 2020.

[8] N. Sharma, K. Chaudhry, and C. C. Rao, "Vehicular pollution prediction modelling: a review of highway dispersion models," *Transport Reviews*, vol. 24, no. 4, pp. 409–435, 2004.

[9] R. Cook *et al.*, "Resolving local-scale emissions for modeling air quality near roadways," *Journal of the Air & Waste Management Association*, vol. 58, no. 3, pp. 451–461, 2008.

[10] O. G. Sutton, "Micrometeorology: a study of physical processes in the lowest layers of the earth's atmosphere," 1953.

[11] J. M. Stockie, "The mathematics of atmospheric dispersion modeling," *Siam Review*, vol. 53, no. 2, pp. 349–372, 2011.

[12] J. R. Zimmerman and R. S. Thompson, *User's guide for HIWAY: a highway air pollution model*. US Environmental Protection Agency, Office of Research and Development …, 1975.

[13] D. P. Chock, "A simple line-source model for dispersion near roadways," *Atmospheric Environment (1967)*, vol. 12, no. 4, pp. 823–829, 1978.

[14] S. T. Rao and M. T. Keenan, "Suggestions for improvement of the EPA-HIWAY model," *Journal of the Air Pollution Control Association*, vol. 30, no. 3, pp. 247–256, 1980.

[15] S. T. Rao, G. Sistla, M. T. Keenan, and J. S. Wilson, "An evaluation of some commonly used highway dispersion models," *Journal of the Air Pollution Control Association*, vol. 30, no. 3, pp. 239–246, 1980.

[16] A. Y. Watson, R. R. Bates, and D. Kennedy, "Atmospheric transport and dispersion of air pollutants associated with vehicular emissions," in *Air Pollution, the Automobile, and Public Health*, National Academies Press (US), 1988, pp. 77–98.

[17] D. Heist *et al.*, "Estimating near-road pollutant dispersion: A model inter-comparison," *Transportation Research Part D: Transport and Environment*, vol. 25, pp. 93–105, 2013.

[18] K. Jones and A. Wilbur, "A User's Manual for the CALINE-2 Computer Program," 1976.

[19] P. E. Benson, "Caline 4-A Dispersion Model for Predictiong Air Pollutant Concentrations Near Roadways," California State Department of Transportation, Sacramento, California (NTIS PB 85 211498/AS), Federal Highway Administration Report FHWA/CA/TL-84/15 Federal Highway Administration Report FHWA/CA/TL-84/15, 1984.

[20] A. K. Luhar and R. Patil, "A general finite line source model for vehicular pollution prediction," *Atmospheric Environment (1967)*, vol. 23, no. 3, pp. 555–562, 1989.

[21] P. A. Eckhoff and T. N. Braverman, "Addendum to the User's Guide to CAL3QHC Version 2.0 (CAL3QHCR User's Guide," 1995.

[22] J. Den Boeft, H. Eerens, W. Den Tonkelaar, and P. Zandveld, "CAR International: A simple model to determine city street air quality," *Science of the total environment*, vol. 189, pp. 321–326, 1996.

[23] D. Hall, A. Spanton, F. Dunkerley, M. Bennett, and R. Griffiths, *A Review of Dispersion Model Inter-comparison Studies Using ISC, R91, AERMOD and ADMS.* Environment Agency, 2000.

[24] M. Khare and P. Sharma, "Performance evaluation of general finite line source model for Delhi traffic conditions," *Transportation Research Part D: Transport and Environment*, vol. 4, no. 1, pp. 65–70, 1999.

[25] J. Kukkonen, J. Harkonen, J. Walden, A. Karppinen, and K. Lusa, "Validation of the dispersion model CAR-FMI against measurements near a major road," *International journal of environment and pollution*, vol. 16, no. 1–6, pp. 137–147, 2001.

[26] S. T. Rao, G. Sistla, R. E. Eskridge, and W. B. Petersen, "Turbulent diffusion behind vehicles: Evaluation of ROADWAY models," *Atmospheric Environment (1967)*, vol. 20, no. 6, pp. 1095–1103, Jan. 1986, doi: 10.1016/0004-6981(86)90141-1.

[27] H. Q. Bang, V. H. N. Khue, N. T. Tam, and K. Lasko, "Air pollution emission inventory and air quality modeling for Can Tho City, Mekong Delta, Vietnam," *Air Qual Atmos Health*, vol. 11, no. 1, pp. 35–47, Jan. 2018, doi: 10.1007/s11869-017-0512-x.

[28] A. Dėdelė and A. Miškinytė, "Estimation of inter-seasonal differences in NO 2 concentrations using a dispersion ADMS-Urban model and measurements," *Air Quality, Atmosphere & Health*, vol. 8, no. 1, pp. 123–133, 2015.

[29] K. L. Kenty *et al.*, "Application of CALINE4 to roadside NO/NO2 transformations," *Atmospheric Environment*, vol. 41, no. 20, pp. 4270–4280, 2007.

[30] J. Bluett, G. Kuschel, S. Xie, M. Unwin, and J. Metcalfe, "The development, use and value of a long-term on-road vehicle emission database in New Zealand," *Air Quality and Climate Change*, vol. 47, no. 3, p. 17, 2013.

[31] US EPA, "Air Quality Dispersion Modeling - Preferred and Recommended Models," *US EPA*, Nov. 02, 2016. https://www.epa.gov/scram/air-quality-dispersion-modeling-preferred-and-recommended-models (accessed Nov. 07, 2020).

[32] S. Gokhale and S. Pandian, "A semi-empirical box modeling approach for predicting the carbon monoxide concentrations at an urban traffic intersection," *Atmospheric Environment*, vol. 41, no. 36, pp. 7940–7950, Nov. 2007, doi: 10.1016/j.atmosenv.2007.06.065.

[33] H. Cai and S. Xie, "Traffic-related air pollution modeling during the 2008 Beijing Olympic Games: The effects of an odd-even day traffic restriction scheme," *Science of The Total Environment*, vol. 409, no. 10, pp. 1935–1948, Apr. 2011, doi: 10.1016/j.scitotenv.2011.01.025.

[34] C. W. Milando and S. A. Batterman, "Operational evaluation of the RLINE dispersion model for studies of traffic-related air pollutants," *Atmospheric Environment*, vol. 182, pp. 213–224, Jun. 2018, doi: 10.1016/j.atmosenv.2018.03.030.

[35] G. Bowatte *et al.*, "Traffic related air pollution and development and persistence of asthma and low lung function," *Environment International*, vol. 113, pp. 170–176, Apr. 2018, doi: 10.1016/j.envint.2018.01.028.

[36] D. Liang *et al.*, "Errors associated with the use of roadside monitoring in the estimation of acute traffic pollutant-related health effects," *Environmental Research*, vol. 165, pp. 210–219, Aug. 2018, doi: 10.1016/j.envres.2018.04.013.

[37] A. P, O. H, B. Ms, and A.-M. A, "Evaluation of vehicular pollution levels using line source model for hot spots in Muscat, Oman.," *Environ Sci Pollut Res Int*, vol. 27, no. 25, pp. 31184–31201, Jun. 2020, doi: 10.1007/s11356-020-09215-z.

[38] L. Pirjola, M. Kulmala, M. Wilck, A. Bischoff, F. Stratmann, and E. Otto, "Formation of sulphuric acid aerosols and cloud condensation nuclei: an expression for significant nucleation and model comprarison," *Journal of Aerosol Science*, vol. 30, no. 8, pp. 1079–1094, 1999.

[39] H. Korhonen, K. E. Lehtinen, and M. Kulmala, "Multicomponent aerosol dynamics model UHMA: model development and validation," *Atmospheric Chemistry and Physics*, vol. 4, no. 3, pp. 757–771, 2004.

[40] M. Pohjola, L. Pirjola, J. Kukkonen, and M. Kulmala, "Modelling of the influence of aerosol processes for the dispersion of vehicular exhaust plumes in street environment," *Atmospheric Environment*, vol. 37, no. 3, pp. 339–351, 2003.

[41] F. Lurmann, A. Wexler, S. Pandis, S. Musarra, N. Kumar, and J. Seinfeld, "Modelling urban and regional aerosols—II. Application to California's south coast air basin," *Atmospheric Environment*, vol. 31, no. 17, pp. 2695–2715, 1997.

[42] M. Z. Jacobson, "Development and application of a new air pollution modeling system—II. Aerosol module structure and design," *Atmospheric Environment*, vol. 31, no. 2, pp. 131–144, 1997.

[43] Y. Zhang *et al.*, "Development and application of the model of aerosol dynamics, reaction, ionization, and dissolution (MADRID)," *Journal of Geophysical Research: Atmospheres*, vol. 109, no. D1, 2004.

[44] N. S. Holmes and L. Morawska, "A review of dispersion modelling and its application to the dispersion of particles: An overview of different dispersion models available," *Atmospheric Environment*, vol. 40, no. 30, pp. 5902–5928, Sep. 2006, doi: 10.1016/j.atmosenv.2006.06.003.

[45] J. Levitin, J. Härkönen, J. Kukkonen, and J. Nikmo, "Evaluation of the CALINE4 and CAR-FMI models against measurements near a major road," *Atmospheric Environment*, vol. 39, no. 25, pp. 4439–4452, 2005.

[46] B. Broderick and R. O'Donoghue, "Spatial variation of roadside C2–C6 hydrocarbon concentrations during low wind speeds: Validation of CALINE4 and COPERT III modelling," *Transportation Research Part D: Transport and Environment*, vol. 12, no. 8, pp. 537–547, 2007.

[47] S. Righi, P. Lucialli, and E. Pollini, "Statistical and diagnostic evaluation of the ADMS-Urban model compared with an urban air quality monitoring network," *Atmospheric Environment*, vol. 43, no. 25, pp. 3850–3857, 2009.

[48] A. Agharkar, "Model Validation and Comparative Performance Evaluation of MOVES/CALINE4 and Generalized Additive Models for Near-Road Black Carbon Prediction," Ph.D., University of Cincinnati, Cincinnati, OH, USA, 2017.

[49] S. Majumder, "Emission load distribution and prediction of NO2 and PM10 using ISCST3 and CALINE4 line source modeling," *Applied Journal of Environmental Engineering Science*, vol. 5, no. 1, pp. 5–1, 2019.

[50] M. Selvakumar, S. Geetha, and S. Muthu Lakshmi, "Prediction of Air Pollution Due to Mobile Sources Using Line Source Models," in *Advances in Construction Materials and Sustainable Environment*, Springer, 2022, pp. 573–583.

[51] Z. Xu, Y. Kang, Y. Cao, and Z. Li, "Deep amended COPERT model for regional vehicle emission prediction," *Science China Information Sciences*, vol. 64, no. 3, pp. 1–3, 2021.

[52] US Environmental Protection Agency, "User's guide for the industrial source complex (ISC3) dispersion models." US Environmental Protection Agency and Research Triangle Park, North Carolina, 1995.

[53] M. M. Kimmlingen, *Modeling of gasoline emissions from stationary and mobile sources at Port Everglades*. Florida Atlantic University, 2003.

[54] S. Batterman *et al.*, "Dispersion modeling of traffic-related air pollutant exposures and health effects among children with asthma in Detroit, Michigan," *Transportation research record*, vol. 2452, no. 1, pp. 105–113, 2014.

[55] "CERC > Environmental software > ADMS 5 > Input and output." https://www.cerc.co.uk/environmental-software/ADMS-model/data.html (accessed Oct. 18, 2021).

[56] P. Vijay, S. M. Shiva Nagendra, S. Gulia, M. Khare, M. Bell, and A. Namdeo, "Performance Evaluation of UK ADMS-Urban Model and AERMOD Model to Predict the PM10 Concentration for Different Scenarios at Urban Roads in Chennai, India and Newcastle City, UK," in *Urban Air Quality Monitoring, Modelling and Human Exposure Assessment*, S. M. Shiva Nagendra, U. Schlink, A. Müller, and M. Khare, Eds. Singapore: Springer, 2021, pp. 169–181. doi: 10.1007/978-981-15-5511-4_12.

[57] K. C. Silverman, J. G. Tell, E. V. Sargent, and Z. Qiu, "Comparison of the industrial source complex and AERMOD dispersion models: case study for human health risk assessment," *J Air Waste Manag Assoc*, vol. 57, no. 12, pp. 1439–1446, Dec. 2007, doi: 10.3155/1047-3289.57.12.1439.

[58] B. Zou, F. Benjamin Zhan, J. Gaines Wilson, and Y. Zeng, "Performance of AERMOD at different time scales," *Simulation Modelling Practice and Theory*, vol. 18, no. 5, pp. 612–623, May 2010, doi: 10.1016/j.simpat.2010.01.005.

[59] D. Finn *et al.*, "Tracer studies to characterize the effects of roadside noise barriers on near-road pollutant dispersion under varying atmospheric stability conditions," *Atmospheric Environment*, vol. 44, no. 2, pp. 204–214, Jan. 2010, doi: 10.1016/j.atmosenv.2009.10.012.

[60] A. Venkatram, V. Isakov, E. Thoma, and R. Baldauf, "Analysis of air quality data near roadways using a dispersion model," *Atmospheric Environment*, vol. 41, no. 40, pp. 9481–9497, Dec. 2007, doi: 10.1016/j.atmosenv.2007.08.045.

[61] M. G. Snyder, A. Venkatram, D. K. Heist, S. G. Perry, W. B. Petersen, and V. Isakov, "RLINE: A line source dispersion model for near-surface releases," *Atmospheric Environment*, vol. 77, pp. 748–756, Oct. 2013, doi: 10.1016/j.atmosenv.2013.05.074.

[62] "All Projects | Sonoma Technology." https://www.sonomatech.com/projects/631 (accessed Aug. 20, 2022).

[63] "CERC > Environmental software > ADMS-Roads model." http://www.cerc.co.uk/environmental-software/ADMS-Roads-model.html (accessed Aug. 20, 2022).

[64] "Air Quality Modeling | Ohio University." https://www.ohio.edu/engineering/air-quality/research/air-quality-modeling (accessed Aug. 20, 2022).

[65] A. Kumar, "Pollutant Dispersion in the Planetary Boundary Layer," Ph.D., University of Waterloo, Waterloo, Ontario, Canada, 1978.

[66] Y. T. Yu, S. Xiang, and K. E. Noll, "Evaluation of the Relationship between Momentum Wakes behind Moving Vehicles and Dispersion of Vehicle Emissions Using Near-Roadway Measurements," *Environmental Science & Technology*, vol. 54, no. 17, pp. 10483–10492, 2020.

[67] R. Paine *et al., AERMOD: model formulation and evaluation results*. National Exposure Research Laboratory, Office of Research and Development …, 1999.

[68] K. Zhang and S. Batterman, "Near-road air pollutant concentrations of CO and PM2. 5: A comparison of MOBILE6. 2/CALINE4 and generalized additive models," *Atmospheric Environment*, vol. 44, no. 14, pp. 1740–1748, 2010.

[69] P. E. Benson, "Modifications to the Gaussian vertical dispersion parameter, σz, near roadways," *Atmospheric Environment (1967)*, vol. 16, no. 6, pp. 1399–1405, 1982.

[70] M. G. Snyder and ; David K. Heist, "User's Guide for R-LINE Model Version 1.2 A Research LINE source model for near-surface releases," Atmospheric Exposure Research Branch Atmospheric Modeling and Analysis Division.

[71] D. P. Chock, "General Motors sulfate dispersion experiment," *Boundary-Layer Meteorology*, vol. 18, no. 4, pp. 431–451, 1980.

[72] Y.-T. Yu, "Parameterization of Vertical Dispersion Coefficient (σ z) near Roadway: Vehicle Wake, Density and Types," Ph.D., Illinois Institute of Technology, Chicago, Illinois, USA, 2020.

[73] V. Akula, "Estimating the convective velocity scale for diffusion applications," *Boundary-Layer Meteorology*, vol. 15, no. 4, pp. 447–452, 1978.

[74] S. Thykier-Nielsen, S. Deme, and T. Mikkelsen, "Description of the atmospheric dispersion module RIMPUFF," *Riso National Laboratory, PO Box*, vol. 49, 1999.

[75] A. Kumar, "Effects of cross-wind shear on horizontal dispersion," *Journal of Environmental Engineering*, vol. 112, no. 1, pp. 1–11, 1986.

[76] Á. Leelőssy, F. Molnár, F. Izsák, Á. Havasi, I. Lagzi, and R. Mészáros, "Dispersion modeling of air pollutants in the atmosphere: a review," *Open Geosciences*, vol. 6, no. 3, pp. 257–278, 2014.

[77] R. Baldauf *et al.*, "Traffic and Meteorological Impacts on Near-Road Air Quality: Summary of Methods and Trends from the Raleigh Near-Road Study," *Journal of the Air & Waste Management Association*, vol. 58, no. 7, pp. 865–878, Jul. 2008, doi: 10.3155/1047-3289.58.7.865.

[78] S. V. H. Madiraju, G. R. PVS, and R. K. K, "Prototype of Eco-Friendly Indoor Air Purifier to Reduce Concentrations of CO2, SO2 and NO2," *Nature Environment and Pollution Technology*, vol. 19, no. 2, pp. 747–753, 2020, doi: 10.46488/NEPT.2020.v19i02.030.

[79] P. Nimmatoori and A. Kumar, "Development and evaluation of a ground-level area source analytical dispersion model to predict particulate matter concentration for different particle sizes," *Journal of Aerosol Science*, vol. 66, pp. 139–149, Dec. 2013, doi: 10.1016/j.jaerosci.2013.08.014.

[80] V. Gudivaka and A. Kumar, "An evaluation of four box models for instantaneous dense-gas releases," *Journal of Hazardous Materials*, vol. 25, no. 1–2, pp. 237–255, 1990.

[81] R. M. Riswadkar and A. Kumar, "Evaluation of the industrial source complex short-term model in a large-scale multiple source region for different stability classes," *Environmental Monitoring and Assessment*, vol. 33, no. 1, pp. 19–32, 1994.

[82] V. C. Patel and A. Kumar, "Evaluation of three air dispersion models: ISCST2, ISCLT2, and SCREEN2 for mercury emissions in an urban area," *Environmental Monitoring and Assessment*, vol. 53, no. 2, pp. 259–277, 1998.

[83] A. Kumar, N. K. Bellam, and A. Sud, "Performance of an industrial source complex model: Predicting long-term concentrations in an urban area," *Environmental Progress*, vol. 18, no. 2, pp. 93–100, 1999.

[84] A. Kumar, J. Luo, and G. F. Bennett, "Statistical evaluation of lower flammability distance (LFD) using four hazardous release models," *Process Safety Progress*, vol. 12, no. 1, pp. 1–11, 1993.

[85] S. Ahuja, "Evaluation of MESOPUFF-II-SOx transport and deposition in the Great Lakes region," 1996, vol. 72, pp. 283–299.

[86] "Model Evaluation." http://www.eng.utoledo.edu/aprg/courses/dm/hmodel.html (accessed Feb. 10, 2022).

[87] J. W. Boylan and A. G. Russell, "PM and light extinction model performance metrics, goals, and criteria for three-dimensional air quality models," *Atmospheric environment*, vol. 40, no. 26, pp. 4946–4959, 2006.

[88] A. S. Moursi, N. El-Fishawy, S. Djahel, and M. A. Shouman, "An IoT enabled system for enhanced air quality monitoring and prediction on the edge," *Complex & Intelligent Systems*, vol. 7, no. 6, pp. 2923–2947, 2021.

[89] A. G. Asuero, A. Sayago, and A. González, "The correlation coefficient: An overview," *Critical reviews in analytical chemistry*, vol. 36, no. 1, pp. 41–59, 2006.

[90] P. Amoatey, H. Omidvarborna, H. A. Affum, and M. Baawain, "Performance of AERMOD and CALPUFF models on SO2 and NO2 emissions for future health risk assessment in Tema Metropolis," *Human and Ecological Risk Assessment: An International Journal*, vol. 25, no. 3, pp. 772–786, 2019.

[91] H. M. Zwain, B. K. Nile, A. M. Faris, M. Vakili, and I. Dahlan, "Modelling of hydrogen sulfide fate and emissions in extended aeration sewage treatment plant using TOXCHEM simulations," *Scientific reports*, vol. 10, no. 1, pp. 1–11, 2020.

[92] S. W. Kang, "Sensitivity analysis of four air quality models," Master's Thesis, University of Toledo, Toledo, Ohio, USA, 1986.

[93] P. Nimmatoori and A. Kumar, "Application and sensitivity analysis of two screening dispersion models (SCREEN3 AND AERSCREEN) for a ground-level area source," *International Journal of Environmental Science and Engineering Research (IJESER)*, vol. 4, no. 2, p. 12, 2013.

[94] S. V. H. Madiraju and A. Kumar, "Development and Evaluation of SLINE 1.0, a Line Source Dispersion Model for Gaseous Pollutants by Incorporating Wind Shear Near the Ground under Stable and Unstable Atmospheric Conditions," *Atmosphere*, vol. 12, no. 5, p. 618, 2021.

[95] A. Bhat, A. Kumar, and K. Czajkowski, "Development and evaluation of a dispersion model to predict downwind concentrations of particulate emissions from land application of class B biosolids in unstable conditions," *Indoor and outdoor air pollution*, pp. 29–40, 2011.

[96] S. V. H. Madiraju and A. Kumar, "Examination of the Performance of a Three-Phase Atmospheric Turbulence Model for Line-Source Dispersion Modeling Using Multiple Air Quality Datasets," *J*, vol. 5, no. 2, pp. 198–213, 2022, doi: https://doi.org/10.3390/j5020015.

[97] S. V. H. Madiraju and A. Kumar, "An Intercomparison of Performance and Sensitivity of Four Generic Mobile Source Dispersion Models," presented at the International Graduate Studies Congress, Jun. 2021.

[98] D. L. Ermak, "An analytical model for air pollutant transport and deposition from a point source," *Atmospheric Environment (1967)*, vol. 11, no. 3, pp. 231–237, 1977.

[99] D. Richter and M. Chamecki, "Inertial Effects on the Vertical Transport of Suspended Particles in a Turbulent Boundary Layer," *Boundary-Layer Meteorol*, vol. 167, no. 2, pp. 235–256, May 2018, doi: 10.1007/s10546-017-0325-3.

[100] L. D. Sabin, J. H. Lim, M. T. Venezia, A. M. Winer, K. C. Schiff, and K. D. Stolzenbach, "Dry deposition and resuspension of particle-associated metals near a freeway in Los Angeles," *Atmospheric Environment*, vol. 40, no. 39, pp. 7528–7538, 2006.

[101] US EPA, "AERMOD deposition algorithms – science document(revised draft). Research Triangle Park." US EPA, 2009.

[102] S. V. H. Madiraju and A. Kumar, "Development of an Analytical Line Source Dispersion Model to Predict Ground Level Concentrations for Particulate Matter (PM) of Different Particle Size Ranges," *Environmental Sciences Proceedings*, vol. 8, no. 1, p. 13, 2021.

[103] R. A. Johnson, M. Anderson, E. Lilly, and C. Hok, "Implementation of CALINE4," Nov. 1988, Accessed: Oct. 18, 2021. [Online]. Available: https://scholarworks.alaska.edu/handle/11122/10357

[104] S. R. Hanna, B. A. Egan, J. Purdum, and J. Wagler, "Evaluation of the ADMS, AERMOD, and ISC3 dispersion models with the OPTEX, Duke Forest, Kincaid, Indianapolis and Lovett field datasets," *International Journal of Environment and Pollution*, vol. 16, no. 1–6, pp. 301–314, 2001.

[105] B. Jungers, T. Kear, and D. Eisinger, "A survey of air quality dispersion models for project level conformity analysis," *The California Department of Transportation*, 2006.

[106] J. C. Chang and S. R. Hanna, "Technical descriptions and user's guide for the BOOT statistical model evaluation software package, version 2.0," *George Mason University and Harvard School of Public Health, Fairfax, Virginia, USA*, 2005.

[107] S. V. H. Madiraju and A. Kumar, "Performance of Simple Mobile Source Dispersion Models using Three-Phase Turbulence Model," Jul. 2022, vol. 16, p. 30. doi: https://doi.org/10.3390/ecas2022-12847.

[108] A. Kadiyala, D. Kaur, and A. Kumar, "Development of hybrid genetic-algorithm-based neural networks using regression trees for modeling air quality inside a public transportation bus," *Journal of the Air & Waste Management Association*, vol. 63, no. 2, pp. 205–218, 2013.

Appendix A

Performance of a Simple Mobile Source Dispersion Model Using Three-Phase Turbulence Model

A.1 Introduction

Dispersion and chemical transformation in the atmosphere using mathematical or numerical techniques is called air pollution dispersion modeling. The dispersion modeling is based on the physics and chemistry involved in the process of advection/dispersion of contaminants and could predict and estimate the concentrations of contaminants by considering the origin of source, composition, emissions, traffic data, and meteorology. Analytical/numerical techniques are used to simulate ground-level concentration in air quality models. Typical inputs of air quality modeling include source information, meteorological data, and the surrounding terrain.

The small-scale, irregular air motions characterized by winds that vary in speed and direction are called turbulence in the atmosphere. Atmospheric turbulence is vital in causing the mixture and distribution of atmospheric gasses, water vapor, and other substances and hence it is an important parameter in air quality modeling. Along with the atmospheric turbulence, other critical parameters in air quality modeling are atmospheric stability, initial vertical plume spread, downwind distance, wind velocity, additional spread due to vehicular wake, thermal turbulence, road width, residence time, and mixing height of mobile source dispersion.

Published in: "The 5th International Electronic Conference on Atmospheric Sciences", session "Atmospheric Techniques, Instruments, and Modeling" on 25 July 2022 by MDPI https://doi.org/10.3390/ecas2022-12847.

The improvement in the performance of mobile source models over the last 50 years is achieved by improving the theoretical basis of the dispersion equations and developing dispersion coefficients based on either theory or field experiments. Madiraju and Kumar (2021) proposed a new Three-Phase turbulence model to calculate the vertical spread of mobile source plume by combining the current concepts of atmospheric turbulence and plume spread observations based on field data. The purpose of this study is to simulate the ground level concentrations using a basic model without following the three-phase turbulence model (MODEL-A) and compare results with the same basic model using dispersion coefficients for point sources (called MODEL-B and with following the three-phase turbulence model). Statistical indicators are used to assess the performance of the basic model under these two cases.

A.2 Performance Evaluation

The performance of the basic model is assessed initially by simulating the ground level concentrations of the air pollutants with multiple data sets without and with implementing the TPT model. The performance measures (discussed in section 4.3) are then computed by running through a model evaluation software (BOOT in this study). BOOT results are compared to identify the performance change after implementing the TPT model.

A.2.1 Evaluation Tool

BOOT has been primarily used to evaluate the performance of air dispersion models. It provides concise information on model performance. The current study uses Version 2.0 of the BOOT software. This software is significant in providing the summary of confidence limit analyses based on percentile confidence limits. It also provides a summary of performance measures for the considered dispersion models.

A.2.2 Performance Measures

It is necessary to consider multiple performance measures, as each measure has advantages and disadvantages and there is not a single measure that is universally applicable to all conditions. The relative advantages of each performance measure are partly determined by the distribution of the variable of interest. Linear measures of FB (Fractional Bias) and NMSE (Normalized Mean Square Error) are strongly influenced by infrequently occurring high observed and predicted concentrations. The fraction of predictions within a factor of two of observations (FA2), on the other hand, is the most robust measure, because it is not overly influenced by high and low outliers. Along with FB, NMSE, and FA2; the correlation coefficient (r) is also an important performance measure used in this study. The ideal values and suggested ranges of performance measures for better performing model are presented in Table 2. FB_{FN} can be considered as the underpredicting (false-negative) component of FB. Similarly, FB_{FP} can be considered as the overpredicting (false-positive) component of FB, i.e., only those (Co- Observed concentration in the field, Cp-Predicted concentration using a mathematical model) pairs with Cp > Co are considered in the calculation. All these performance measures are simulated using BOOT software.

A.2.3 Results

The ground-level concentrations (that are simulated using the basic model) are run through the BOOT software. The BOOT software output results generated for the three data sets for stable and unstable atmospheric conditions are listed in Table 3. In the BOOT analysis, it was considered that MODEL-A is the basic model without following the TPT model and MODEL-B is also the same basic model following the TPT model.

In the BOOT output file 'N' represents the number of data points considered in each data set. Each block represents each data set considered to run the BOOT software.

Since the basic model used in this study is a widely used model by many researchers and students, all the performance measures (statistical indicators) computed are in the satisfactory range suggested in the literature. In the nominal (median) results, the mean and standard deviation values of MODEL-A are significantly close enough when compared with observed values. But the MODEL-B results show that the mean and standard deviations values of the basic model have improved. The nominal results also indicate that all the other statistical indicators also improved slightly.

The mean values of the model predicted concentrations for Data set 1 (stable), Data set 2 (stable) of MODEL-A are close to the observed values. Data set 2 is unstable Data set 3 is stable, and the unstable of MODEL-B is close to observed values. The sigma values of the model predicted concentrations for Data set 1 and data set 3 stables of MODEL-A are close to the observed values and MODEL-B sigma values are close to observed values in all the other data sets.

The Bias values of MODEL-A and MODEL-B are higher than the ranges of a better-performing model. But the values of MODEL-B are slightly improved than MODEL-A. The Bias value for a perfect model is 0, which is practically impossible.

NMSE emphasizes the scatter in the complete dataset. NMSE reflects both systematic and unsystematic (random) errors in the concentrations. The ideal value of a perfect model will be 0 [96]. However, the results indicate that MODEL-A and MODEL-B have better NMSE values. The best NMSE value observed for MODEL-A for data set 2 (both stability conditions) and data set 3

(unstable condition) is 0.11. The best NMSE value is observed for MODEL-B for data set 2 (unstable condition) and data set 3 (unstable condition) is 0.11.

The correlation coefficient gives an indication of the linear relationship between the predicted and observed values. A perfect model has a correlation coefficient value of 1. Model-A and MODEL-B have correlation coefficients ranging from 0.58 to 0.74 and 0.67-to 0.8 in all three data sets. This indicates that MODEL-B predicted concentrations are more significantly correlated than MODEL-A.

The FA2 is defined as the percentage of predictions within a factor of two of the observed values. The ideal value for the factor of two is 1 (100%). The fraction of predictions within a factor of two of observations. The air quality model with more than 0.8 value of Fa2 is called a better performing model. The highest values of Fa2 for MODEL-A and MODEL-B are observed as 0.81 and 0.88 respectively for data set 1 for unstable atmospheric conditions.

Table 3. BOOT output results for the simple model for the three considered data sets at stable and unstable atmospheric conditions.

Model	MEAN	SIGMA	BIAS	NMSE	r	Fa2	FB	HIGH	2nd HIGH	FBfn	FBfp	MOEfn	MOEfp
MODEL A													
Data 1a	1.9x10^05	2.5x10^05	12.36	0.35	0.73	0.79	-0.261	2.0x10^06	1.8x10^06	0.195	0.456	0.875	0.614
Data 1b	1.8x10^05	1.2x10^04	14.33	0.47	0.72	0.81	-0.285	2.1x10^06	1.9x10^06	0.398	0.683	0.762	0.477
Data 2a	1.7x10^04	1.1x10^04	9.52	0.11	0.69	0.73	-0.265	3.5x10^05	3.0x10^05	0.182	0.447	0.848	0.583
Data 2b	1.2x10^04	1.0x10^04	11.98	0.11	0.74	0.76	-0.266	1.7x10^05	1.5x10^05	0.489	0.755	0.661	0.395
Data 3a	3.0x10^05	2.0x10^04	10.13	0.17	0.58	0.79	-0.334	1.6x10^06	1.1x10^06	0.357	0.691	0.713	0.379
Data 3b	4.4x10^05	1.4x10^05	20.11	0.11	0.66	0.74	-0.257	2.0x10^06	1.5x10^06	0.417	0.674	0.613	0.356
MODEL B													
Data 1a	2.8x10^05	6.3x10^04	7.69	0.26	0.78	0.82	-0.179	2.5x10^06	1.9x10^06	0.197	0.376	0.973	0.794
Data 1b	2.5x10^05	4.2x10^04	6.78	0.34	0.77	0.88	-0.198	2.1x10^06	1.7x10^06	0.674	0.872	0.496	0.298
Data 2a	3.3x10^04	2.4x10^04	8.22	0.1	0.73	0.78	-0.17	3.3x10^05	3.1x10^05	0.317	0.487	0.853	0.683
Data 2b	2.7x10^04	1.1x10^04	11.2	0.09	0.8	0.81	-0.172	1.1x10^05	1.1x10^05	0.337	0.509	0.833	0.661
Data 3a	3.1x10^05	1.4x10^05	5.67	0.13	0.67	0.79	-0.221	1.3x10^06	1.2x10^06	0.277	0.498	0.763	0.542
Data 3b	4.6x10^05	4.5x10^04	15.35	0.09	0.71	0.76	-0.147	1.5x10^06	1.2x10^06	0.355	0.502	0.655	0.508

The FB values for both the models are less than 0.5 and close to 0, which means both MODEL-A and MODEL-B are better performing. However, it can be observed that all the FB values are negative, which means that most of the model predictions are less than the observed values (under-predicting). If the point of (FB_{FN}, FB_{FP}) = (2, 0) means that predictions are zero everywhere, but all observations are finite. If the point of (FB_{FN}, FB_{FP}) = (0, 2) means that observations are zero everywhere, but all predictions are finite. Since both FB_{FN} and FB_{FP} have values greater than 0 and less than 2 which means all the observations and predictions are finite. If $FB_{FN} = FB_{FP} = 0$; then a model can be called as a perfect model.

A.3. Conclusions

Overall, the TPT model was implemented in a basic mobile source dispersion model, and the performance was assessed. Three data sets were used to assess and simulate the model predicted concentrations and compare them with the observed data. BOOT software is used to generate the comparison results. A comparison of results for the basic model with and without following the TPT model is given in Table 3 using the three data sets for stable and unstable atmospheric conditions. Various performance measures include meaning, sigma, bias, NMSE, correlation coefficient, Fa2, and FB. The results indicate that there is a slight improvement in the model performance of the basic model after following the TPT model. Improvement in FB, NMSE, Fa2, and r values are visible. The nominal results also show that the mean and standard deviation values of the simulations computed using MODEL-B are better than the MODEL-A. Finally, these results indicate that following a separate turbulence model for the mobile source could improve model predictions.